COMPUTATIONAL FLUID DYNAMICS AND TWO-DIMENSIONAL HYDRAULIC MODELING STUDY-MODEL VALIDATION AND INITIAL PRODUCTION RUNS

PRELIMINARY STUDY REPORT

BRUNSWICK HYDROELECTRIC PROJECT

(FERC NO. 2284)



Submitted by:

Brookfield Renewable
Brookfield White Pine Hydro LLC
150 Main Street
Lewiston, ME 04240

Prepared by:

GOMEZ AND SULLIVAN ENGINEERS

August 2026

Brookfield

TABLE OF CONTENTS

1.0 Introduction 1
2.0 Goals and Objectives 2
3.0 Study Area 2
4.0 Methods 7
4.1 Data Collection 7
4.2 CFD Model Development 10
4.2.1 Physical Geometry 10
4.2.2 Physical Processes 11
4.2.3 Computational Mesh and Boundary Conditions 12
4.2.4 Flow Sources 14
4.3 2D Model Development 23
4.3.1 Physical Geometry 23
4.3.2 Physical Processes 23
4.3.3 Computational Mesh and Boundary Conditions 23
5.0 Simulations 28
5.1 Model Validation 28
5.1.1 Forebay Model 28
5.1.2 Tailrace Model 29
5.1.3 Bypass Channel Model 29
5.2 Production Runs 31
5.2.1 Forebay Model 31
5.2.2 Tailrace Model 31
5.2.3 Bypass Channel Model 32
6.0 Results 34
6.1 Model Validation 34
6.1.1 Forebay Model 34
6.1.2 Tailrace Model 35
6.2 Production Runs 36
6.2.1 Forebay Model 36
6.2.2 Tailrace Model 37
6.2.3 Bypass Channel Model 37
7.0 References 87

LIST OF TABLES

Table 5.1-1: Summary of Validation Run Simulation Conditions 30
Table 5.2-1: Summary of Hydraulic Capacities and Operating Levels 33
Table 5.2-2: Summary of Production Run Simulation Conditions 33
Table 6.1.1-1: Summary Statistics of the Difference Between Simulated and Field Measured Velocities at all ADCP Nodes for all Forebay Validation Transects 38
Table 6.1.2-1: Summary Statistics of the Difference Between Simulated and Field Measured Velocities at all ADCP Nodes for all Tailrace Validation Transects 38
Table 6.2.3-1: Summary of Bypass Channel Model Results at the Falls 38

LIST OF FIGURES

Figure 3.0-1: Project Study Area 4
Figure 3.0-2: Project Overview 5
Figure 3.0-3: Overview Map of Project Structures 6
Figure 4.1-1: Brunswick Bathymetric and Topographic Data Collection Extents 8
Figure 4.1-2: Brunswick Velocity Data Collection Transect Locations 9
Figure 4.2.1-1: Shoals Area Bedrock Formations 16
Figure 4.2.1-2: Manual Terrain Adjustments in Shoals area Between Swinging Bridge and Goat Island 17
Figure 4.2.1-3: Overview of Physical Geometry 18
Figure 4.2.3-1: Forebay Model Computational Mesh Layout 19
Figure 4.2.3-2: Tailrace Model Computational Mesh Layout 20
Figure 4.2.4-1: Forebay Model Flow Source Location and Orientation 21
Figure 4.2.4-2: Tailrace Model Flow Source Location and Orientation 22
Figure 4.3-1: Bypass Channel Model Area 25
Figure 4.3.1-1: Terrain Surface Used for Bypass Channel Model 26
Figure 4.3.3-1: Bypass Channel Model Mesh and Boundary Conditions 27
Figure 6.1.1-1: Map of Profile Lines Used for Forebay Model Validation 39
Figure 6.1.1-2: Relative WSEL Comparison for the River Right Channel to the Intake Profile Line 40
Figure 6.1.1-3: Relative WSEL Comparison for the River Left Channel to the Intake Profile Line 41
Figure 6.1.1-4: Simulated and Field Measured Velocities at Transect on River Right of Goat Island 42

Figure 6.1.1-5: Simulated and Field Measured Velocities at Transect on River Left of Goat Island....43
Figure 6.1.1-6: Simulated and Field Measured Velocities at Transect Below Goat Island....44
Figure 6.1.1-7: Rocks in vicinity of Goat Island not Resolved in the Forebay CFD Model....45
Figure 6.1.1-8: Simulated and Field Measured Velocities at Intake Transect....46
Figure 6.1.2-1: Map of Profile Line Used for Tailrace Model Validation....47
Figure 6.1.2-2: Relative WSEL Comparison for the Tailrace Profile Line....48
Figure 6.1.2-3: Simulated and Field Measured Velocities at TR1....49
Figure 6.1.2-4: Simulated and Field Measured Velocities at TR2....50
Figure 6.1.2-5: Simulated and Field Measured Velocities at TR3....51
Figure 6.1.2-6: Simulated and Field Measured Velocities at TR4....52
Figure 6.1.2-7: Simulated and Field Measured Velocities at TR5....53
Figure 6.2.1-1: Location of Forebay Model Velocity Planes....54
Figure 6.2.1-2: Simulated Velocities at Three Locations in Front of the Intake for Highest Production Flow (7,595 cfs)....55
Figure 6.2.1-3: Velocity Magnitude and Orientation for Highest Production Flow (7,595 cfs) 50 feet Upstream of Intake....56
Figure 6.2.1-4: Velocity Magnitude and Orientation for Highest Production Flow (7,595 cfs) 100 feet Upstream of Intake....57
Figure 6.2.1-5: Velocity Magnitude and Orientation for Highest Production Flow (7,595 cfs) 150 feet Upstream of Intake....58
Figure 6.2.1-6: Simulated Velocities at Three Locations in Front of the Intake for Lowest Production Flow (1,320 cfs)....59
Figure 6.2.1-7: Velocity Magnitude and Orientation for Lowest Production Flow 50 feet Upstream of Intake....60
Figure 6.2.1-8: Velocity Magnitude and Orientation for Lowest Production Flow 100 feet Upstream of Intake....61
Figure 6.2.1-9: Velocity Magnitude and Orientation for Lowest Production Flow 150 feet Upstream of Intake....62
Figure 6.2.2-1: Location of Tailrace Model Velocity Planes....63
Figure 6.2.2-2: Simulated Velocities at Three Locations Downstream of the Powerhouse for Highest Production Flow (7,595 cfs)....64
Figure 6.2.2-3: Simulated Velocities at Three Locations Downstream of the Powerhouse for Lowest Production Flow (1,320 cfs)....64
Figure 6.2.2-4: Velocity Magnitude and Orientation for Highest Production Flow (7,595 cfs) 50 feet Downstream of Powerhouse....65

Figure 6.2.2-5: Velocity Magnitude and Orientation Highest Production Flow (7,595 cfs) 100 feet Downstream of Powerhouse 66
Figure 6.2.2-6: Velocity Magnitude and Orientation for Highest Production Flow (7,595 cfs) 150 feet Downstream of Powerhouse 67
Figure 6.2.2-7: Velocity Magnitude and Orientation for Lowest Production Flow (1,320 cfs) 50 feet Downstream of Powerhouse 68
Figure 6.2.2-8: Velocity Magnitude and Orientation for Lowest Production Flow (1,320 cfs) 100 ft Downstream of Powerhouse....69
Figure 6.2.2-9: Velocity Magnitude and Orientation for Lowest Production Flow (1,320 cfs) 150 ft Downstream of Powerhouse....70
Figure 6.2.3-1: Simulated Depths in the Bypass Channel (100 cfs)....71
Figure 6.2.3-2: Simulated Velocities in the Bypass Channel (100 cfs)....72
Figure 6.2.3-3: Simulated Depths in the Bypass Channel (930 cfs)....73
Figure 6.2.3-4: Simulated Velocities in the Bypass Channel (930 cfs)....74
Figure 6.2.3-5: Simulated Depths in the Bypass Channel (1,760 cfs)....75
Figure 6.2.3-6: Simulated Velocities in the Bypass Channel (1,760 cfs)....76
Figure 6.2.3-7: Simulated Depths in the Bypass Channel (2,690 cfs)....77
Figure 6.2.3-8: Simulated Velocities in the Bypass Channel (2,690 cfs)....78
Figure 6.2.3-9: Simulated Depths in the Bypass Channel (3,625 cfs)....79
Figure 6.2.3-10: Simulated Velocities in the Bypass Channel (3,625 cfs)....80
Figure 6.2.3-11: Simulated Depths in the Bypass Channel (7,250 cfs)....81
Figure 6.2.3-12: Simulated Velocities in the Bypass Channel (7,250 cfs)....82
Figure 6.2.3-13: Simulated Depths in the Bypass Channel (10,875 cfs)....83
Figure 6.2.3-14: Simulated Velocities in the Bypass Channel (10,875 cfs)....84
Figure 6.2.3-15: Simulated Depths in the Bypass Channel (14,500 cfs)....85
Figure 6.2.3-16: Simulated Velocities in the Bypass Channel (14,500 cfs)....86

LIST OF ABBREVIATIONS AND DEFINITIONS

2D	two-dimensional
3D	three-dimensional
ADCP	Acoustic Doppler Current Profiler
BWPH	Brookfield White Pine Hydro LLC.
CAD	computer aided design
CFD	Computational Fluid Dynamics
CFR	Code of Federal Regulations
cfs	cubic feet per second
ESRI	Environmental Systems Research Institute
FAVOR	Fractional Area/Volume Obstacle Representation
FERC	Federal Energy Regulatory Commission
Flow-3D	FLOW-3D® software from Flow Science, Inc.
ft/s	feet per second
HEC-RAS	Hydrologic Engineering Center's River Analysis System
Licensee	Brookfield White Pine Hydro LLC.
LiDAR	Light Detection and Ranging
MaineDOT	Maine Department of Transportation
MCS	model coordinate system
MDMR	Maine Department of Marine Resources
ME	Maine
MMBTU	Merrymeeting Bay Trout Unlimited
msl	Mean Sea Level
NAD83	North American Datum of 1983
NGVD29	National Geodetic Vertical Datum of 1929
NOAA	National Oceanic and Atmospheric Administration
NOI	Notice of Intent
PAD	Pre-Application Document
Project	Brunswick Hydroelectric Project (FERC No. 2284)
PSP	Proposed Study Plan
RANS	Reynolds Averaged Navier-Stokes
RNG	Renormalized Group
RTK-GPS	Real Time Kinematic Global Positioning System
SPCS	State Plane Coordinate System
STL	Stereolithography format

SWE	Shallow Water Equations
TIN	triangulated irregular network
USFWS	United States Fish and Wildlife Service
VOF	Volume of Fluid
WSEL	water surface elevation

1.0 INTRODUCTION

Brookfield White Pine Hydro LLC (BWPH, Licensee), is in the process of relicensing the 19-megawatt Brunswick Hydroelectric Project (Project) (FERC No. 2284) with the Federal Energy Regulatory Commission (FERC). The Project is located on the Androscoggin River in the Town of Brunswick, Maine (ME) to the south and the Town of Topsham, ME to the north. The Project straddles the border between the Cumberland and Sagadahoc counties. The original license was issued on February 9, 1979 and expires on February 28, 2029.

The Licensee is using FERC's Integrated Licensing Process as established in Title 18 Code of Federal Regulations (CFR), Part 5. The Licensee filed a Pre-Application Document (PAD) and Notice of Intent (NOI) to seek a new license for the Project on February 21, 2024.[1] The PAD provides a description of the Project, including its structures, operations, and potentially affected environmental resources.

The Licensee distributed the PAD and NOI simultaneously to Federal and state resource agencies, local governments, Native American tribes, members of the public, and others thought to be interested in the relicensing proceeding. Following the filing of the PAD, FERC prepared and issued Scoping Document 1 on April 16, 2024. FERC also held agency and public scoping meetings and a site visit on May 7, 2024. The FERC Process Plan and Schedule provided agencies and interested parties an opportunity to file comments on the PAD and Scoping Document 1 and requested studies by June 20, 2024. FERC subsequently issued Scoping Document 2 on July 29, 2024.

The Licensee filed a Proposed Study Plan (PSP) on August 2, 2024 and held Study Plan Meetings on August 28 and October 9, 2024. The Revised Study Plan was filed in accordance with the Integrated Licensing Process schedule on December 2, 2024. FERC issued a Study Plan Determination on December 30, 2024.

In the Revised Study Plan, the Licensee proposed to conduct Computational Fluid Dynamics (CFD) modeling in the vicinity of the Project forebay/downstream fish entrance, as well as in the Project tailrace/near the entrance of the upstream fish passage facility. Additionally, the Licensee proposed to conduct two-dimensional (2D) hydraulic modeling in the channel downstream of the Tainter gate section of the spillway. This study would provide a better understanding of flow field conditions that exist in these areas, and how these conditions may be affecting migratory fish behavior and movements. The results of the modeling effort would be coupled with the Upstream and Downstream Passage Alternatives Study to evaluate modifications to the existing upstream and downstream fish passage systems at the Project. The United States Fish and Wildlife Service (USFWS), Merrymeeting Bay Trout Unlimited (MMBTU), and Maine Department of Marine Resources (MDMR) submitted comments regarding the proposed CFD modeling on November 1 (USFWS and MMBTU) and November 15, 2024 (MDMR). FERC subsequently issued the Study Plan Determination on December 30, 2024 which accepted the proposed CFD and 2D modeling study with minor changes as proposed by USFWS, MMBTU, and MDMR.

[1] **https://elibrary.ferc.gov/eLibrary/filelist?accession_Number=20240221-5163.**

2.0 GOALS AND OBJECTIVES

The goal of this study is to determine the flow field conditions and how they may be affecting migratory fish behavior and movements in the vicinity of the Project forebay/downstream fishway entrance, the Project tailrace/near the entrance of the upstream fish passage facility, and in the channel downstream of the Tainter gate section of the spillway. The information from this study was coupled with the *Upstream and Downstream Passage Alternatives Study* to evaluate potential modifications to the upstream and downstream fish passage facilities at the Project.

The objective of this study is to develop a series of layered drawings that show velocity magnitude and orientation under various operational conditions. The results of the modeling demonstrate velocities and flow orientations in the vicinity of the Project's upstream and downstream fish passage facility entrances, as well as in the channel downstream of the Tainter gate section of the spillway.

3.0 STUDY AREA

The Project is located on the Androscoggin River at the head-of-tide at approximately river mile 6 in the Towns of Brunswick and Topsham, ME. The Project straddles the border between Cumberland and Sagadahoc counties. The Project dam is the downstream most dam on the mainstem of the Androscoggin River. The dam and powerhouse span the Androscoggin River immediately above the U.S. Route 201 bridge connecting Topsham and Brunswick, ME, at a site originally known as Brunswick Falls.

The Project impoundment extends approximately 4.5 miles upstream from the Brunswick Dam to the tailwater area of the Pejepscot Dam. Approximately 550 feet upstream of the Project powerhouse, Goat Island splits the channel and influences the velocities to the powerhouse. Additionally, there is an area of shallow shoals that extend from the upstream end of Goat Island approximately 400 feet. Finally, the Androscoggin Swinging Bridge crosses the impoundment approximately 1,500 feet upstream of the Project powerhouse.

Downstream of the Project, the river is split into two channels, which rejoin underneath the U.S. Route 201 bridge. The river right channel is the tailrace and the river left channel is a bypass channel. The bypass channel extends from the Tainter gate section of the spillway approximately 500 feet downstream to a small natural falls before merging with the tailrace. Figure 3.0-1 provides a map overview of the Project area with features labeled.

Figure 3.0-2 provides a map overview of the Project structures. The 125-foot-wide powerhouse is located along the river right side of the Androscoggin River. The powerhouse contains three turbine-generator units with Unit 1 being located closest to the river right shore and Unit 3 being located furthest from the river right shore. Unit 1 has an adjustable hydraulic capacity range of 2,741 cubic feet per second (cfs) to 5,075 cfs, while Units 2 and 3 are not adjustable and operate at approximately 1,200 cfs each. The upstream and downstream fish passage facilities are integral with the powerhouse, as shown in Figure 3.0-3. Water discharged through the powerhouse (i.e., whether through a turbine or fish passage facility) enters a tailrace with a maximum depth of approximately 12 feet, a width of approximately 96 feet, and a length of approximately 300 feet.

The tailrace consists of excavated rock with a U-shaped cross section. Tailwater elevations can be tidally influenced for total river flows up to approximately 35,000 cfs.

The upstream fish passage entrance is located adjacent to the powerhouse, while the exit flume, which has trashracks with 5.75-inch clear spacing, is located between Unit 1 and the shore. The upstream fish passage structure (vertical slot fishway) passes a total flow of approximately 100 cfs[2] and consists of a series of pools and weirs. The upstream fish passage facility is operated from May 1 through November 15 as river conditions allow (i.e., typically up to a total river flow of 20,000 cfs. The downstream fish passage entrance is located between Unit 1 and Unit 2 and is covered by a traskrack that has 3.5-inch clear spacing, while the exit discharges from the downstream face of the powerhouse. The downstream fish passage structure passes approximately 20 cfs and consists of a surface sluice leading to an 18-inch diameter pipe. The downstream fish passage facility is operated from April 1 through December 31.

[2] 30 cfs passes through the fishway with an additional 70 cfs passed via an attraction water system consisting of a gravity fed pipe from the impoundment to a diffusion area at the lower end of the fishway

Figure 3.0-1: Project Study Area



Figure 3.0-2: Project Overview

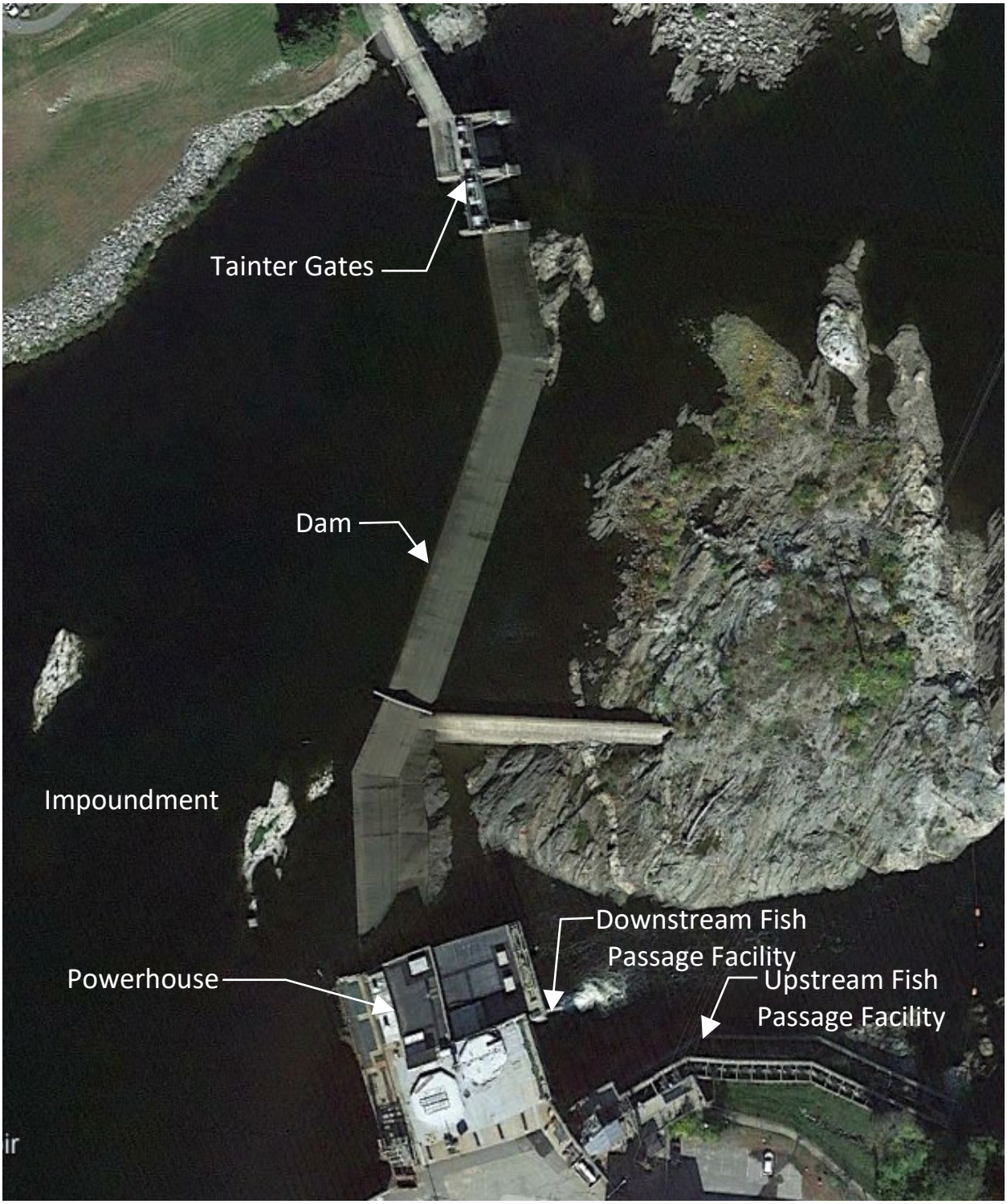
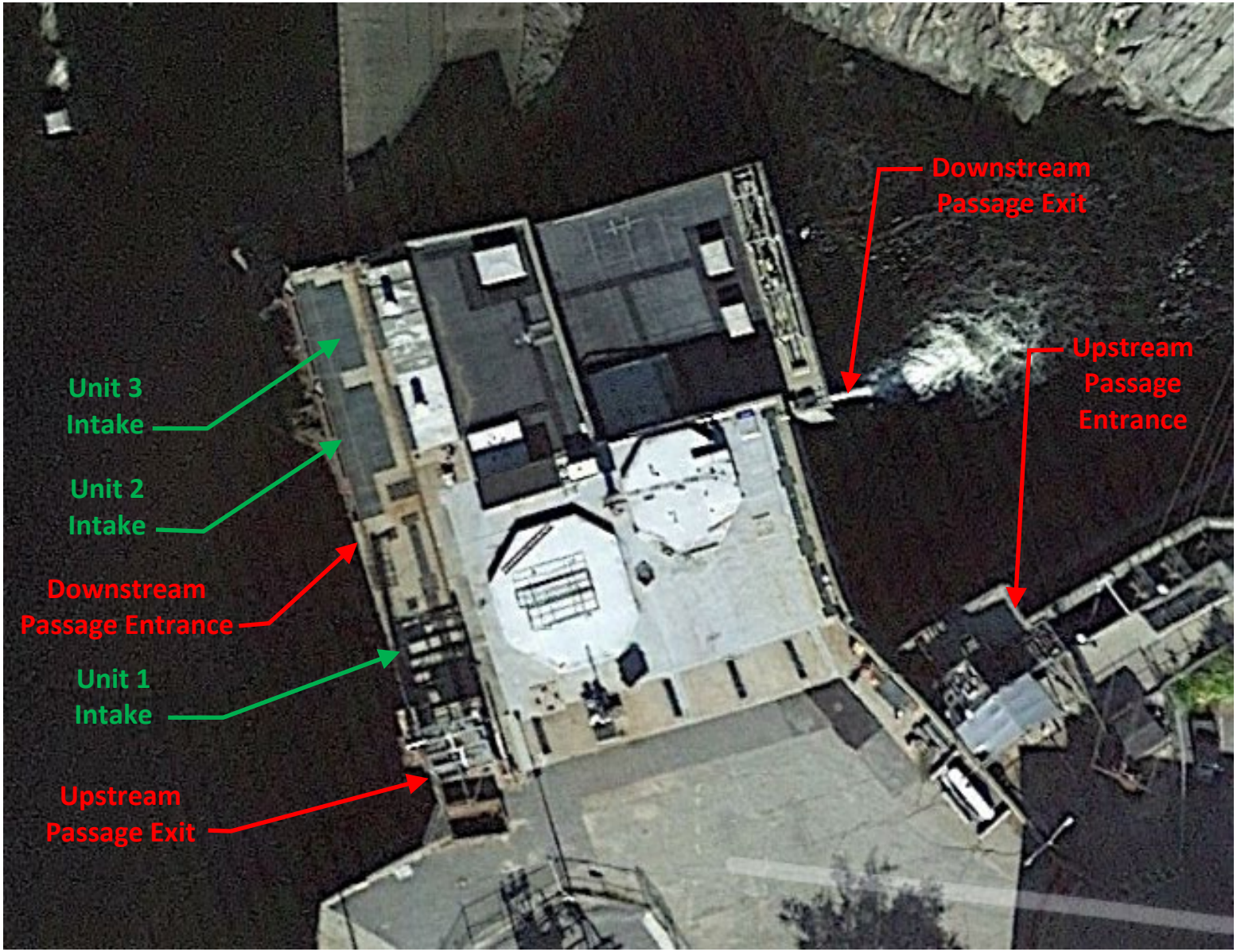


Figure 3.0-3: Overview Map of Project Structures



4.0 METHODS

Two separate CFD models (i.e., forebay model and tailrace model) and a 2D hydraulic model were developed to gain a better understanding of flow field conditions that exist in the vicinity of the upstream and downstream fish passage facility entrances and in the channel below the spillway. The forebay and tailrace models each include large-scale and small-scale models to evaluate various scenarios at the spatial scales needed to evaluate the flow field conditions. The CFD models discussed herein were developed and run using the FLOW-3D® software from Flow Science, Inc. (Flow-3D); specifically, FLOW-3D HYDRO (solver version 25.1.0.20250326 win64 HYDRO HPC 1.1.0, interface version 25.1.0.20250319) was utilized. The following sections outline the data collection efforts, development of each model, and validation of the models.

4.1 Data Collection

In June and September 2025, the Licensee completed various data collection efforts for the purpose of model development and validation. The impoundment water surface elevation (WSEL) or headpond was held approximately 0.5 feet below the spillway crest to allow for safe conditions while data were collected by boat near the Project. A bathymetric survey was performed which encompassed the width of the river and extended approximately 2,500 feet upstream from the dam. Downstream of the dam, bathymetric data was collected in the river left channel downstream of the Tainter gates and in the tailrace extending approximately 1,000 feet from the powerhouse face. A boat mounted Acoustic Doppler Current Profiler (ADCP) was used to collect water depth and water velocity data simultaneously. A Real Time Kinematic Global Positioning System (RTK-GPS) was also mounted to the boat to collect WSEL and georeference the ADCP data. Additional topographic elevations were collected using the RTK-GPS to supplement the bathymetric data in areas inaccessible by boat. A total station unit was used to collect elevations along the bedrock falls at the bottom of the river left channel downstream of the Tainter gates. Figure 4.1-1 shows the extent of the topographic and bathymetric data collection efforts. The boat-mounted ADCP and RTK-GPS were also used to collect velocity data within the impoundment on either side of Goat Island, in front of the powerhouse and fishways (downstream and upstream), and within the tailrace. Velocity data were not captured in the river left channel downstream of the Tainter gates because the Tainter gates were closed and the impoundment drawn down for safety reasons, resulting in no flow in the channel. Figure 4.1-2 shows the location of velocity transect data collection efforts.

Figure 4.1-1: Brunswick Bathymetric and Topographic Data Collection Extents

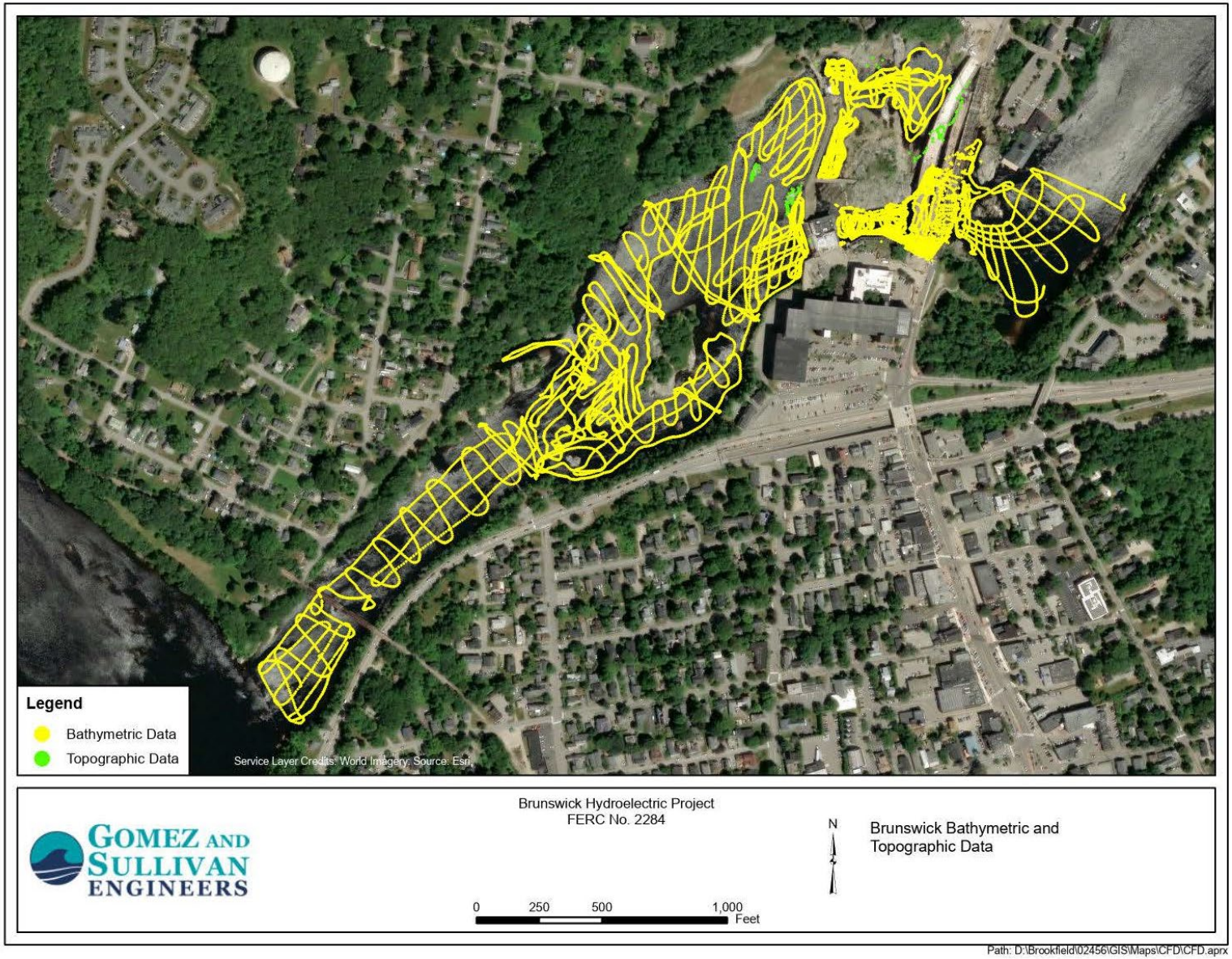
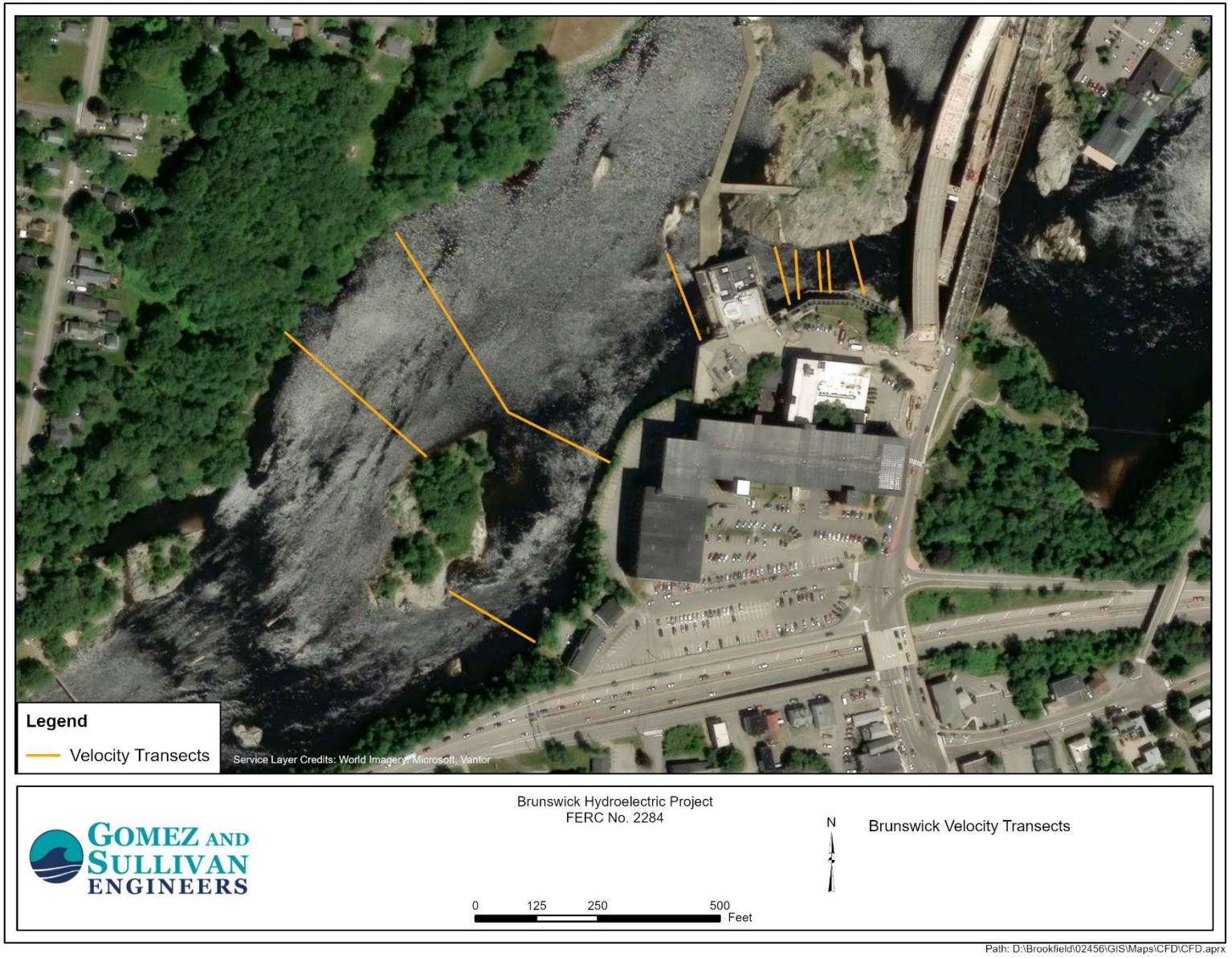


Figure 4.1-2: Brunswick Velocity Data Collection Transect Locations



4.2 CFD Model Development

Flow-3D is a general-purpose CFD software that employs numerical techniques to solve the equations of motion for fluids to obtain transient, three-dimensional (3D) solutions to multi-scale, multi-physics flow problems (Flow Science, 2025). Flow-3D solves the Reynolds Averaged Navier-Stokes (RANS) equations. Significant inputs for the models include geometry of the Project structures and surrounding terrain, the physical processes to be analyzed, and a computational mesh with boundary conditions. The following sections describe the model features used for simulations in this study.

4.2.1 Physical Geometry

The physical geometry of the Project structures (e.g., spillway, draft tubes, fish passage structures) was developed in a computer aided design (CAD) software, specifically AutoDesk® Civil 3D® 2020, Version 13.7.1276.0 Civil 3D 2025.2.1. The Project structure's physical geometry was developed as a 3D solid based on available Project drawings and field surveyed data, with a focus on the portions of the structure that affect the hydraulic flow characteristics. The physical geometry of the terrain was developed as a triangulated irregular network (TIN) using geographic information systems software, specifically the Environmental Systems Research Institute (ESRI) ArcGIS Pro Version 3.6.4 software. The TIN was developed using the June and September 2025 bathymetric and topographic data collected as part of this study, as well as a bathymetric data collected downstream of the Project under the Route 201 Bridge provided by Maine Department of Transportation (MaineDOT), and a 2020 Light Detection and Ranging (LiDAR) collection obtained from the United States Geological Survey (2026). Terrain breaklines were manually defined within the TIN to account for the location and elevation of Project structures. Additionally, manual modifications were made throughout the model validation process to improve simulation of hydraulics in the shoals area. ADCP collection efforts could not adequately capture the terrain within the shoals due to water depths that are too shallow to provide accurate ADCP data or not passable with a boat. Photos of this area from a time when the impoundment was drawn down show that multiple substantial bedrock vanes exist which direct flow towards the river left channel, as well as significant irregular channel bottom geometry due to the substrate (Figure 4.2.1-1). To adequately capture this area, a ridgeline was created in the TIN across the river right channel and connecting to the upstream end of Goat Island to represent the natural bedrock vanes and direct more flow towards the river left channel (Figure 4.2.1-2). Additionally, roughness was added in the river left and right channels to better represent the substrate roughness not captured due to limited ADCP information and the need for relatively large computational cell sizes (i.e., 8 feet) to reduce simulation time and increase model stability for the large-scale model described in Section 4.2.3. The roughness height for the river left and river right shoals was set to 6 feet and 9 feet, respectively. The roughness heights were developed using a Manning's roughness value of 0.105 that considers the substrate material (i.e., jagged and irregular rock cut), streamwise variation in cross section shape and size (i.e., channel split), and channel obstructions (i.e., bedrock vanes). This Manning's value was converted to a roughness height of approximately 6 feet based on a flow depth of 1.5 feet. This roughness height was increased by as much as three feet, which represents an approximate height of the bedrock vanes, since the TIN does not adequately capture

the undulating bedform[3]. The TIN was then brought into the CAD software to be extruded into a 3D solid. All of the 3D solids (i.e., Project structures and terrain) were initially developed using the National Geodetic Vertical Datum of 1929 (NGVD29)[4] and a projected coordinate system, specifically the Maine West Zone of the State Plane Coordinate System (SPCS) with its horizontal datum being the North American Datum of 1983 (NAD83) and linear unit being the United States Survey Foot. The 3D solids were rotated[5] within the CAD software to align the powerhouse with a coordinate axis which allows for a more efficient CFD analysis with regards to the required computational mesh spacing and the resulting computational time. Flow-3D requires physical geometry developed in other software to be saved in the Stereolithography format (STL) which does not recognize negative values in any coordinate direction. Since the invert elevation of the powerhouse draft tubes is less than elevation 0 feet, all 3D solids were vertically translated by +100 feet to obtain the vertical datum for the model coordinate system (MCS) within the CAD software prior to exporting them as STL files[6]. Finally, once imported into Flow-3D, the horizontal coordinates of the STL files were translated to improve the computational efficiency of the model[7].

Figure 4.2.1-3 depicts the physical geometry of the structures and terrain utilized for all scenarios analyzing existing conditions. The purpose of the physical geometry is to define the solid objects which may affect the flow of water in areas of interest. Accordingly, additional STL files were placed in some analyses to block out areas where water is not expected to go or where results are not required. Another STL was also added to not allow flow in the area downstream of the spillway just to the left of the powerhouse tailrace, as water level fluctuations in this shallow backwatered area caused significant model instability. These additional STL files increase model efficiency and decrease the computational time required to complete a model run without impacting pertinent results in the area of interest.

4.2.2 Physical Processes

The conditions being simulated within the CFD models represent complex flow conditions, which are controlled to varying extents by several physical processes. While some of the processes, such as gravity, are well understood and their effects can be computed directly and without significant computational effort, others, such as turbulence, are more complex and can only be approximated through computationally intensive processes. The Flow-3D software allows the selection of different sub-models for various physical processes, depending on the type of flow being simulated, and the specific information of interest, so that the dominant physical processes for the specific flow condition can be simulated without unnecessarily expending computational power to

[3] Mannings roughness values are bulk resistance coefficients that account for roughness, as well as other loss mechanisms such as form drag, secondary flows, and momentum losses. Ks is an "equivalent roughness height" and while mathematically appropriate for modeling, should not be physically interpreted as representing bathymetry at any scale.

[4] Some source data was provided in the North American Vertical Datum of 1988 (NAVD88), for which this study used an elevation conversion from NAVD88 to the NGVD29 of +0.646 feet (i.e., NGVD29 = NAVD88 + 0.646 feet.

[5] The 3D solids were rotated by -108.0271 degrees around a point located on the river right corner of the powerhouse, specifically 3,005,081.7491 feet East and 396,146.7223 feet North in the SPCS.

[6] The elevation conversion from NGVD29 to the MCS is +100 feet (i.e., MCS(Z) = NGVD29 + 100)

[7] The model would not run when using the large X and Y coordinates associated with the SPCS. As such, a translation of -3,005,081.7491 feet in the X-direction and -396,146.7223 feet in the Y-direction was utilized to convert from the SPCS to the MCS (i.e., MCS(X) = SPCS(X) - 3,005,081.7491 and MCS(Y) = SPCS(Y) - 396,146.7223).

model processes that have minimal impacts on the flow of interest. For these free surface flow CFD models, gravitational forces with viscosity, dynamically computed turbulence, and no-slip or partial slip wall shear boundary conditions were included in the simulations. A Renormalized Group (RNG) model was used to evaluate turbulence. These conditions were expected to have a significant impact on the flow patterns within the river, while other physical processes (e.g., air entrainment) are not expected to have an appreciable impact on information of interest.

The default fluid properties (e.g., density, viscosity) in Flow-3D for "Water at 20 C" were used for each model. The free water surfaces are simulated in Flow-3D using the Volume of Fluid (VOF) technique. This method models the free water surface by tracking the amount of fluid that is in each 3D cell over time. In other words, at any given time a cell can either be empty, full or partially full of water. Partially full cells contain the free water surface. The variable used to track this is called the fluid fraction. The VOF technique consists of three parts, a scheme to describe the shape and location of the free surface, a method to track the evolution of the shape and location of the free surface through time and space, and a means for applying boundary conditions to the free surface. The VOF method assumes a single fluid (water) and does not include the movement of the air above the water. For this study, it was assumed that the air has no significant effect on the movement of the water and as such it was neglected. The default Flow-3D VOF solver options were used for each model.

4.2.3 Computational Mesh and Boundary Conditions

In Flow-3D, a fully structured computational grid is applied to the solid models to create the computational domain (i.e., the area where fluid flow is analyzed). Flow-3D uses the Fractional Area/Volume Obstacle Representation (FAVOR) method to block out parts of the computational domain (volumes and areas) that are obstructed by the solid models (e.g., below the bathymetric surface, within the powerhouse superstructure). An appropriate computational grid setup is required to reasonably predict hydraulic conditions in a CFD model. The computational grid is created by one or more mesh blocks that are aligned with either a Cartesian or Cylindrical coordinate system. In general, a smaller grid cell size provides more accurate solutions, but also increases the time to obtain a reasonable solution. If multiple mesh blocks are used, they can either abut one another, or one mesh block can be partially or completely contained within another (i.e., nested meshes). Flow-3D generally prefers adjacent grids of different sizes to be at a 2:1 ratio for mass balance purposes (e.g., 4-foot cells transitioning to 2-foot cells or 8-foot cells).

CFD models require boundary conditions at all edges of all mesh blocks to perform the flow computations. With nested meshes, where a finer mesh is embedded inside a larger area coarser mesh, the boundary conditions for the finer mesh are defined by the results from the coarser mesh. When the finer mesh is within the same model as the coarser mesh, these are referred to as symmetry boundaries in Flow-3D, which assumes that the same flow conditions occur on either side of the boundary (i.e., there are no gradients in the values computed by the model across the boundary). As such, the model has one mesh which completely contains all other meshes, and boundary conditions are only required for the outmost computational mesh. Similarly, when an entire model is nested within a larger model, a Grid Overlay boundary can be used in Flow-3D, to utilize the computational results from the larger model to define the boundary conditions for the nested model. The forebay model and tailrace model each consist of two models (i.e., large-scale and small-scale). The large-scale model uses relatively large cells to evaluate flow patterns over a

larger extent, while the small-scale model is nested inside the large-scale model and uses smaller cells to evaluate flow patterns near fishway entrances and exits in more detail. The mesh configuration, including cell sizes and areas of refinement, was assessed and refined as part of the model validation process. The following sections provide a description of the final mesh configuration for the forebay and tailrace models.

Forebay Model

A large-scale model[8] was developed from the Androscoggin Swinging Bridge to approximately 100 feet downstream of the powerhouse covering the entire width of the river, while a small-scale model was developed from approximately 540 feet upstream of the powerhouse to 28 feet into the powerhouse covering the entire river right bank to approximately 6 feet out from the river left edge of the powerhouse As shown in Figure 4.2.3-1, the large-scale model used 8-foot cells to reduce computational run time and improve model stability, while the small-scale model used 2-foot cells.

Unique boundary conditions were only required on the edges of the 8-foot mesh block for the large-scale forebay model, as the 2-foot cells for the small-scale model utilized grid overlay boundaries which utilize results from the large-scale model. As a reminder, the x-axis is parallel to the face of the powerhouse (positive in the right-to-left direction, looking downstream), the y-axis is perpendicular to the face of the powerhouse (positive in the upstream direction), and the z-axis is oriented with gravity acting in the negative-z direction. The X Min (river right) and X Max (river left) boundaries in the 8-foot mesh block are far enough from the river that no flow is expected to cross these boundaries for the range of flows analyzed in this study. As such, these boundaries were defined as symmetry boundaries (i.e., no gradients across the boundary). The Z Min boundary is located below the lowest ground elevations and was set as a wall, since no flow would pass through the boundary. The Z Max boundary is located above the expected WSEL for the range of flows analyzed and was set as a pressure boundary with a fluid fraction of zero (i.e., atmospheric conditions). The Y Max boundary is located above Goat Island near the Androscoggin River Swinging Bridge, and acts as the inflow boundary to the model. As such, the Y Max boundary was set as a volume flow rate boundary. The boundary sets the inflow discharge and computes the fluid elevation using an automatic flow natural inlet boundary. The flow direction vector was set such that flow is in the streamwise direction, perpendicular to the river cross section. The Y Min (downstream) boundary was set as a rating curve with a wide flow range and a very narrow fluid elevation range to allow for model stability. Default water properties (e.g., density and viscosity) in Flow-3D were used for the Forebay Models.

Tailrace Model

A large-scale model was developed from the middle of the powerhouse to approximately 1,000 feet downstream of the powerhouse covering the entire width of the river, while a small-scale model was developed from near the upstream face of the powerhouse to approximately 400 feet downstream of the powerhouse. As shown in Figure 4.2.3-2, the large-scale model used a combination of 8-foot and 4-foot cells, while the small-scale model used 2-foot cells.

Unique boundary conditions were required on the edges of the 8-foot cell mesh block in the large-scale model and 2-foot cell mesh block for the small-scale model, as the 4-foot cell mesh block of

[8] The term model refers to a separate model entirely with different boundaries and input conditions. Computational meshes or mesh refinement regions are separate meshes within a particular model that have different cell sizes.

the large-scale model utilizes results from the 8-foot cells mesh block in the large-scale model. The X Min (river right) and X Max (river left) boundaries for the large-scale and small-scale models were defined as symmetry boundaries (i.e., no gradients across the boundary) as no flow is expected to cross these boundaries for the range of flows analyzed in this study. The Z Min boundary for the large-scale and small-scale models is located below the lowest ground elevations and was set as a wall, since no flow would pass through the boundary. The Z Max boundary for the large-scale and small-scale models is located above the expected WSEL for the range of flows analyzed and was set as a pressure boundary with a fluid fraction of zero (i.e., atmospheric conditions). The Y Max boundary was defined as a symmetry boundary for the large-scale model and a wall boundary for the small-scale model. No flow is expected across the Y Max boundary for either model. For the large-scale model, the Y Min (downstream) boundary is located approximately 1,000 feet downstream of the powerhouse. This area is tidally influenced but would have a constant fluid elevation over the time scale of the model. As such, the Y Min boundary was set as a rating curve with a wide flow range and a very narrow fluid elevation range, which keeps the fluid elevation in the required range while also allowing a wider range of flow magnitudes to pass without causing instability. Additionally, a 16-foot wave absorbing component was added near the downstream end of the large-scale model to reduce instabilities caused by the multiple shallow backwatered areas within the large-scale model domain. A wave absorbing component smooths fluid elevation instability across the width of the component so that no waves exist on the downstream side of the component. For the small-scale model, the Y Min (downstream) boundary was defined as a grid overlay boundary which utilizes results from the large-scale model.

4.2.4 Flow Sources

Forebay Model

While there are multiple distinct flow structures (upstream fishway, downstream fishway, units 1, 2, and 3), the cell size in the large-scale forebay model does not adequately capture the geometry for all the flow structures. Therefore, a single flow source was used to represent flow into the powerhouse (i.e., through turbines and fish passage structures). Flow from this source was simulated using a mass-momentum source, which assumes a uniform flow distribution from the area defining the flow source. The flow source is located approximately 56 feet upstream of the face of the powerhouse.

The small-scale forebay model includes five flow sources to represent flow through the upstream fishway, downstream fishway, and units 1, 2, and 3. Flow from these sources was simulated using mass momentum sources. The flow sources are located on the upstream face of the powerhouse, or slightly inside the unit intakes. The location and orientation of the flow sources for the large-scale and small-scale forebay model are depicted in Figure 4.2.4-1.

Tailrace Model

The large-scale and small-scale tailrace model includes five flow sources, including the upstream fishway, downstream fishway, and units 1, 2, and 3. Flow from these sources were simulated using mass momentum sources. All flow sources are located on the downstream face of the powerhouse for the large-scale model, while the unit flow sources are located slightly inside the unit intakes for the small-scale model to better simulate the rotational flow patterns created as flow travels through the turbine scroll case. The location and orientation of the flow sources for the large-scale and small-scale tailrace model is depicted in Figure 4.2.4-2. The flow sources consist of freshwater

and thus default water properties (e.g., density and viscosity) in Flow-3D were used for the Tailrace Models.

Figure 4.2.1-1: Shoals Area Bedrock Formations



Photo from Channel showing Roughness in Left Channel



Photo From Shore showing Large Hydraulic Drop in Right Channel

Figure 4.2.1-2: Manual Terrain Adjustments in Shoals Area Between Swinging Bridge and Goat Island



Figure 4.2.1-3: Overview of Physical Geometry

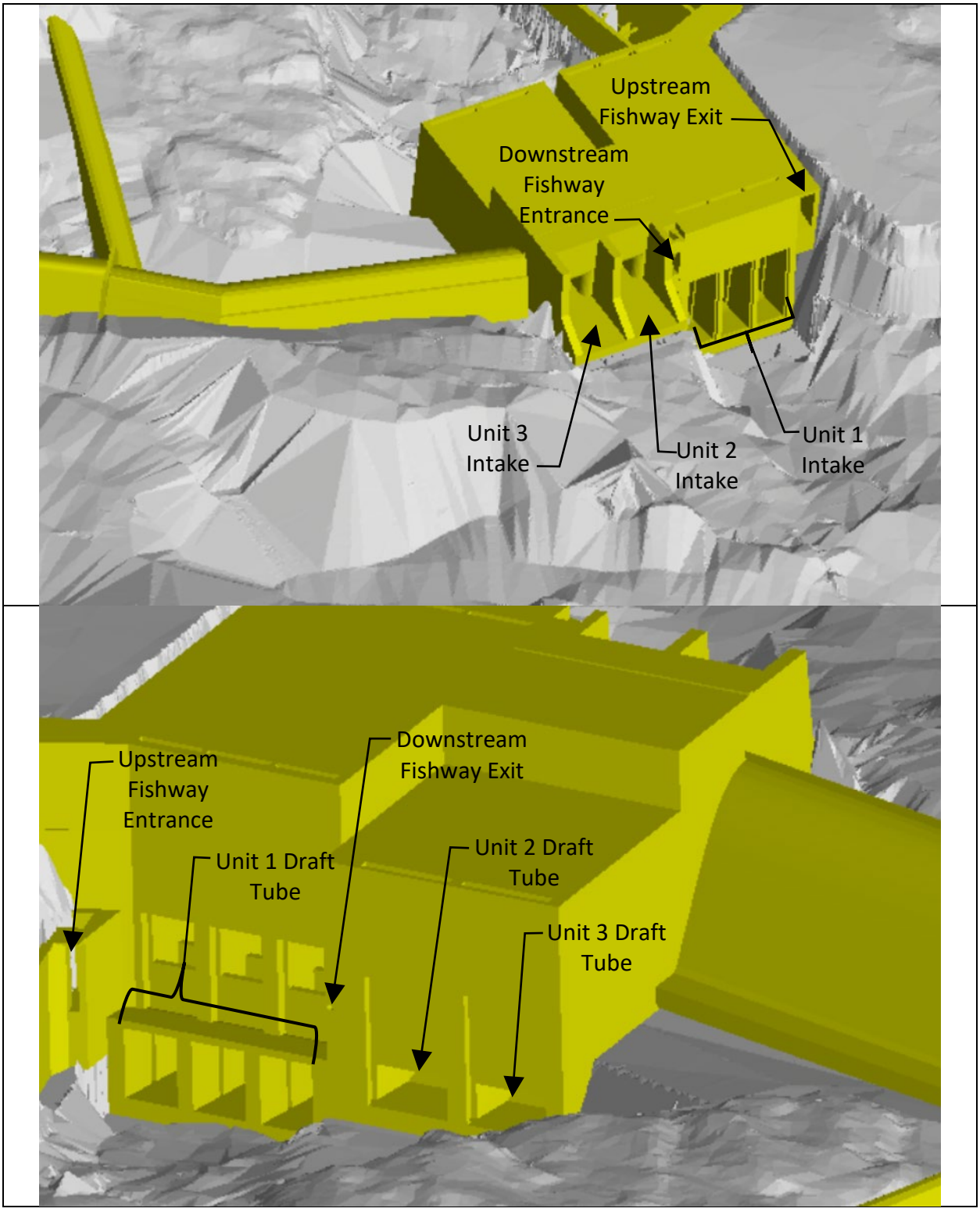


Figure 4.2.3-1: Forebay Model Computational Mesh Layout



Figure 4.2.3-2: Tailrace Model Computational Mesh Layout

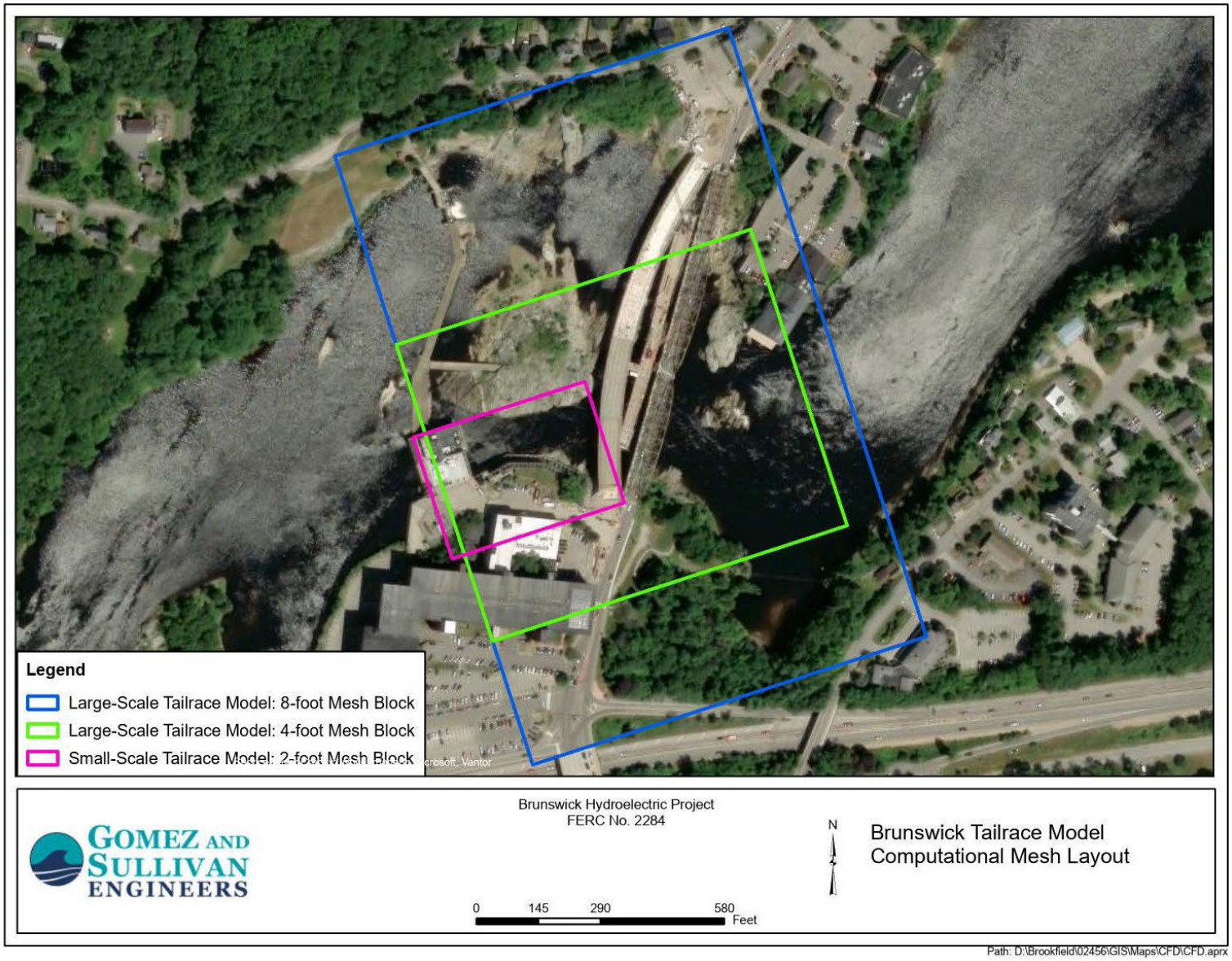
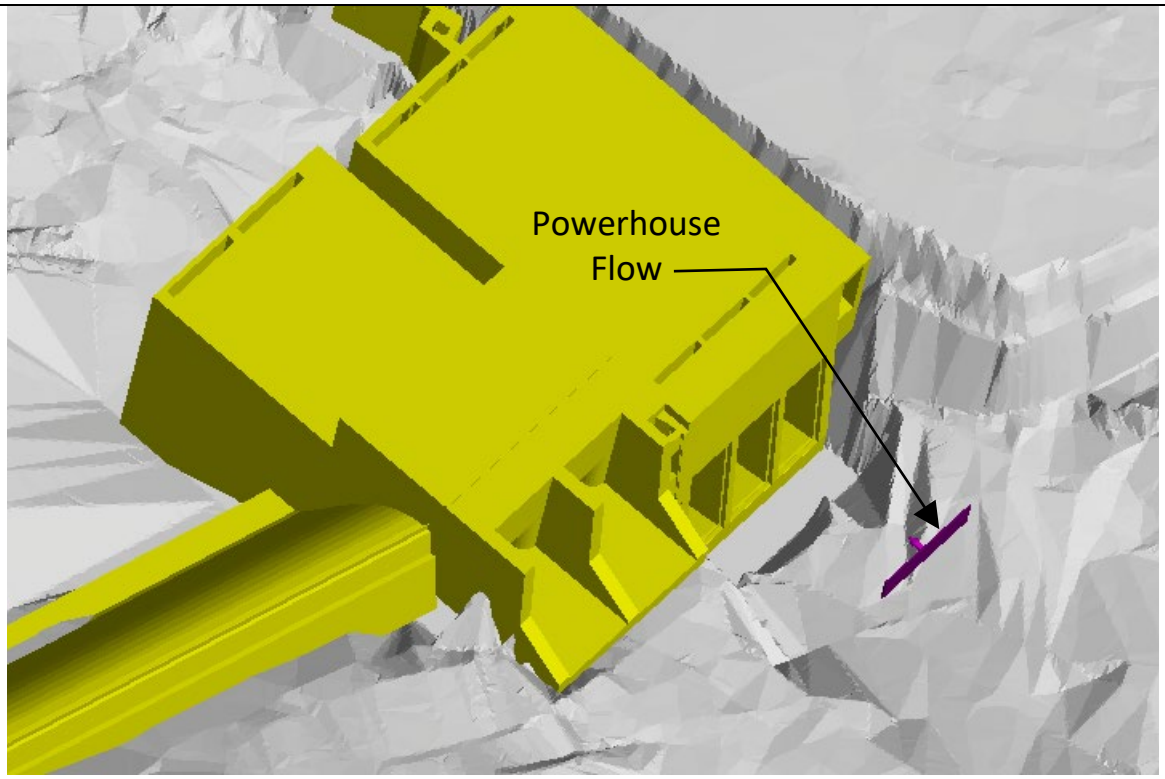
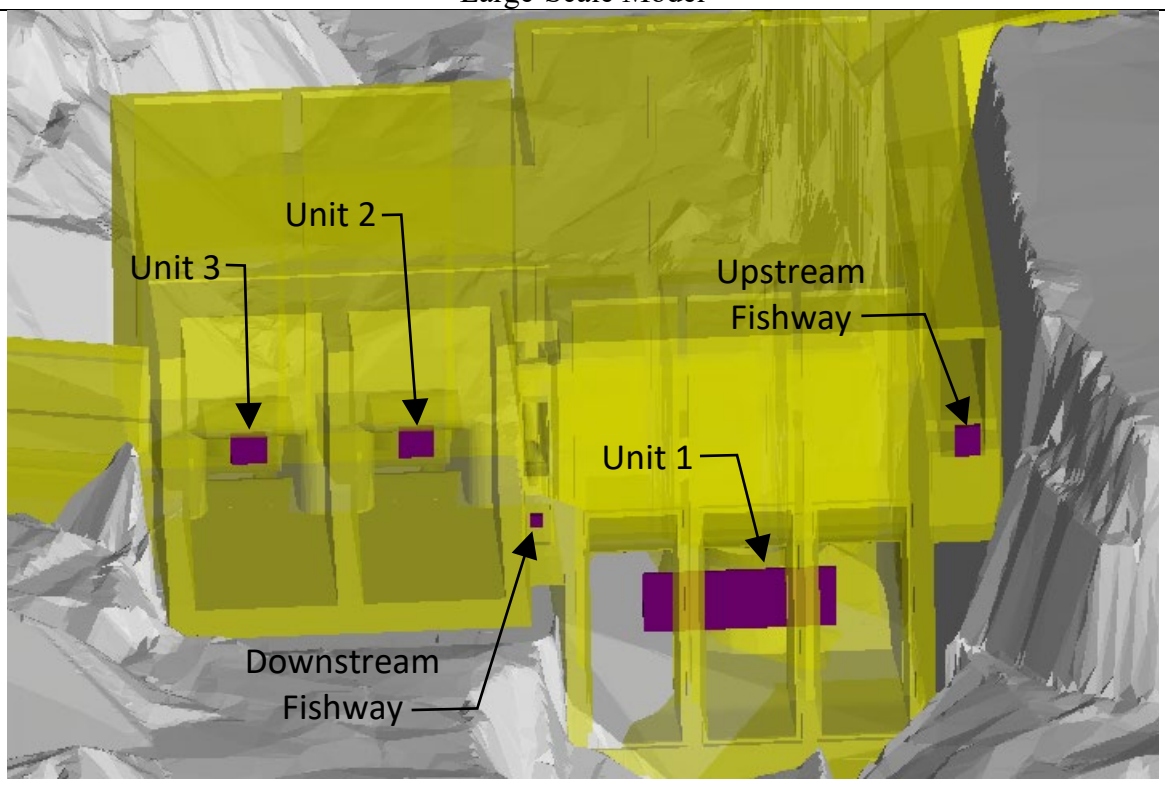


Figure 4.2.4-1: Forebay Model Flow Source Location and Orientation

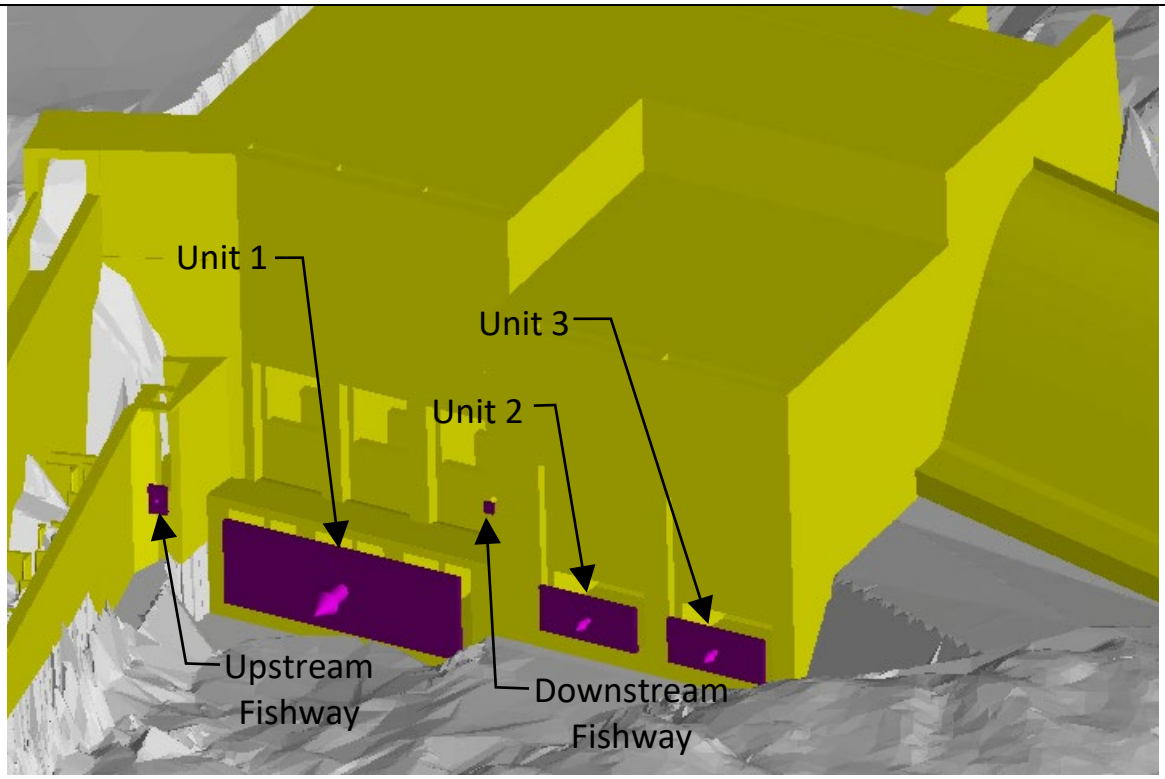


Large-Scale Model

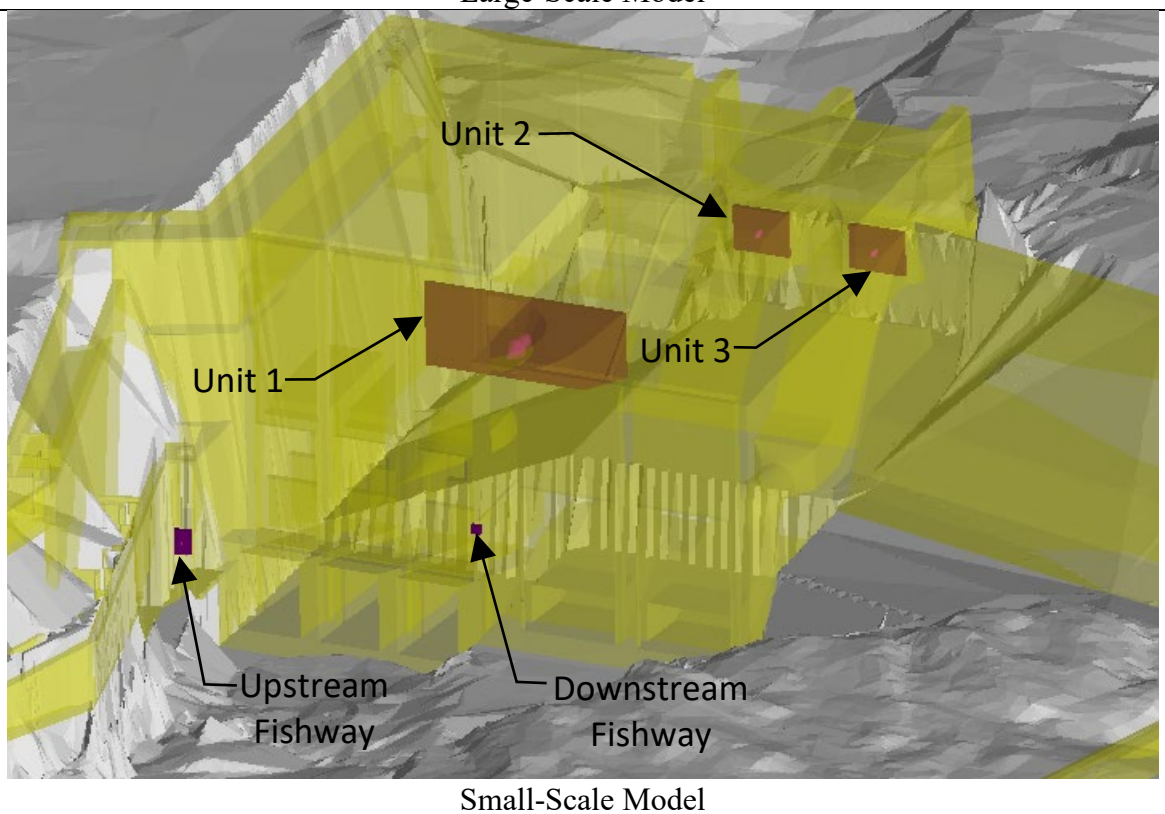


Small-Scale Model

Figure 4.2.4-2: Tailrace Model Flow Source Location and Orientation



Large-Scale Model



Small-Scale Model

4.3 2D Model Development

The Hydrologic Engineering Center's River Analysis System (HEC-RAS) is a hydraulic modeling software developed by the U.S. Army Corps of Engineers that simulates one- and two-dimensional free-surface flow in rivers and floodplains. In 2D applications, HEC-RAS solves the depth-averaged shallow water equations (i.e., SWE or Saint-Venant equations) to compute unsteady flow, WSELs, and velocity fields across a computational grid. Key model inputs include high-resolution terrain data, representation of hydraulic structures, specification of boundary conditions, and selection of computational mesh parameters. The following sections describe these model inputs and setup for a bypass channel model. All spatial data for the bypass channel model were referenced to the Maine West Zone of the SPCS with its horizontal datum being NAD83 and linear unit being the United States Survey Foot while the vertical datum used for the bypass channel model was NGVD29. The model domain extent was selected to include all areas relevant to the analysis, starting at the Tainter gates and continuing downstream of the falls where the river left channel connects to the tailrace, encompassing all water and overbank areas in the region as shown in Figure 4.3-1.

4.3.1 Physical Geometry

The physical geometry for the Project was developed using terrain data and hydraulic structure representations suitable for use in 2D HEC-RAS. The TIN for the bypass channel model is the same TIN used in the CFD model with one change: the spillway and tainter gate structures were added by adjusting the terrain elevations using terrain breaklines based on Project drawings and field surveyed data (these structures were captured in the CFD model using STL files developed separately from the terrain). The TIN was then converted to a raster file (i.e., .tiff), and the processed terrain was imported into HEC-RAS via the RAS Mapper. Figure 4.3.1-1 depicts the terrain surface used for all scenarios analyzed.

4.3.2 Physical Processes

The Saint-Venant equations account for conservation of mass and momentum and are appropriate for representing unsteady flow conditions in rivers and floodplains, as well as across hydraulic structures. HEC-RAS can resolve several physical processes (e.g., gravity, channel friction, and turbulence) during simulations. HEC-RAS 2D does not explicitly resolve three-dimensional turbulence or air-water interactions; instead, these processes are approximated through depth-averaged formulations and empirical parameters. Given the scope and objectives of this study, these assumptions are appropriate and consistent with standard hydraulic modeling practice. Bed resistance was represented using Manning's roughness coefficients. The Manning's roughness coefficient for the model was set to a value of 0.04, which is a common value for a bedrock channel.

Default water properties (e.g., density and viscosity) in HEC-RAS were used for this study. The SWE were solved using a 0.5 second timestep and Eulerian-Lagrangian approach, which uses finite volume numerical methods. Otherwise, the model used default computational settings.

4.3.3 Computational Mesh and Boundary Conditions

HEC-RAS requires that a computational mesh be developed within the 2D flow area. The mesh is composed of polygonal cells, with each cell having up to eight sides (i.e., faces), for which the

model computes flow across each cell face. The 2D flow area mesh for this study was developed within RAS Mapper. Cell size and refinement were developed as part of model validation to balance computational efficiency, model stability, and reasonable solutions for WSEL and velocity. Cell size was generally set to 25 feet for the entire model. A cell size larger than 25 feet was required in the vicinity of the natural falls to improve model stability when computing flow over the falls. Mesh breaklines were used to improve mesh alignment and better simulate flow patterns around key hydraulic control features within the terrain such as the natural falls at the bottom of the bypass channel, natural narrow locations of the channel, and sections of the Tainter gate structure. Boundary conditions were applied at the edges of the 2D flow area to define inflow and outflow conditions. Upstream boundary conditions were specified using flow hydrographs, representing flow through the Tainter gates. Downstream boundary conditions were specified using a stage hydrograph set to a constant water surface elevation to represent tidal conditions. Figure 4.3.3-1 shows the final computational mesh with mesh breakline and boundary condition locations.

Figure 4.3-1: Bypass Channel Model Area

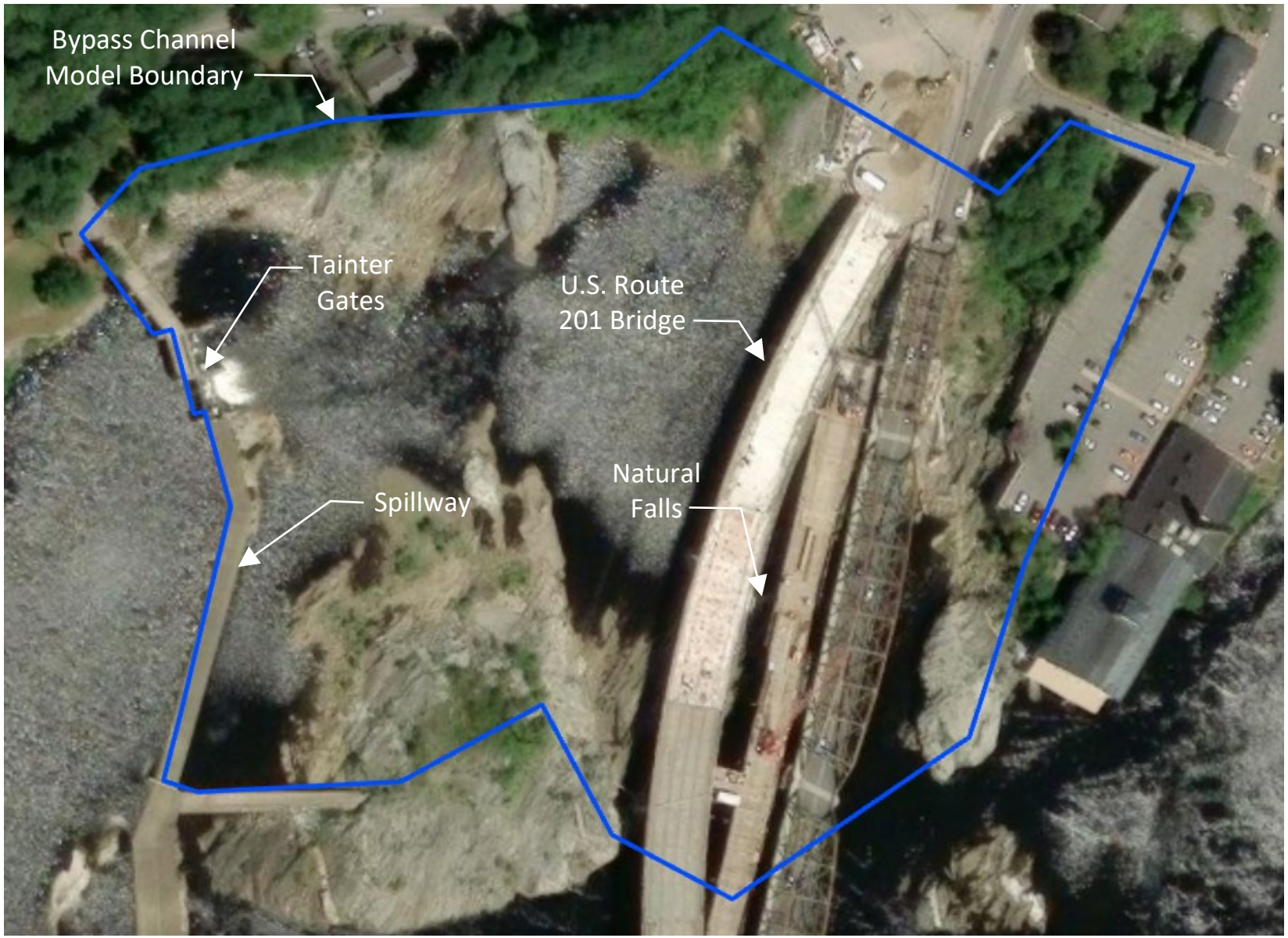


Figure 4.3.1-1: Terrain Surface Used for Bypass Channel Model

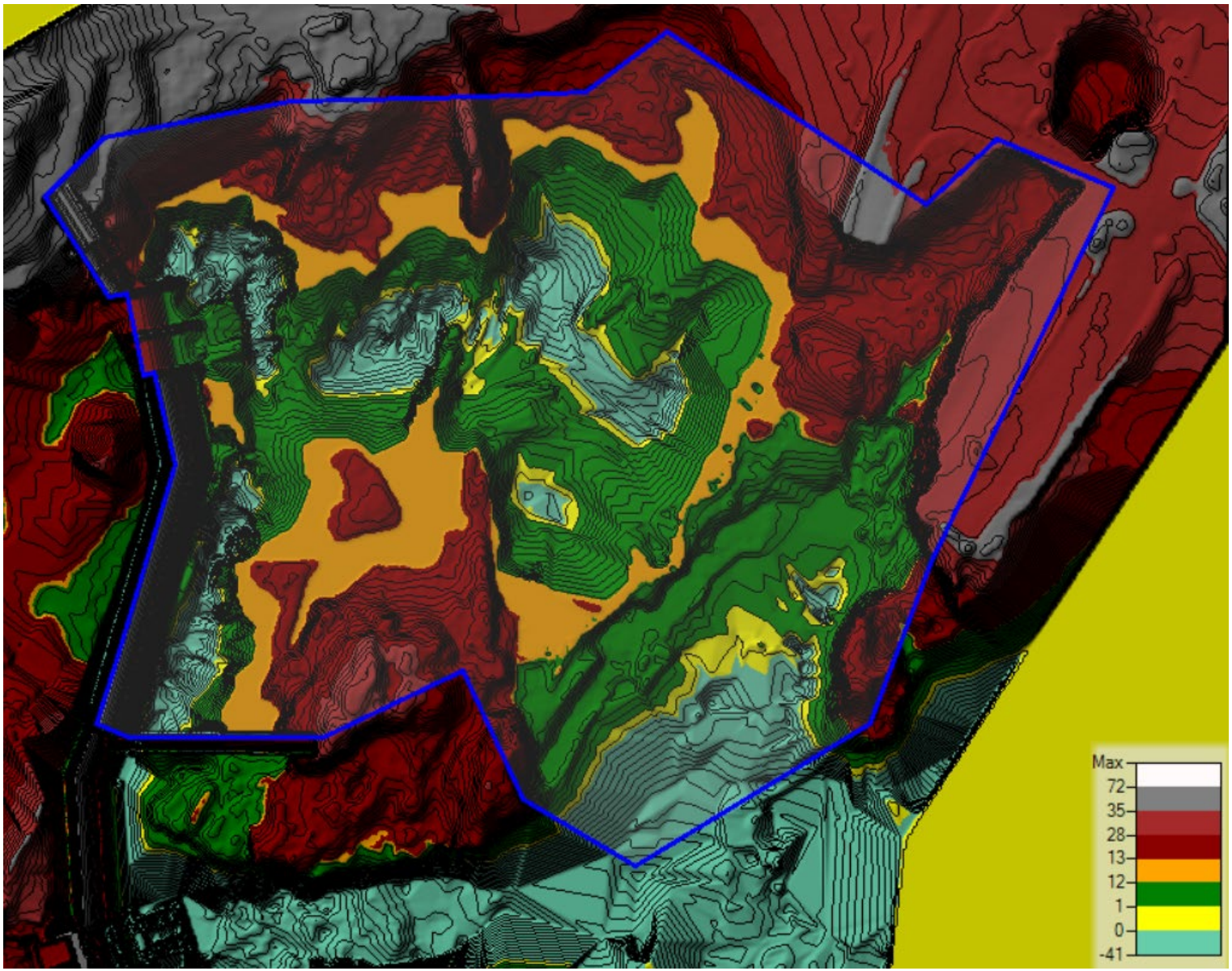
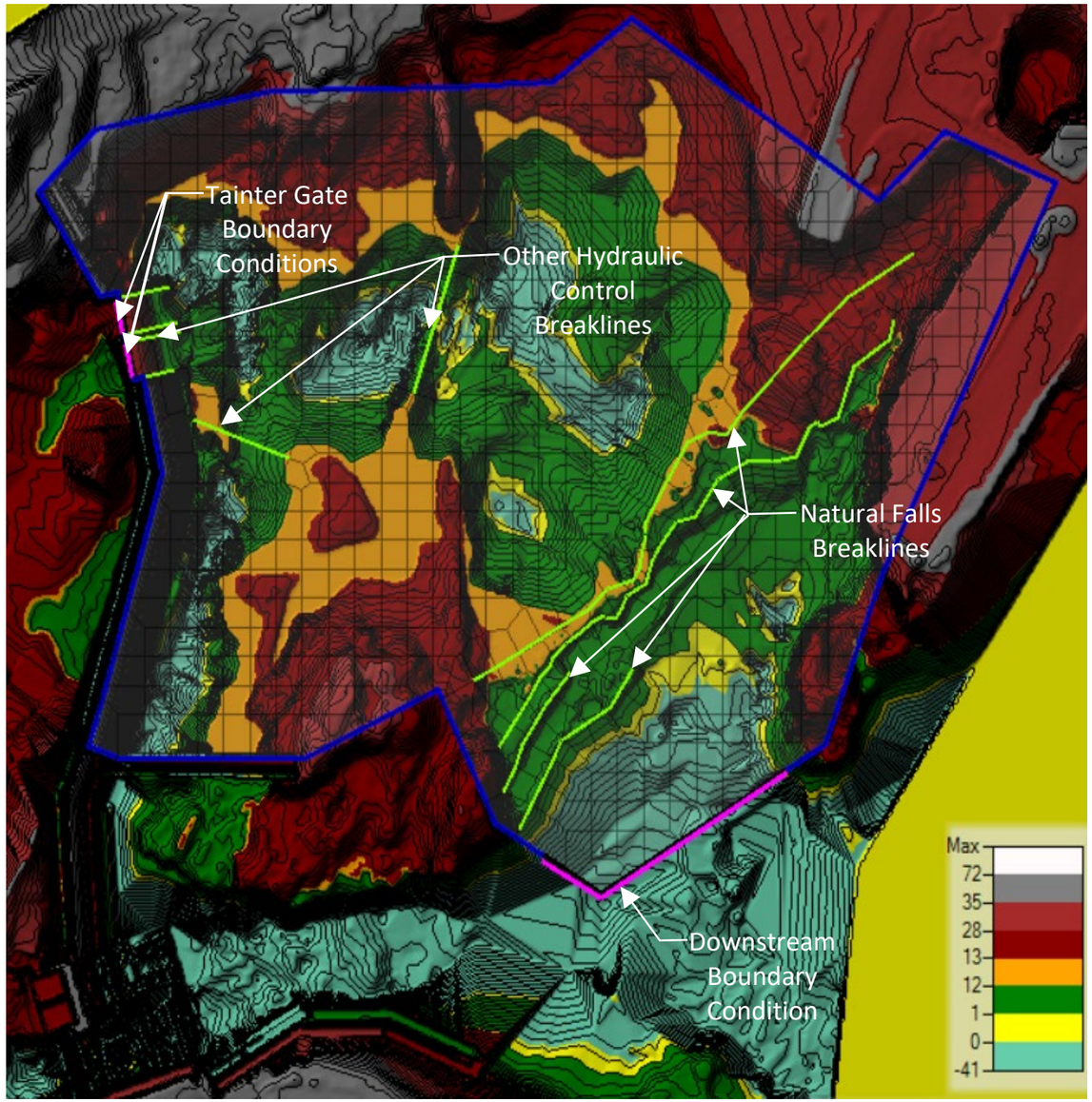
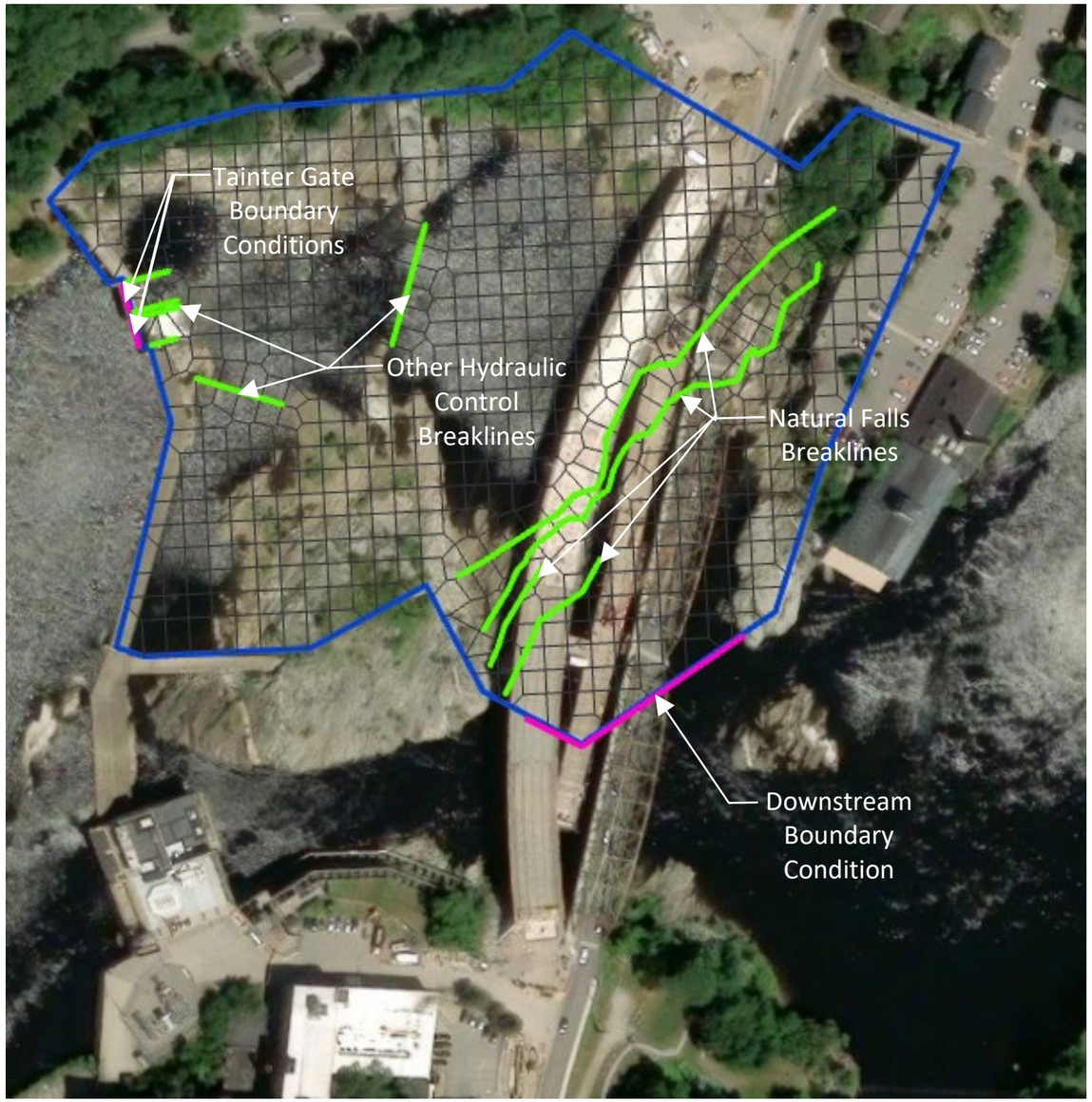


Figure 4.3.3-1: Bypass Channel Model Mesh and Boundary Conditions





5.0 SIMULATIONS

To quickly identify different simulations, a naming convention has been developed which denotes the model, simulation type, simulation number, and if applicable the sub model. The model will be designated as either FB for Forebay or TR for Tailrace for the CFD models and BC for the Bypass Channel model. The simulation type will be designated as either V for validation, or P for production. The simulation number is a sequential numeric designation. Therefore, the first validation simulation for the forebay model would be identified as FB_V-01.

5.1 Model Validation

Model validation is a process used to identify whether the model appropriately represents real world conditions. Flows, WSELs, and velocities collected in June 2025 were used to validate the various models. Field collected data was used to evaluate model performance (e.g., WSELs and velocity distribution), while field collected and operations data were used to define inputs into the models (e.g., flows and initial water levels). Events were chosen for validation of each model, where applicable, based on the river conditions observed during data collection. For the Forebay and Tailrace models, validation of the large-scale model was completed before the small-scale models so that the results from the large-scale model could be used as the boundary conditions for the small-scale model. A summary of conditions for each validation run are provided in Table 5.1-1.

5.1.1 Forebay Model

Three validation runs were completed for the forebay model as described in the following sections.

FB_V-01

The purpose of the first forebay model validation run was to verify the relative hydraulic drop through the shoals area and the flow split around Goat Island under the conditions observed during impoundment bathymetry collection on 6/26/2025. During impoundment bathymetry collection, Unit 1 was operating at approximately 3,289 cfs, Units 2 and 3 were not operating, and the upstream and downstream fishways were operating normally (100 cfs and 20 cfs, respectively), resulting in a total river flow of 3,409 cfs. Therefore, discharge for the upstream boundary condition (i.e., Y Max boundary) and the powerhouse mass source in the large-scale model were set to 3,409 cfs. All other boundary conditions for the large-scale model were defined as described in Section 4.2.3. A small-scale model was not simulated for this validation run.

FB_V-02

The purpose of the second forebay model validation run was to verify the flow split around Goat Island and simulated velocities under the conditions observed during impoundment velocity transect collection on 6/27/2025. During impoundment velocity transect collection, Unit 1 was operating at approximately 2,281 cfs, Units 2 and 3 were not operating, and the upstream and downstream fishways were operating normally (100 cfs and 20 cfs, respectively), resulting in a total river flow of 2,401 cfs. Therefore, discharge for the upstream boundary condition (i.e., Y Max boundary) and the powerhouse mass source in the large-scale model were set to 2,401 cfs. All other boundary conditions for the large-scale model were defined as described in Section 4.2.3. A small-scale model was not simulated for this validation run.

FB_V-03

The purpose of the third forebay model validation run was to verify simulated velocities under the conditions observed during intake velocity transect collection on 6/25/2025. During collection, Unit 1 was operating at approximately 2,563 cfs, Units 2 and 3 were not operating, and the upstream and downstream fishways were operating normally (100 cfs and 20 cfs, respectively), resulting in a total river flow of 2,683 cfs. Therefore, discharge for the upstream boundary condition (i.e., Y Max boundary) and the powerhouse mass source in the large-scale model was set to 2,683 cfs. All other boundary conditions for the large-scale model were defined as described in Section 4.2.3. As described in Section 4.2.3, results from the large-scale model run are used as the boundary conditions for the small-scale model. The discharge for each mass source in the small-scale model were set to the reported flows described above.

5.1.2 Tailrace Model

Two validation runs were completed for the tailrace model as described in the following sections.

TR_V-01

The purpose of the first tailrace model validation run was to verify the relative hydraulic drop under the conditions observed during tailrace bathymetry collection on 6/26/2025. During collection, Unit 1 was operating at approximately 3,289 cfs, Units 2 and 3 were not operating, and the upstream and downstream fishways were operating normally (100 cfs and 20 cfs, respectively), resulting in a total river flow of 3,409 cfs. Therefore, the discharge for each mass source in the large-scale model was set to the reported flows described above. The rating curve for the downstream boundary condition (i.e., Y Min boundary) was set to maintain a water level near that observed during tailrace bathymetry collection. All other boundary conditions for the large-scale model were defined as described in Section 4.2.3. A small-scale model was not simulated for this validation run.

TR_V-02

The purpose of the second tailrace model validation run was to verify simulated velocities under the conditions observed during tailrace velocity transect collection on 6/26/2025. During collection, Unit 1 was not operating, Unit 2 was operating at approximately 1,419 cfs, Unit 3 was operating at approximately 1,392 cfs, and the upstream and downstream fishways were operating normally (100 cfs and 20 cfs, respectively), resulting in a total river flow of 2,931 cfs. Therefore, the discharge for each mass source in the large-scale model was set to the reported flows described above. The rating curve for the downstream boundary condition (i.e., Y Min boundary) was set to maintain a water level near that observed during tailrace velocity transect collection. All other boundary conditions for the large-scale model were defined as described in Section 4.2.3. All boundary conditions for the small-scale model were defined as described in Section 4.2.3, including using results from the large-scale model run to define the downstream boundary condition (i.e., Y Min boundary). The discharge for each mass source in the small-scale model was set to the reported flows described above.

5.1.3 Bypass Channel Model

Safety measures during field work precluded flow from being released into the bypass channel during data collection efforts within the bypass channel model extents. Therefore, no model validation runs were completed for the bypass channel model.

Table 5.1-1: Summary of Validation Run Simulation Conditions

Run Name	Scale	Total Flow (cfs)	Unit 1 Flow (cfs)	Unit 2 Flow (cfs)	Unit 3 Flow (cfs)	Gate 1 Flow (cfs)	Gate 2 Flow (cfs)	Upstream Fishway (cfs)	Downstream Fishway (cfs)	Headpond (feet, NGVD29)	Tailwater (feet, NGVD29)
FB_V-01	Large	3,409	3,289	0	0	-	-	100	20	38.76	-
FB_V-02	Large	2,401	2,281	0	0	-	-	100	20	38.93	-
FB_V-03	Small	2,683	2,563	0	0	-	-	100	20	38.98	-
TR_V-01	Large	3,409	3,289	0	0	-	-	100	20	-	5.31
TR_V-02	Small	2,931	0	1,419	1,392	-	-	100	20	-	2.36

5.2 Production Runs

A production run models a particular operating scenario or change in the Project's operations or structures to inform the evaluation of fish passage conditions at the Project. An initial set of production runs were developed to bracket the range of existing conditions. Additional production runs detailing alternative conditions will be developed later based on the results of the Upstream and Downstream Passage Alternatives Study. Various production runs were developed based on hydraulic capacities and operating levels as summarized in Table 5.2-1. Unit 1 can operate over a range of flows, while Units 2 and 3 have a single operating flow. The maximum discharge through both taintor gates when they are fully open under a normal headpond condition is approximately 14,500 cfs. The upstream and downstream fish passage facilities have a single operating flow. The Project operates in a run-of-river mode with headpond fluctuations of no more than 2 feet. The normal tailwater elevation at the Project is 2.5 feet, NGVD29. The closest tidal gage to the Project is in Portland, ME (NOAA Station 8418150), which has a 116-year period of record. The official daily normal and high tides, as well as the king tide, are currently based on an 18-year epoch running from 1983-2001. Daily high tides at this gage are approximately 5.0 feet higher than the daily mean tide, with the king tide and maximum reported tide being approximately 7.0 feet and 9.6 feet higher than the daily mean tide, respectively. A summary of the conditions simulated for each production run are provided in Table 5.2-2 and are further detailed below.

5.2.1 Forebay Model

FB_P-01

The purpose of the first forebay model production run was to provide results for the maximum operating flow for the Project (7,595 cfs), with Unit 1 operating at approximately 5,075 cfs, Units 2 and 3 operating at 1,200 cfs each, and the upstream and downstream fishways operating normally (100 cfs and 20 cfs, respectively). Therefore, discharge for the upstream boundary condition (i.e., Y Max boundary) and the powerhouse mass source in the large-scale model were set to 7,595 cfs. All other boundary conditions for the large-scale model were defined as described in Section 4.2.3. As described in Section 4.2.3, results from the large-scale model run are used as the boundary conditions for the small-scale model. The discharge for each mass source in the small-scale model were set to the flows described above.

FB_P-02

The purpose of the second forebay model production run was to provide results for the minimum operating flow for the Project (1,320 cfs), with Units 1 and 3 not operating, Unit 2 operating at 1,200 cfs, and the upstream and downstream fishways operating normally (100 cfs and 20 cfs, respectively). Therefore, discharge for the upstream boundary condition (i.e., Y Max boundary) and the powerhouse mass source in the large-scale model were set to 1,320 cfs. All other boundary conditions for the large-scale model were defined as described in Section 4.2.3. As described in Section 4.2.3, results from the large-scale model run are used as the boundary conditions for the small-scale model. The discharges for each mass source in the small-scale model were set to the flows described above.

5.2.2 Tailrace Model

TR_P-01

The purpose of the first tailrace model production run was to provide results for the maximum operating flow for the Project (7,595 cfs), with Unit 1 operating at approximately 5,075 cfs, Units

2 and 3 operating at 1,200 cfs, and the upstream and downstream fishways operating normally (100 cfs and 20 cfs, respectively). Therefore, the discharge for each mass source in the large-scale model was set to the flows described above. The rating curve for the downstream boundary condition (i.e., Y Min boundary) was set to maintain a water level representing a normal tailwater elevation. All other boundary conditions for the large-scale model were defined as described in Section 4.2.3. All boundary conditions for the small-scale model were defined as described in Section 4.2.3, including using results from the large-scale model run to define the downstream boundary condition (i.e., Y Min boundary). The discharge for each mass source in the small-scale model was set to the flows described above.

TR_P-02

The purpose of the second tailrace model production run was to provide results for the minimum operating flow for the Project (1,320 cfs), with Units 1 and 3 not operating, Unit 2 operating at 1,200 cfs, and the upstream and downstream fishways operating normally (100 cfs and 20 cfs, respectively). Therefore, the discharge for each mass source in the large-scale model was set to the flows described above. The rating curve for the downstream boundary condition (i.e., Y Min boundary) was set to maintain a water level representing a normal tailwater elevation. All other boundary conditions for the large-scale model were defined as described in Section 4.2.3. All boundary conditions for the small-scale model were defined as described in Section 4.2.3, including using results from the large-scale model run to define the downstream boundary condition (i.e., Y Min boundary). The discharge for each mass source in the small-scale model was set to the flows described above.

5.2.3 Bypass Channel Model

BC_P-01

This production run considered 50 cfs through Gate 1, 50 cfs through Gate 2, and a tailwater elevation of 2.5 feet, NGVD29.

BC_P-02

This production run considered 1,812.5 cfs through Gate 1, 1812.5 cfs through Gate 2, and a tailwater elevation of 2.5 feet, NGVD29.

BC_P-03

This production run considered 3,625 cfs through Gate 1, 3,625 cfs through Gate 2, and a tailwater elevation of 2.5 feet, NGVD29.

BC_P-04

This production run considered 5,437.5 cfs through Gate 1, 5,437.5 cfs through Gate 2, and a tailwater elevation of 2.5 feet, NGVD29.

BC_P-05

This production run considered 7,250 cfs through Gate 1, 7,250 cfs through Gate 2, and a tailwater elevation of 2.5 feet, NGVD29.

Table 5.2-1: Summary of Hydraulic Capacities and Operating Levels

Parameter	Unit 1 Flow (cfs)	Unit 2 Flow (cfs)	Unit 3 Flow (cfs)	Gate 1 Flow (cfs)	Gate 2 Flow (cfs)	Upstream Fishway Flow (cfs)	Downstream Fishway Flow (cfs)	Headpond (feet, NGVD29)	Tailwater (feet, NGVD29)
Minimum	2,741	1,200	1,200	-	-	-	-	37.4	-
Normal	-	-	-	-	-	100	20	39.4	2.5
Maximum	5,075	1,200	1,200	7,250	7,250	-	-	-	-

Table 5.2-2: Summary of Production Run Simulation Conditions

Run Name	Scale	Total Flow (cfs)	Unit 1 Flow (cfs)	Unit 2 Flow (cfs)	Unit 3 Flow (cfs)	Gate 1 Flow (cfs)	Gate 2 Flow (cfs)	Upstream Fishway Flow (cfs)	Downstream Fishway Flow (cfs)	Headpond (feet, NGVD29)	Tailwater (feet, NGVD29)
FB_P-01	Large	7,595	5,075	1,200	1,200	-	-	100	20	39.4	-
FB_P-02	Small	1,320	0	1,200	0	-	-	100	20	39.4	-
TR_P-01	Large	7,595	5,075	1,200	1,200	-	-	100	20	-	2.5
TR_P-02	Small	1,320	0	1,200	0	-	-	100	20	-	2.5
BC_P-01	-	100	-	-	-	50	50	-	-	-	2.5
BC_P-02	-	3,625	-	-	-	1,812.5	1,812.5	-	-	-	2.5
BC_P-03	-	7,250	-	-	-	3,625	3,625	-	-	-	2.5
BC_P-04	-	10,875	-	-	-	5,437.5	5,437.5	-	-	-	2.5
BC_P-05	-	14,500	-	-	-	7,250	7,250	-	-	-	2.5

6.0 RESULTS

The following sections outline the results of the validation and production runs for the forebay, tailrace, and bypass channel models.

6.1 Model Validation

Model validation was completed to determine if the CFD models provide similar results to field measured changes in WSEL and velocities. The following sections outline the results for the forebay and tailrace model validation. No validation was done for the bypass channel model.

6.1.1 Forebay Model

FB_V-01

The purpose of the first forebay model validation run was to verify the relative hydraulic drop through the shoals area and the flow split around Goat Island under the conditions observed during impoundment bathymetry collection on 6/26/2025. The relative hydraulic drop was evaluated over two impoundment profile lines, starting from the upstream model extents approximately 1,200 feet down the river left and river right channels around Goat Island as shown in Figure 6.1.1-1. Figures 6.1.1-2 and 6.1.1-3 present results of the relative hydraulic change over the two profile lines. The average, median, and maximum difference between the simulated and field measured hydraulic change are 0.01 feet, 0.00 feet, and 0.25 feet respectively for the river left channel and 0.06 feet, 0.04 feet, and 0.35 feet respectively for the river right channel. The median and average difference is less than 0.1 feet and the general trend of the simulated and field measured hydraulic change are similar. The ADCP measures water surfaces resulting from transient conditions such as turbulence, vortex shedding, and velocity shadows. These transient conditions cannot be adequately resolved due to differences in the time scale at which they occur compared to the time averaged results produced when solving the RANS equations in any CFD software. Such transient conditions may occur within the shoals and near Goat Island and likely played a significant role in the difference in water surface elevations between the ACDP and CFD results.

The simulated flow split at a total flow of 3,409 cfs resulted in approximately 62% of the flow being conveyed through the river right channel and 38% through the river left channel. Flow measurements collected in 2012 under a total river flow of approximately 3,300 cfs suggest that 58% of the total river flow was through the river right channel and 42% of the total river flow was through the river left channel.

FB_V-02

The purpose of the second forebay model validation run was to verify the flow split around Goat Island and simulated velocities under the conditions observed during impoundment velocity transect collection on 6/27/2025. The simulated flow split at a total flow of 2,401 cfs resulted in approximately 66% of the flow being conveyed through the river right channel and 34% through the river left channel. The measured field data showed a flow split of approximately 60% in the river right channel and 40% in the river left channel.

Three velocity transects were used to compare simulated and field measured velocity magnitude and orientation within the impoundment. One transect is located directly below Goat Island and there are transects on either side of Goat Island, as shown in Figure 4.1-2. The simulated and field

measured velocity magnitude and orientation for each transect were compared to verify the large-scale forebay model. Table 6.1.1-1 summarizes relevant statistical information regarding the difference between simulated and field measured velocities. For this table, and any other like it, a positive difference indicates the simulated velocity is higher than the field measured velocity, and a negative difference indicates the simulated velocity is lower than the field measured velocity. Figures 6.1.1-4 through 6.1.1-6 show plots of simulated and field measured velocity magnitude and orientation for each transect. Velocities were generally higher in the river right channel and lower in the river left channel than the field measured, which is consistent with the noted difference between the simulated and field measured flow split around Goat Island (i.e., higher flows in the right channel and lower flows in the left channel). The river right and river left velocity transects also indicate that the location of the highest velocities for the simulated velocities differ from the location of the highest velocities for the field measured velocities. Several factors (i.e., spatial scale and time scale) introduce limitations with being able to reproduce ADCP measurements. For spatial scale, limitations with data collection (i.e., large rocks and shallow flow conditions) in combination with the computational cell size led to poor definition of the terrain in the model and is likely the leading cause for discrepancies between the simulated and field measured velocity distribution. For example, a large rock in the right channel (see Figure 6.1.1-7) likely pushes flow to the left side of the channel (as observed from the field measurements). However, this rock is not resolved within the model domain, leading to higher flows to the right side of the right channel. For time scale, the ADCP captures transient behavior (e.g., vortices, persistent eddies, and secondary flow patterns), which occur on a different time scale than the time averaged results produced when solving the RANS equations in any CFD software. The simulated velocity distribution downstream of Goat Island was more representative of the field measured velocity distribution than the comparison of velocity distributions from each individual channel.

FB_V-03

The purpose of the third forebay model validation run was to verify simulated velocities under the conditions observed during intake velocity transect collection on 6/25/2025. A velocity transect was measured directly in front of the intake to evaluate velocities in front of the powerhouse. The simulated and field measured velocity magnitude and orientation for the transect were compared to verify the small-scale forebay model. Table 6.1.1-1 summarizes relevant statistical information regarding the difference between simulated and field measured velocities. Figure 6.1.1-8 shows plots of simulated and field measured velocity magnitude and orientation for the transect for the model and field measurements. The general trend of higher velocities in front of Unit 1 is similar between the simulated and field measured velocities. As discussed in the results for FB_V-02, spatial and time scale considerations introduce limitations with being able to reproduce ADCP measurements.

6.1.2 Tailrace Model

TR_V-01

The purpose of the first tailrace model validation run was to verify the relative hydraulic drop within the model extents under the conditions observed during tailrace bathymetry collection on 6/26/2025. The relative hydraulic drop was evaluated over one profile line, starting from 340 feet downstream of the powerhouse[9] and extending to the downstream boundary condition as shown

[9] Water levels under these flow conditions were collected via boat mounted equipment, for which access within approximately 340 feet of the powerhouse is restricted by a boat barrier.

in Figure 6.1.2-1. Figure 6.1.2-2 presents results of the relative hydraulic change over the profile line. The average, median, and maximum difference between the simulated and field measured hydraulic change for the profile line is 0.05 feet, -0.00 feet, and 0.52 feet respectively.

The simulated WSEL indicates that the tailrace is a flat-water region with little change, which is representative of the site conditions observed during data collection. However, the field data shows relatively large fluctuations in WSEL from approximately station 740 to 900. These areas of large WSEL fluctuation correspond with where the field crew turned the boat due to various data collection considerations encountered in the field (e.g., channel geometry, bathymetric file size). The distance between the water surface and the instrument sensor is defined during equipment setup. This distance varies more drastically when the boat is turning, which leads to less accurate water level measurements. Additionally, the ADCP measures water surfaces resulting from transient conditions such as turbulence, vortex shedding, and velocity shadows. These transient conditions cannot be adequately resolved due to differences in the time scale at which they occur compared to the time averaged results produced when solving the RANS equations in any CFD software. Such transient conditions may occur near the bedrock ledge where the field crew was turning the boat due to the sudden change of the flow direction of the water, and likely played a significant role in the difference in water surface elevations between the ACDP and CFD results.

TR_V-02

The purpose of the second tailrace model validation run was to verify simulated velocities under the conditions observed during tailrace velocity transect collection on 6/26/2025. Five velocity transects were measured in the Project tailrace, as depicted in Figure 4.1-2. The simulated and field measured velocity magnitude and orientation for each transect were compared to verify the small-scale tailrace model. Table 6.1.2-1 summarizes relevant statistical information regarding the difference between simulated and field measured velocities. Figures 6.1.2-3 through 6.1.2-7 show plots of simulated and field measured velocity magnitude and orientation for each transect. These figures show that the simulated velocity distribution is similar to the field measured velocity distribution.

6.2 Production Runs

Productions runs were completed to bracket the range of operating conditions that occur at the Project. The following sections outline the results for the forebay, tailrace, and bypass channel.

6.2.1 Forebay Model

To demonstrate results from the small-scale forebay model important for evaluating hydraulic conditions near the intake, figures showing a vertical plane of velocity magnitudes and orientations were developed. Figure 6.2.1-1 shows the location of these velocity planes.

FB_P-01

The purpose of the first forebay model production run was to provide results for the maximum operating flow for the Project (7,595 cfs), as described in Section 5.2.1. Figure 6.2.1-2 through 6.2.1-5 shows plots of simulated velocities from the small-scale model at three transects in front of the intake. In general, velocities are less than 3 feet per second (ft/s) in front of the intake.

FB_P-02

The purpose of the second forebay model production run was to provide results for the minimum operating flow for the Project (1,320 cfs), as described in Section 5.2.1. Figure 6.2.1-6 through 6.2.1-9 shows plots of simulated velocities from the small-scale model at three transects in front of the intake. In general, velocities are less than 1 ft/s in front of the intake.

6.2.2 Tailrace Model

To demonstrate results from the small-scale tailrace model important for evaluating hydraulic conditions near the upstream fish passage entrance, figures showing a vertical plane of velocity magnitudes and orientations were developed. Figure 6.2.2-1 shows the location of these velocity planes.

TR_P-01

The purpose of the first tailrace model production run was to provide results for the maximum operating flow for the Project (7,595 cfs), as described in Section 5.2.2. Figure 6.2.2-2 and Figure 6.2.2-4 through 6.2.2-6 show plots of simulated velocities from the small-scale model at three transects downstream of the powerhouse. Appendix A also contains plan view plots of simulated velocities within the tailrace at various depths from the small-scale model. Due to the geometry of the channel, maximum velocities in the tailrace reach approximately 12 ft/s.

TR_P-02

The purpose of the second tailrace model production run was to provide results for the minimum operating flow for the Project (1,320 cfs), as described in Section 5.2.2. Figure 6.2.2-3 and Figure 6.2.2-7 through 6.2.2-9 show plots of simulated velocities from the small-scale model at three transects downstream of the powerhouse. Appendix A also contains plan view plots of simulated velocities within the tailrace at various depths from the small-scale model. Due to the geometry of the channel, maximum velocities in the tailrace reach approximately 7 ft/s.

6.2.3 Bypass Channel Model

Due to the high velocities and hydraulic drop along the falls, modeling accurate results directly on the falls becomes difficult. As such, model data from upstream of the falls was used to estimate the mean critical depth and its associated velocity over the falls, as presented in Table 6.2.3-1. It is anticipated that flow over the falls becomes supercritical, thus maximum water depths over the falls may be less than the estimated mean critical depth and minimum velocities may be greater than the estimated mean velocity presented in Table 6.2.3-1. The simulated depths and velocities for all simulated flows are shown in Figure 6.2.3-1 through Figure 6.2.3-16. Higher flows provide more favorable depths and less favorable velocities for fish trying to traverse up the falls. It must be noted that the minimum crest elevation of the falls is approximately 12 feet, NGVD29. Therefore, normal tides are approximately 6.70 feet below the falls crest, the king tide, which occurs approximately once a month, is approximately 4.64 feet below the falls crest, and the maximum reported tide is about 2.05 feet above the falls crest. Higher tidal conditions improve the possibility of fish traversing up the falls, but the tidal conditions that would allow for upstream passage occur rarely for most fish species, other than those that have the ability to complete larger vertical leaps, such as Salmonids.

Table 6.1.1-1: Summary Statistics of the Difference Between Simulated and Field Measured Velocities at all ADCP Nodes for all Forebay Validation Transects

Transect	Simulation	Minimum (ft/s)	Percent of Total Less Than -3.0 ft/s Difference	Percent Between -3.0 and -2.0 ft/s Difference	Percent Between -2.0 and -1.0 ft/s Difference	Percent Between -1.0 and 0.0 ft/s Difference	Percent Between 0.0 and 1.0 ft/s Difference	Percent Between 1.0 and 2.0 ft/s Difference	Percent Between 2.0 and 3.0 ft/s Difference	Percent of Total Greater Than 3.0 ft/s Difference	Maximum (ft/s)
River Right of Goat Island	FB_V-02	-3.02	0.02%	0.14%	2.91%	18.49%	30.32%	48.13%	0.00%	0.00%	1.71
River Left of Goat Island	FB_V-02	-2.60	0.00%	0.31%	1.50%	73.52%	24.67%	0.00%	0.00%	0.00%	0.99
Below Goat Island	FB_V-02	-3.52	0.05%	0.27%	2.74%	38.14%	58.79%	0.00%	0.00%	0.00%	0.94
Intake	FB_V-03	-3.59	0.10%	1.85%	11.56%	44.34%	39.95%	1.33%	0.56%	0.30%	4.18

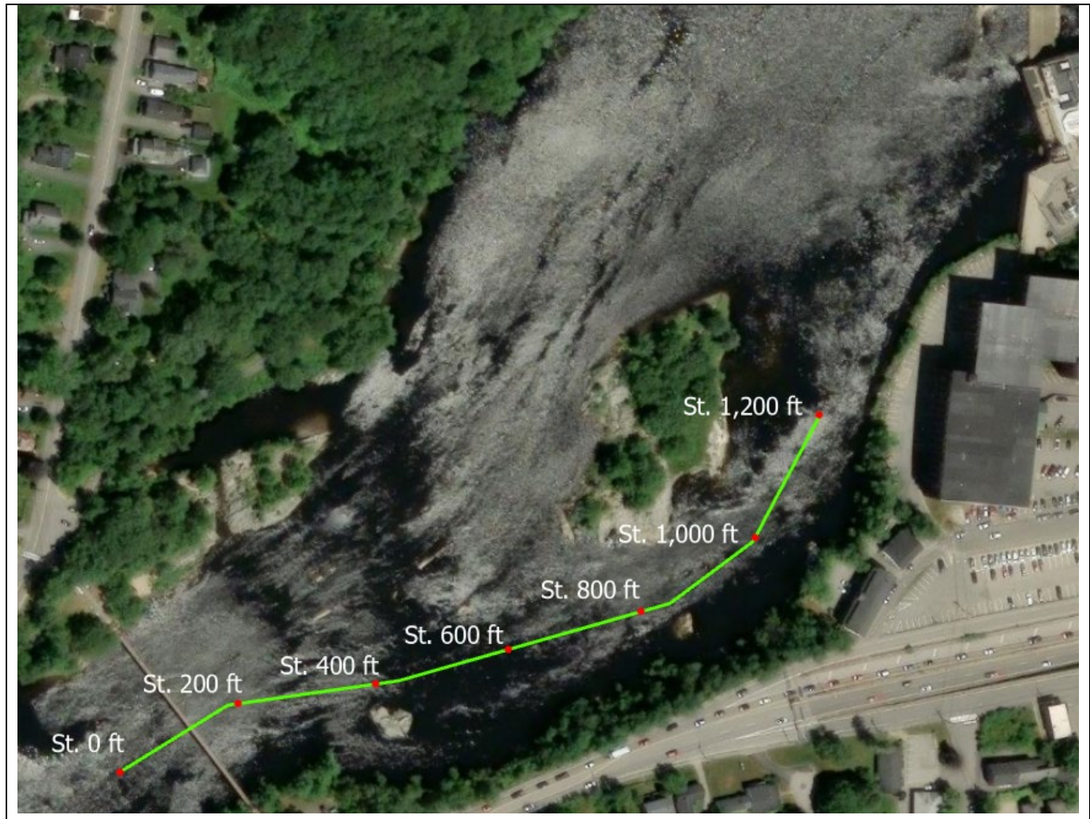
Table 6.1.2-1: Summary Statistics of the Difference Between Simulated and Field Measured Velocities at all ADCP Nodes for all Tailrace Validation Transects

Transect	Simulation	Minimum (ft/s)	Percent of Total Less Than -3.0 ft/s Difference	Percent Between -3.0 and -2.0 ft/s Difference	Percent Between -2.0 and -1.0 ft/s Difference	Percent Between -1.0 and 0.0 ft/s Difference	Percent Between 0.0 and 1.0 ft/s Difference	Percent Between 1.0 and 2.0 ft/s Difference	Percent Between 2.0 and 3.0 ft/s Difference	Percent of Total Greater Than 3.0 ft/s Difference	Maximum (ft/s)
TR1 (Upstream)	TR_V-02	-4.94	3.82%	6.80%	11.76%	22.52%	13.74%	20.68%	10.91%	9.77%	5.21
TR2	TR_V-02	-6.05	4.05%	4.12%	10.01%	23.14%	27.47%	22.07%	8.45%	0.71%	3.47
TR3	TR_V-02	-3.58	0.98%	6.60%	17.24%	28.00%	37.04%	9.41%	0.73%	0.00%	2.69
TR4	TR_V-02	-3.73	4.26%	14.95%	21.88%	35.05%	21.29%	2.38%	0.20%	0.00%	2.79
TR5 (Downstream)	TR_V-02	-3.61	0.87%	9.05%	21.50%	31.85%	18.54%	18.19%	0.00%	0.00%	1.98

Table 6.2.3-1: Summary of Bypass Channel Model Results at the Falls

Flow (cfs)	Mean Critical Depth (feet)	Mean Velocity at Mean Critical Depth (ft/s)
100	0.06	1.37
930	0.38	3.48
1,760	0.77	4.99
2,690	1.04	5.78
3,625	1.27	6.40
7,250	1.95	7.93
10,875	2.49	8.96
14,500	2.96	9.76

Figure 6.1.1-1: Map of Profile Lines Used for Forebay Model Validation



River Right Channel to Intake



River Left Channel to Intake

Figure 6.1.1-2: Relative WSEL Comparison for the River Right Channel to the Intake Profile Line

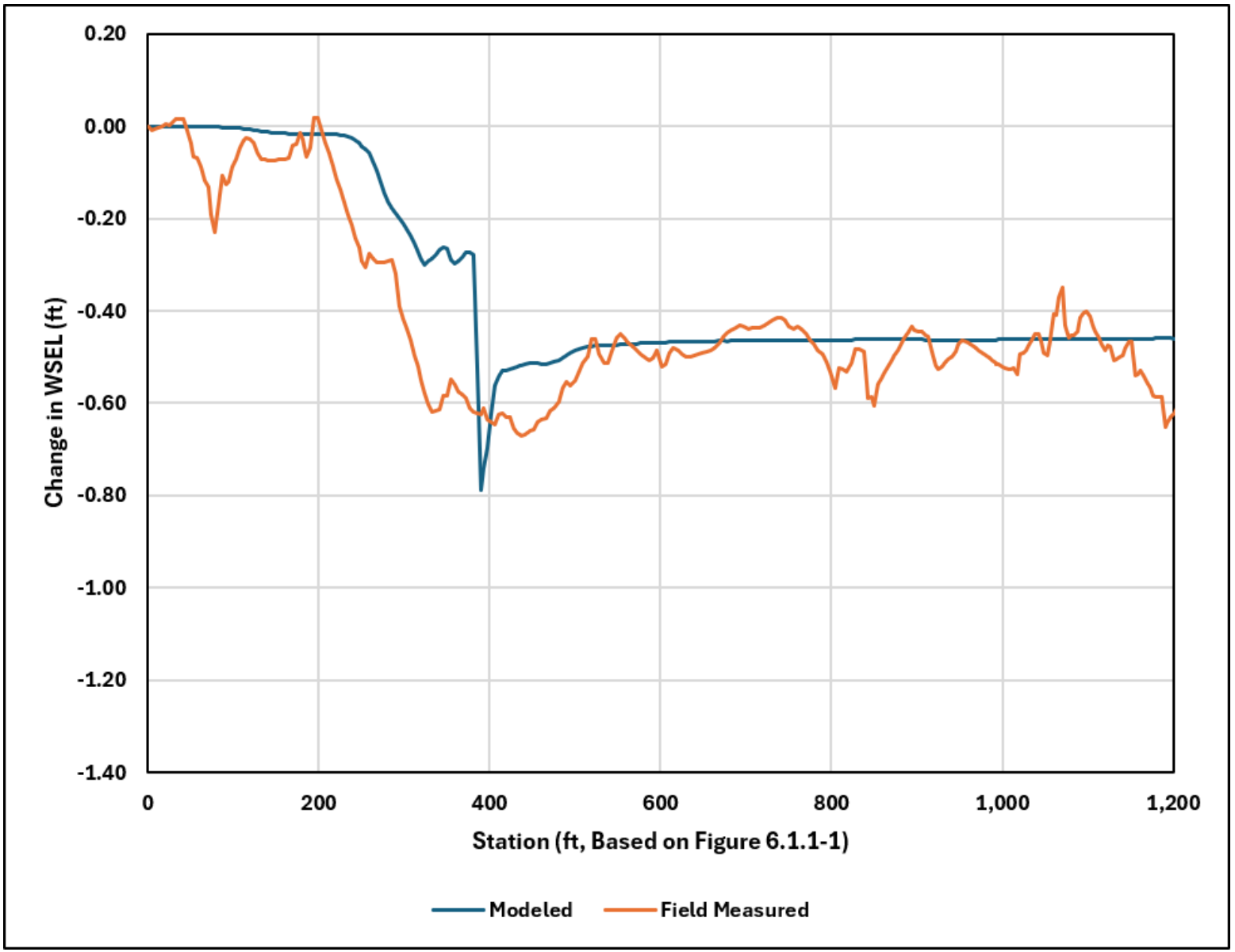


Figure 6.1.1-3: Relative WSEL Comparison for the River Left Channel to the Intake Profile Line

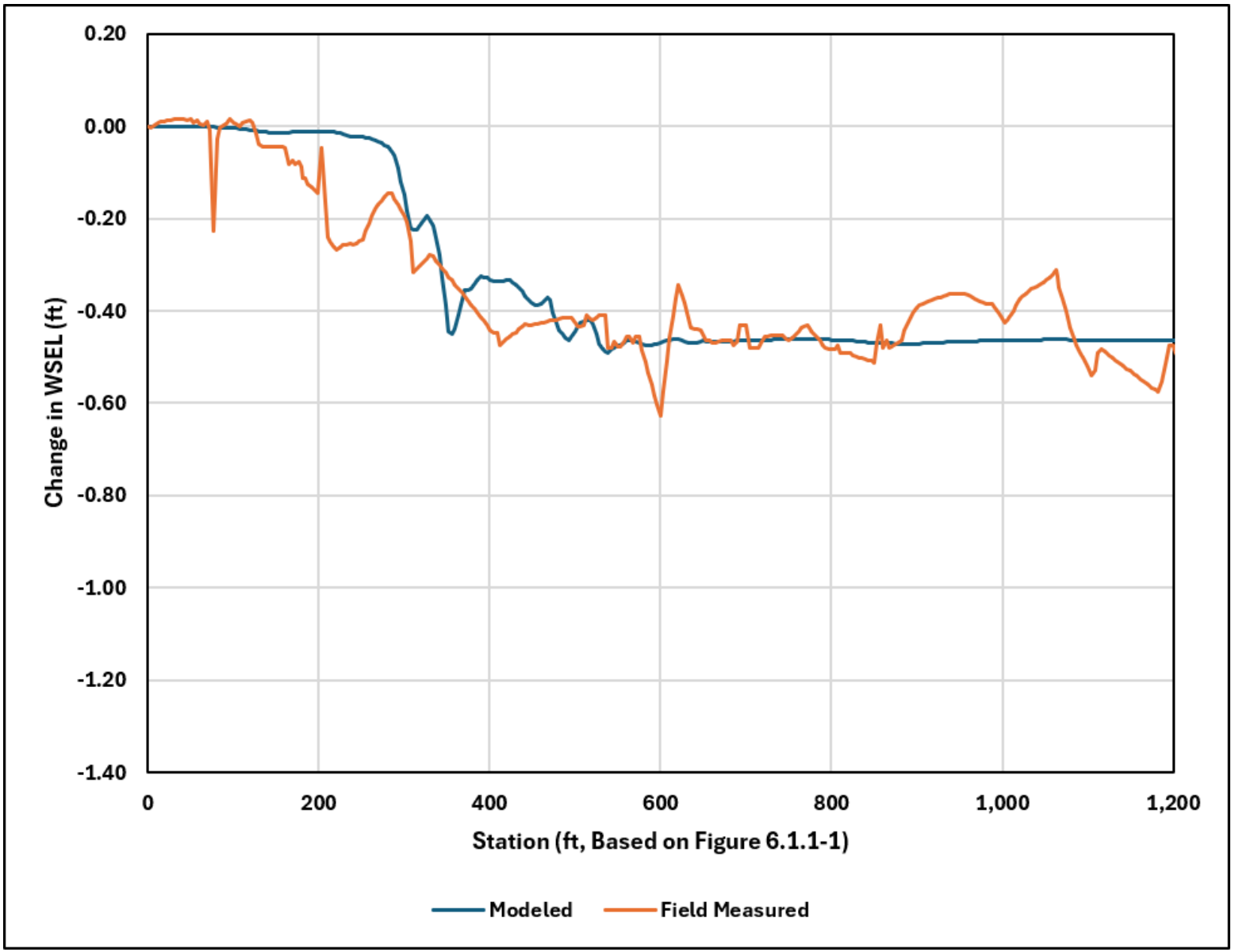
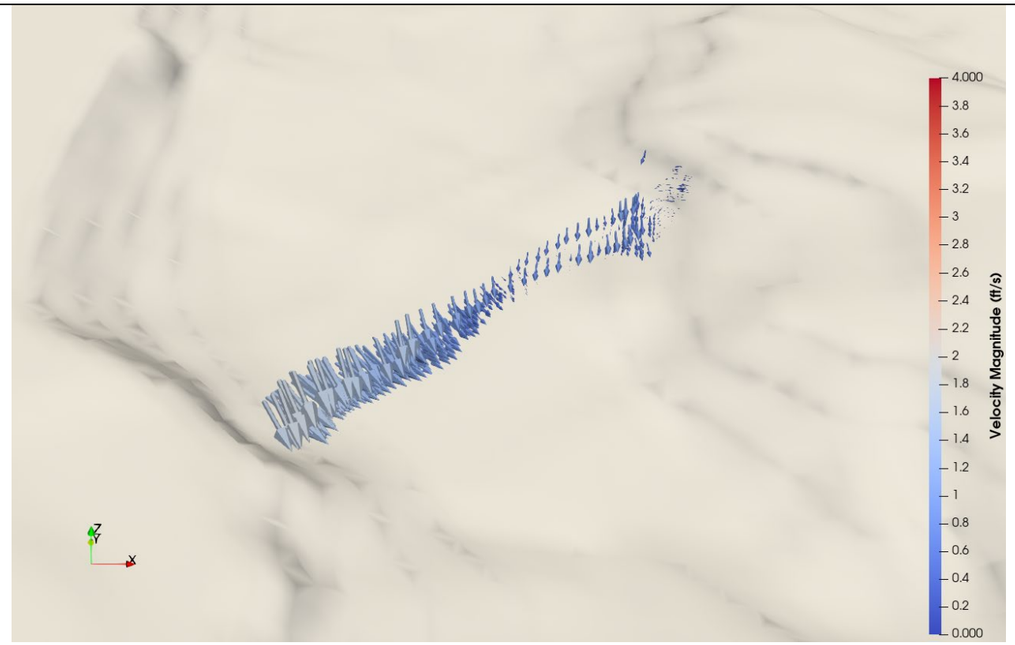
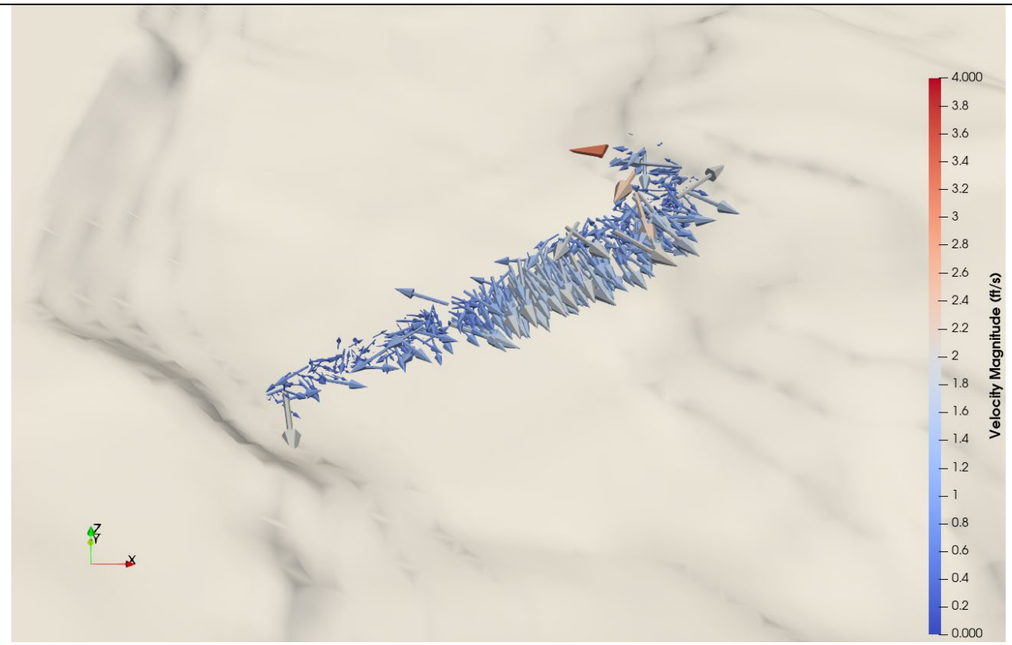


Figure 6.1.1-4: Simulated and Field Measured Velocities at Transect on River Right of Goat Island

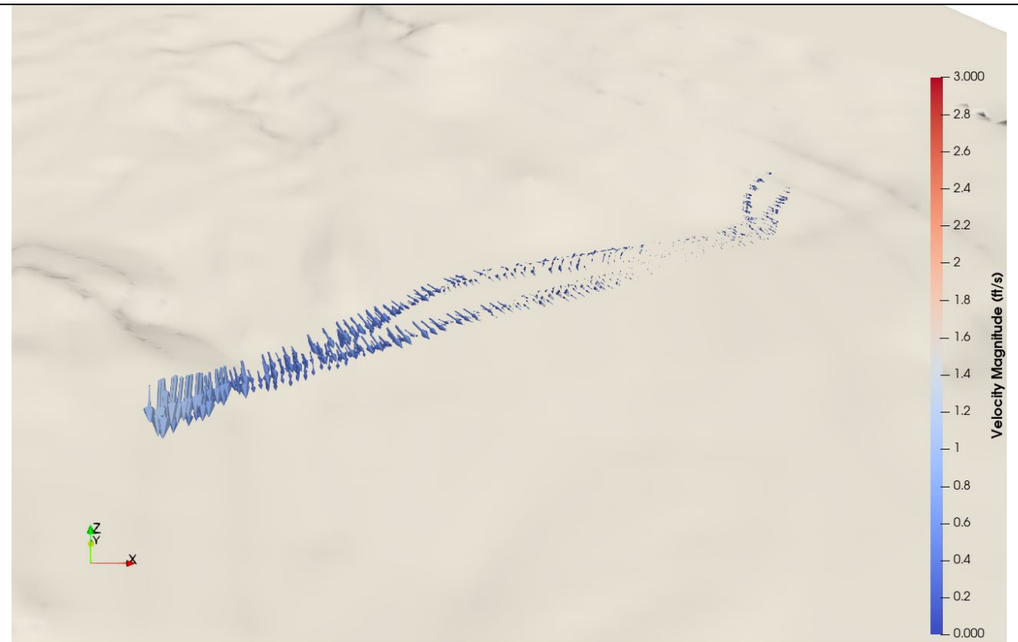


Simulated Velocities

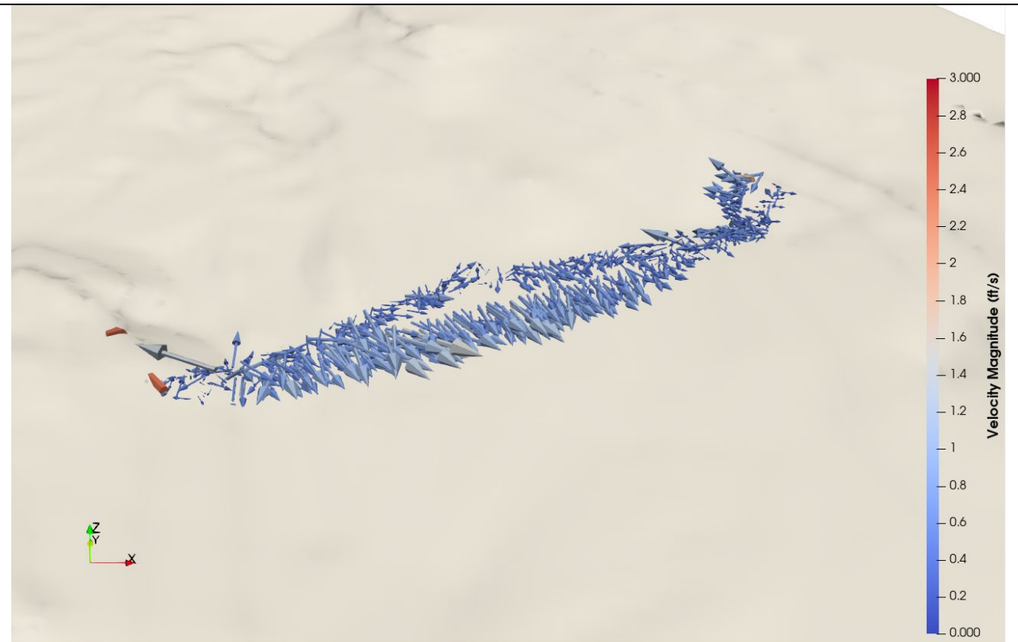


Field Measured Velocities

Figure 6.1.1-5: Simulated and Field Measured Velocities at Transect on River Left of Goat Island

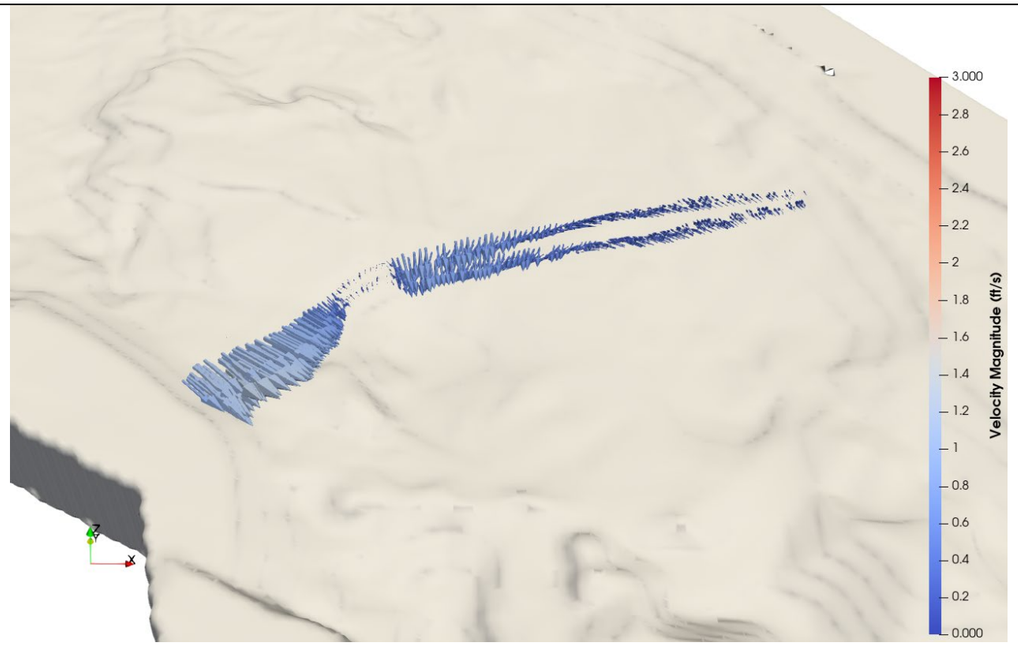


Simulated Velocities

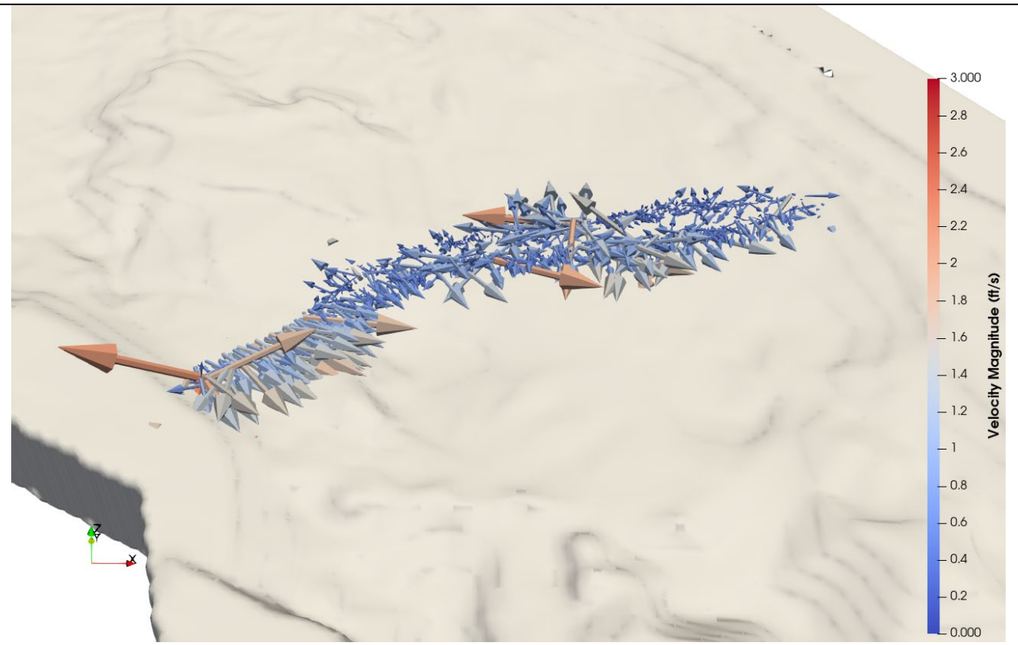


Field Measured Velocities

Figure 6.1.1-6: Simulated and Field Measured Velocities at Transect Below Goat Island



Simulated Velocities



Field Measured Velocities

Figure 6.1.1-7: Rocks in vicinity of Goat Island not Resolved in the Forebay CFD Model

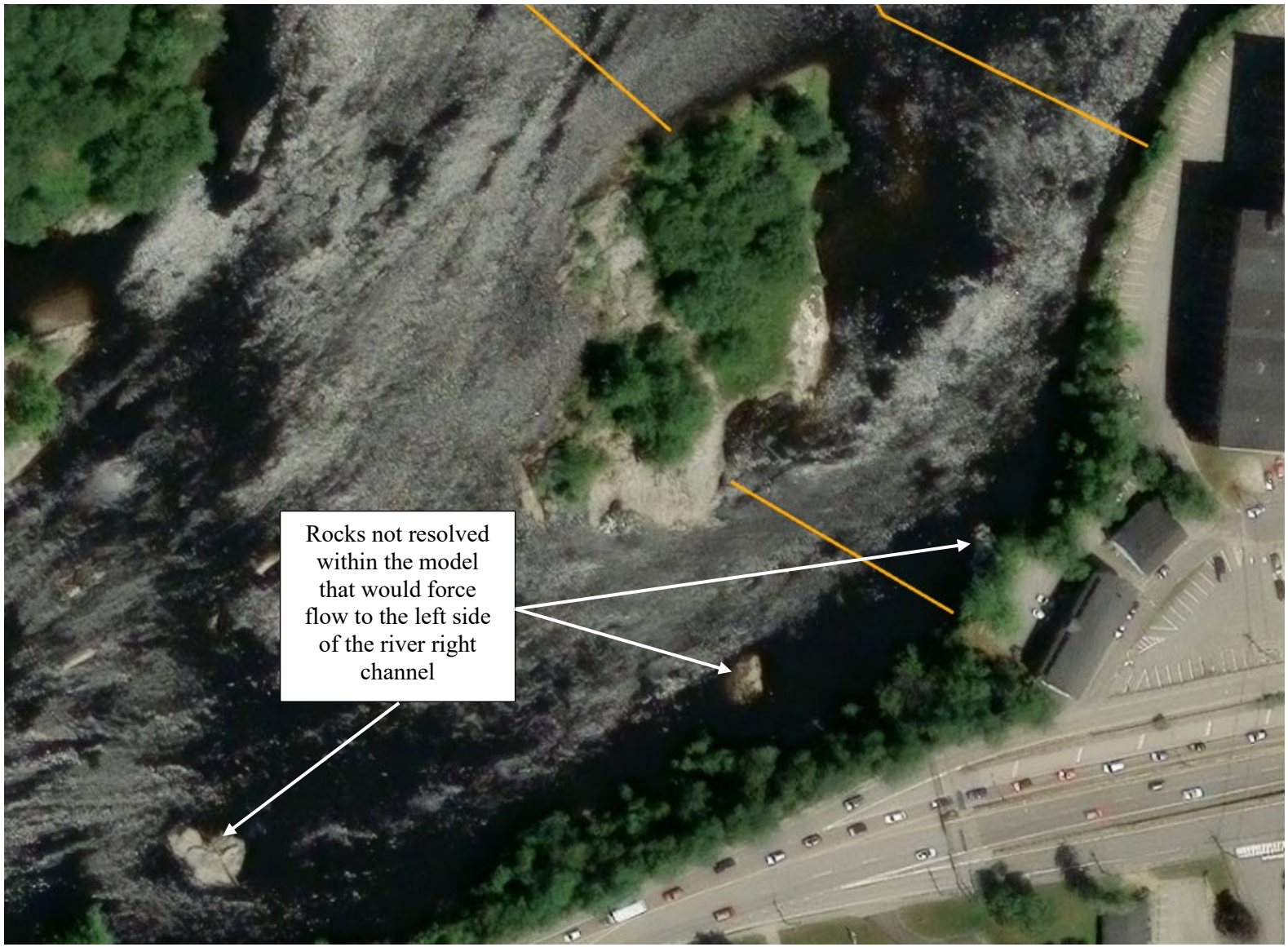
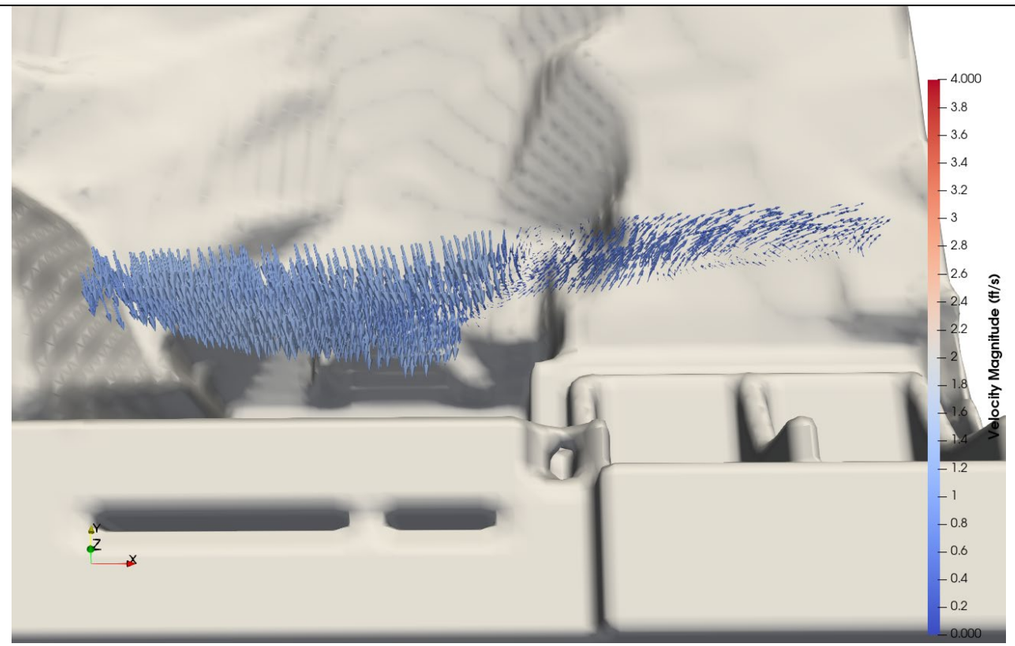
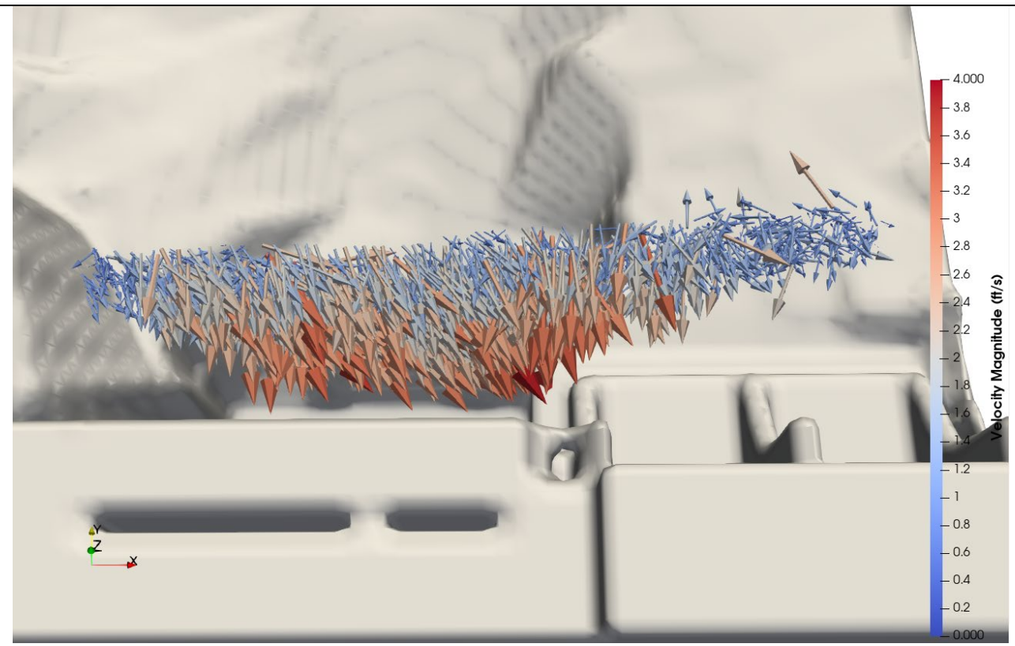


Figure 6.1.1-8: Simulated and Field Measured Velocities at Intake Transect



Simulated Velocities



Field Measured Velocities

Figure 6.1.2-1: Map of Profile Line Used for Tailrace Model Validation

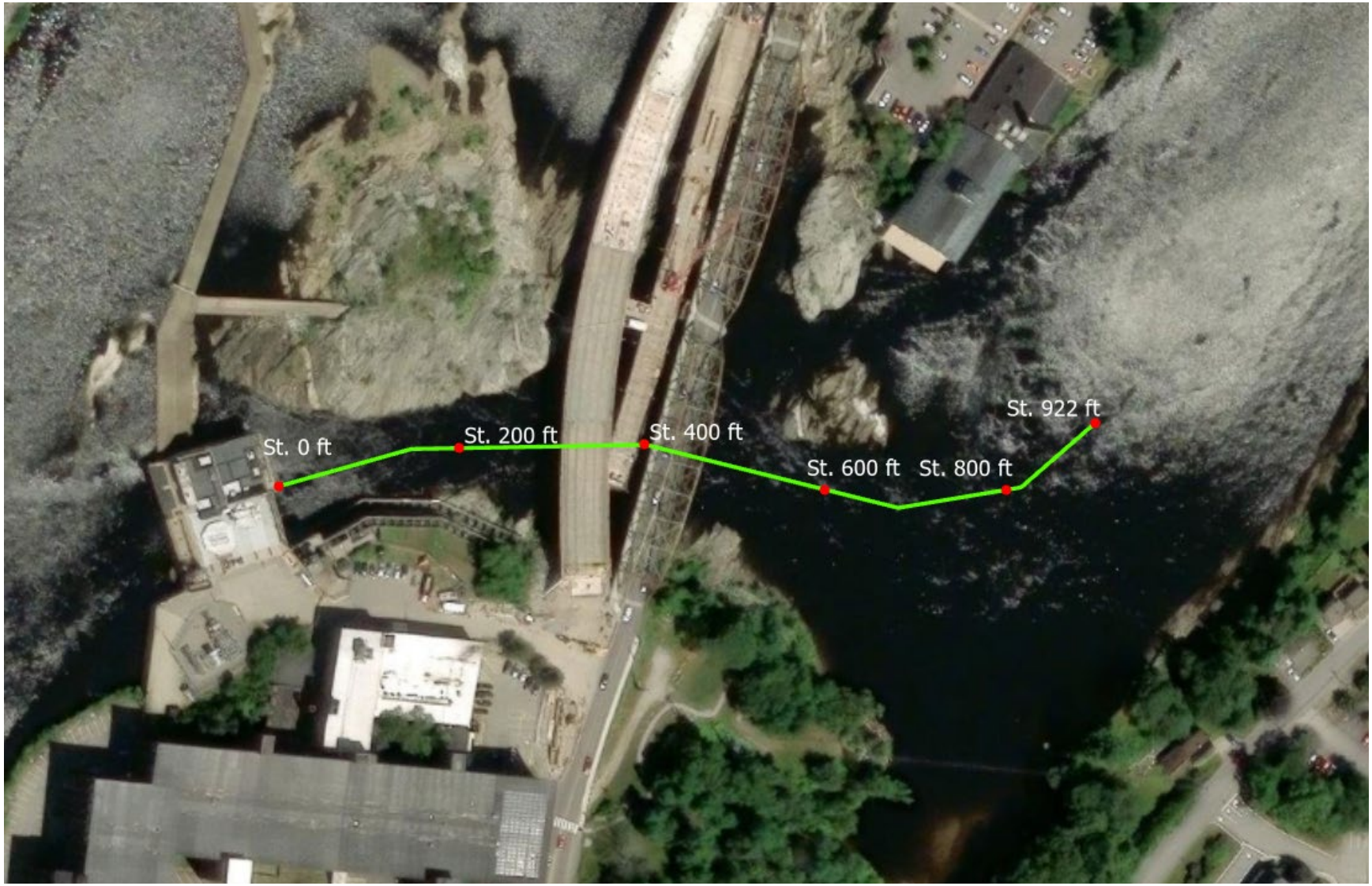


Figure 6.1.2-2: Relative WSEL Comparison for the Tailrace Profile Line

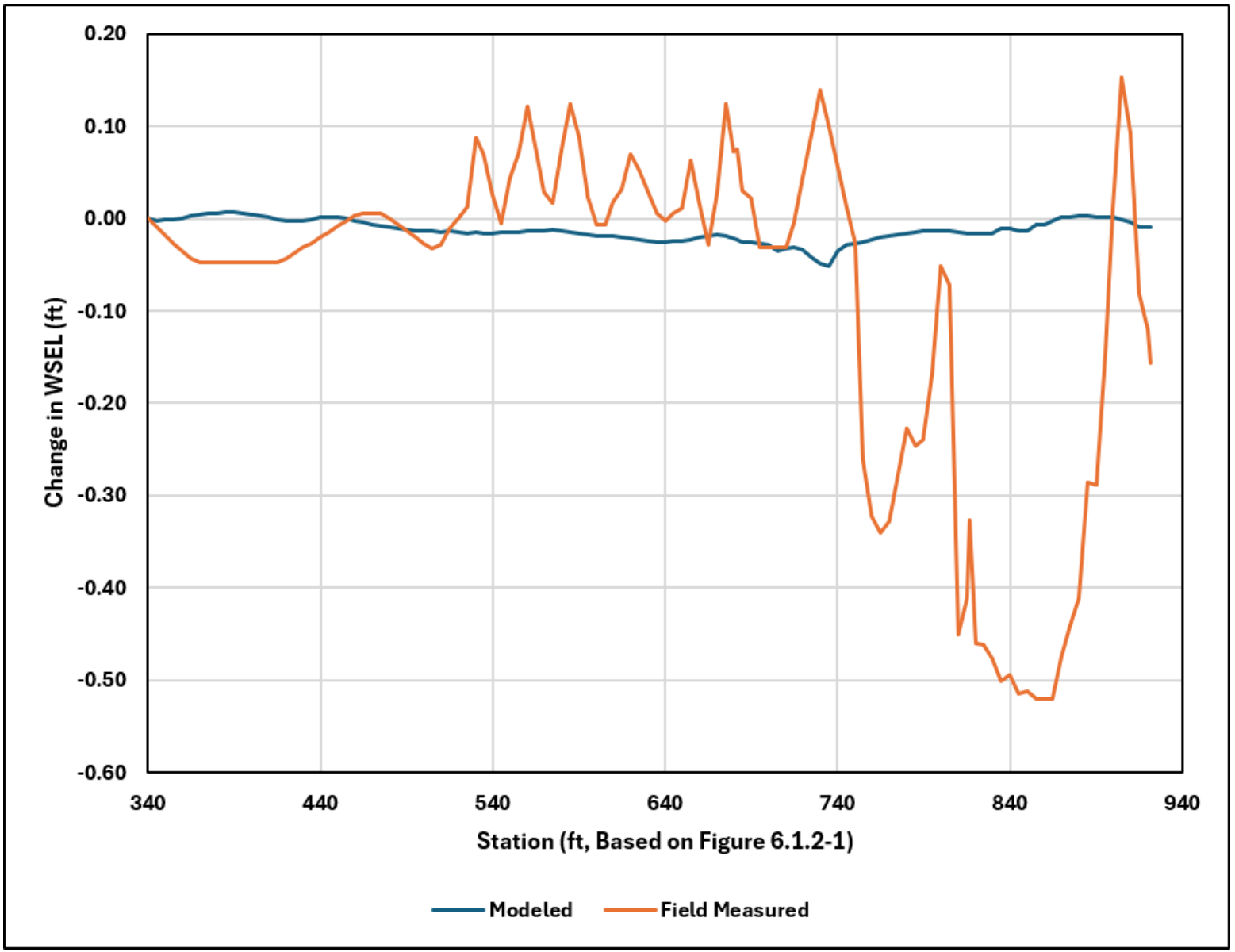
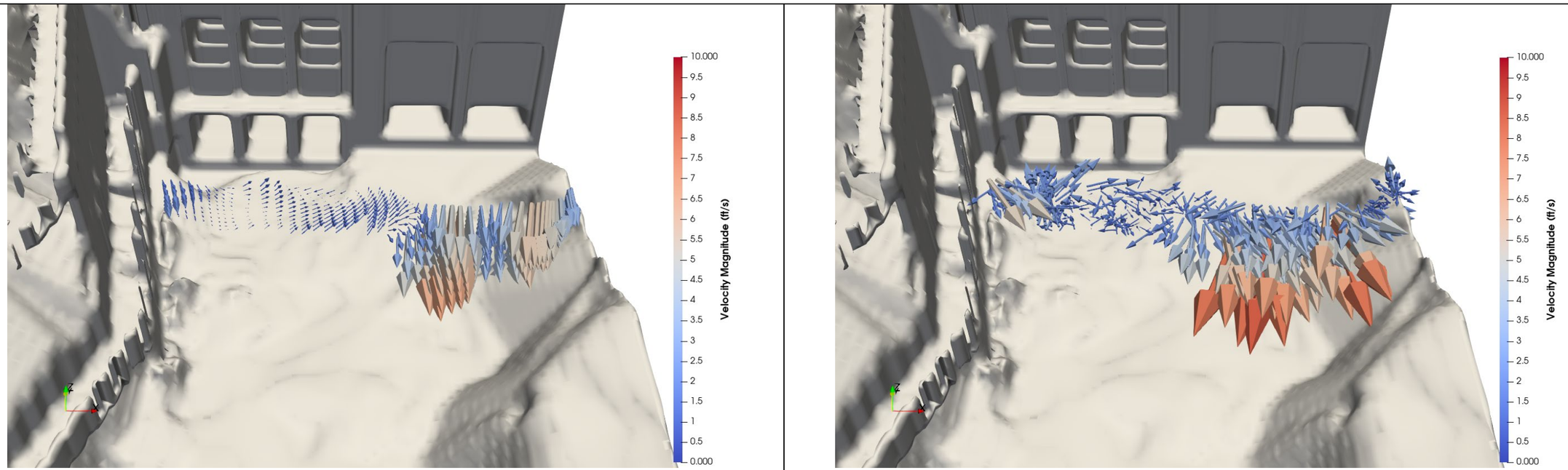


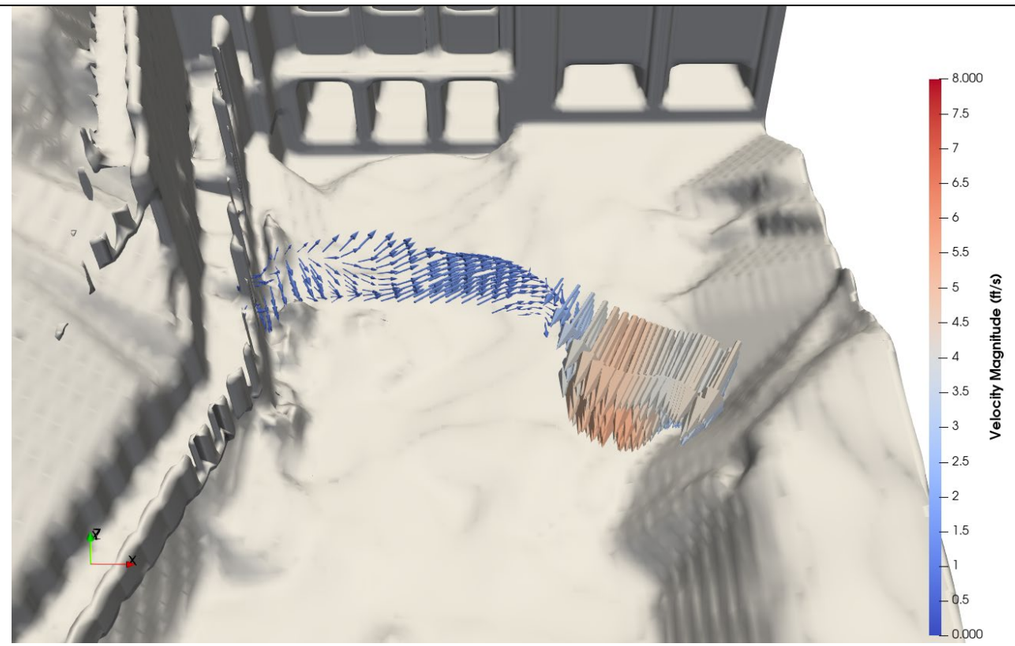
Figure 6.1.2-3: Simulated and Field Measured Velocities at TR1



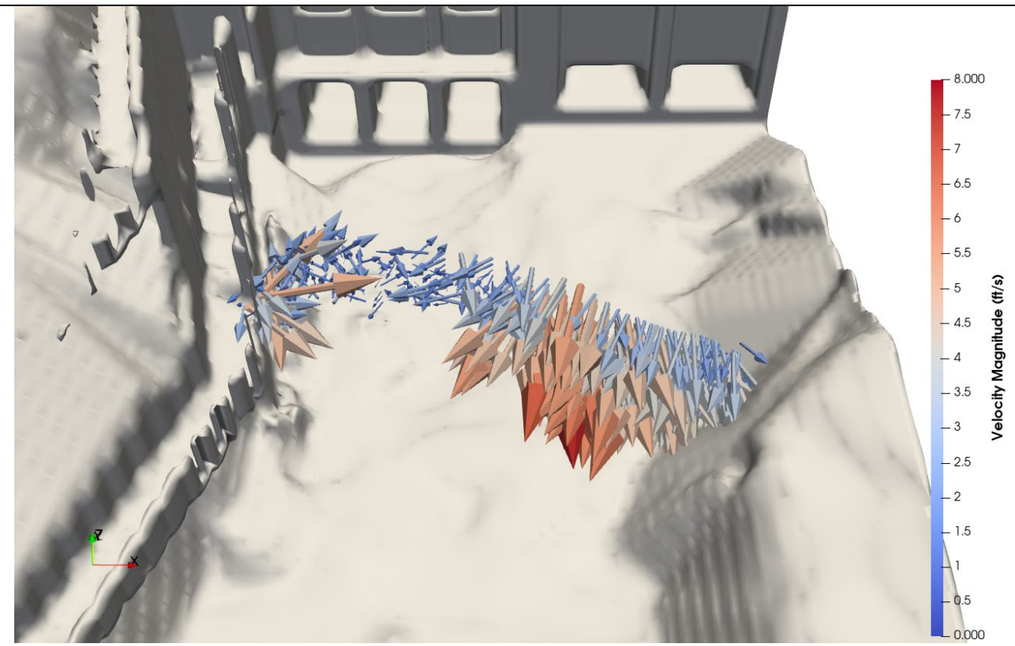
Simulated Velocities

Field Measured Velocities

Figure 6.1.2-4: Simulated and Field Measured Velocities at TR2

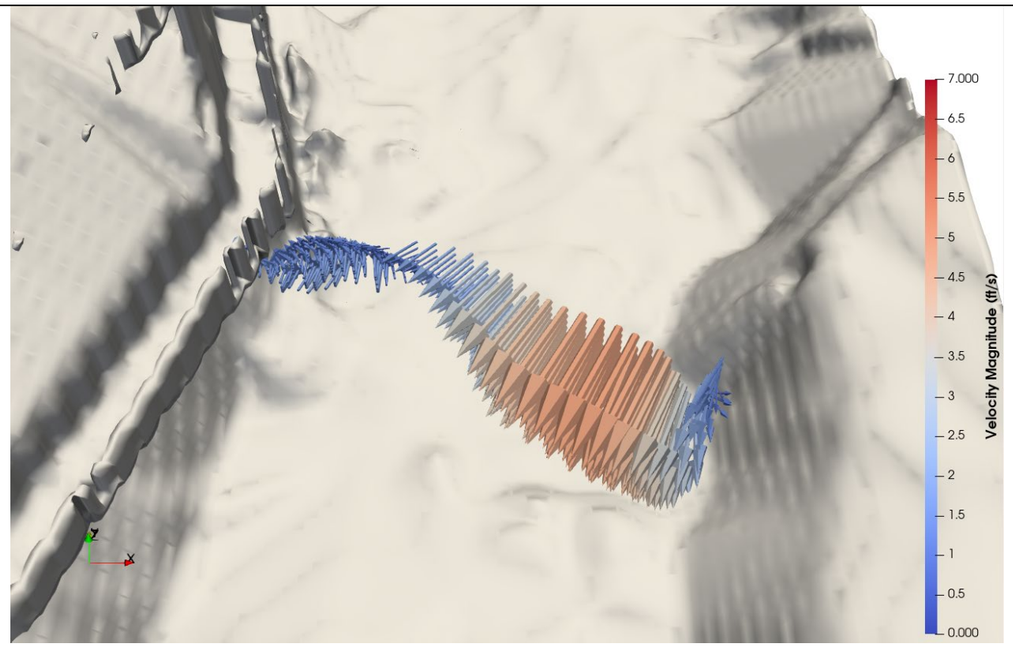


Simulated Velocities

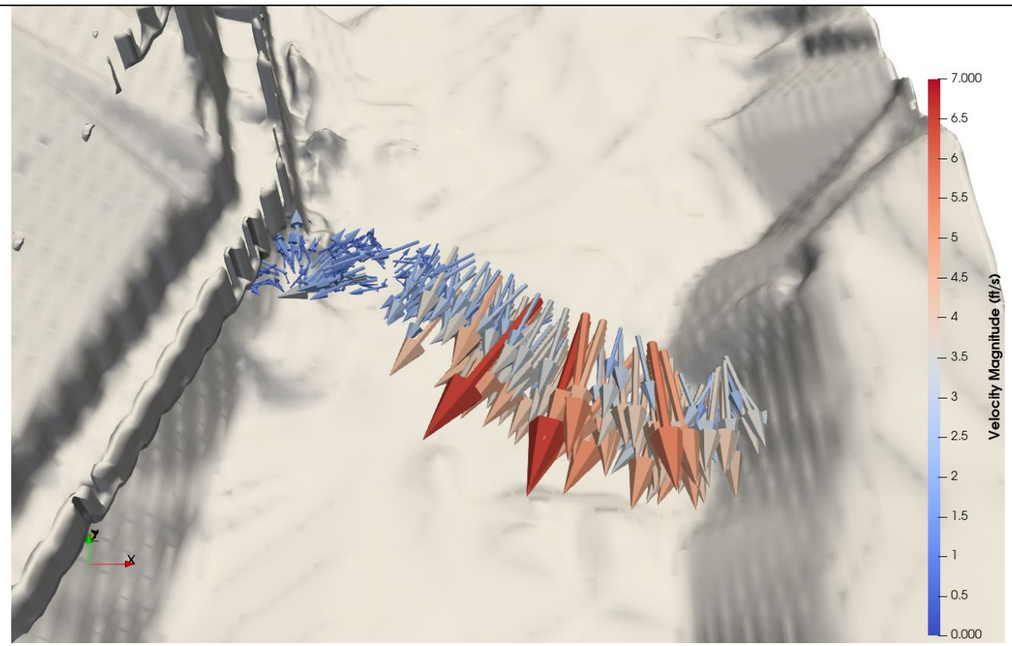


Field Measured Velocities

Figure 6.1.2-5: Simulated and Field Measured Velocities at TR3

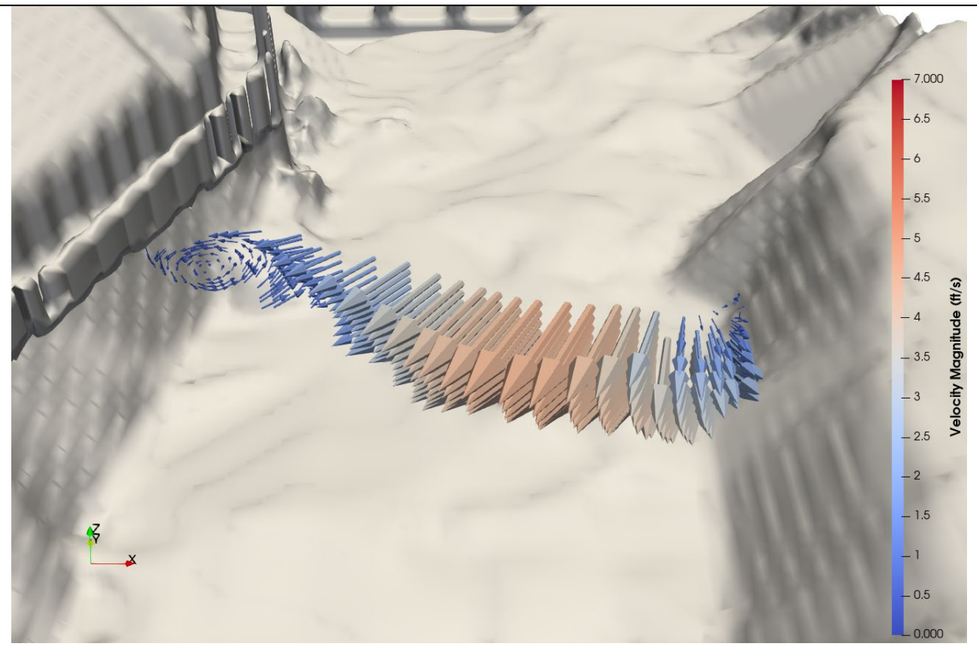


Simulated Velocities

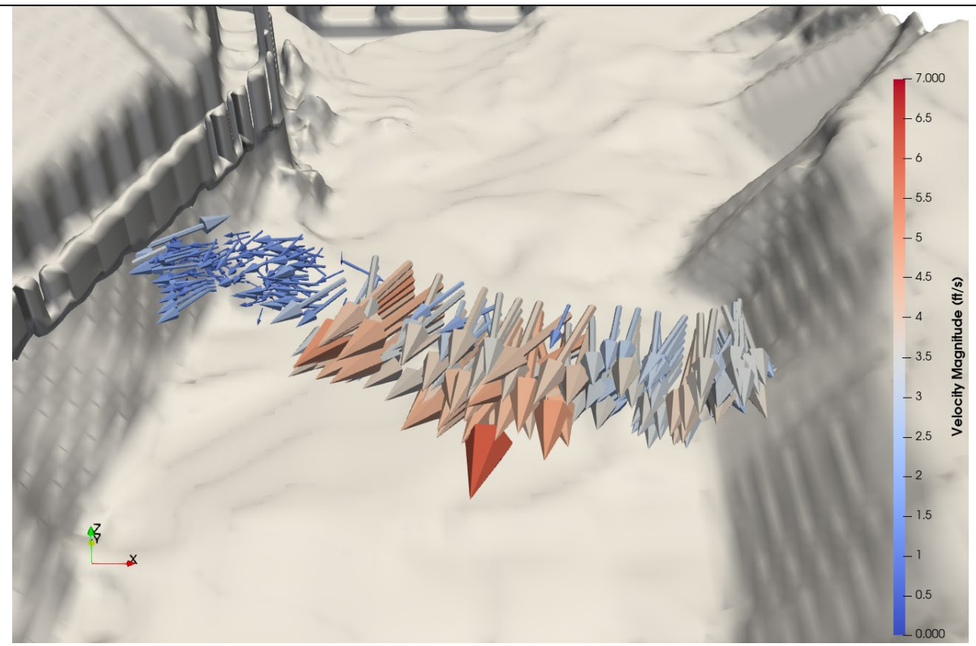


Field Measured Velocities

Figure 6.1.2-6: Simulated and Field Measured Velocities at TR4

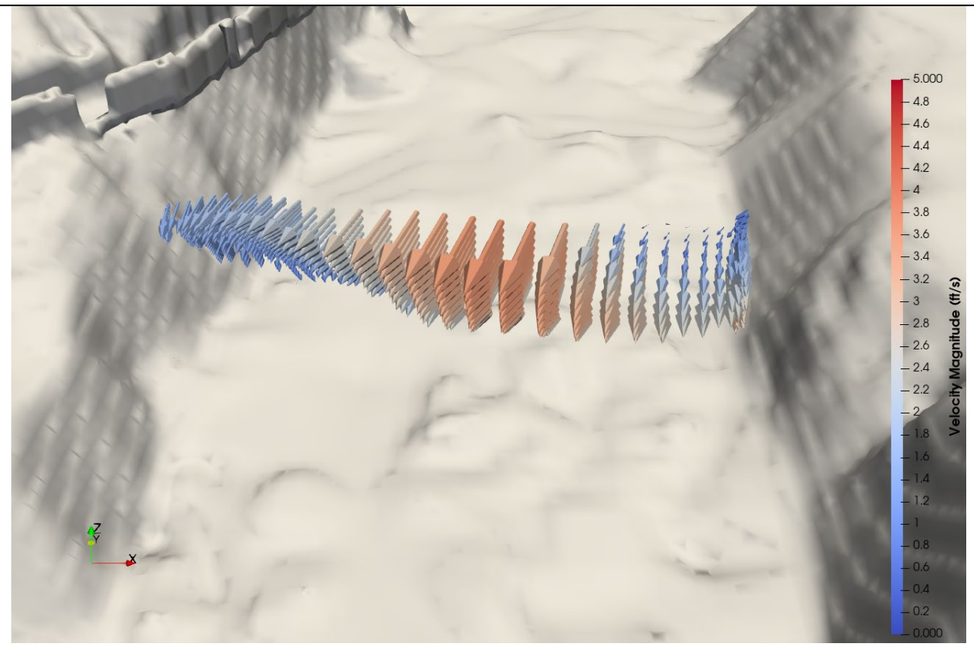


Simulated Velocities

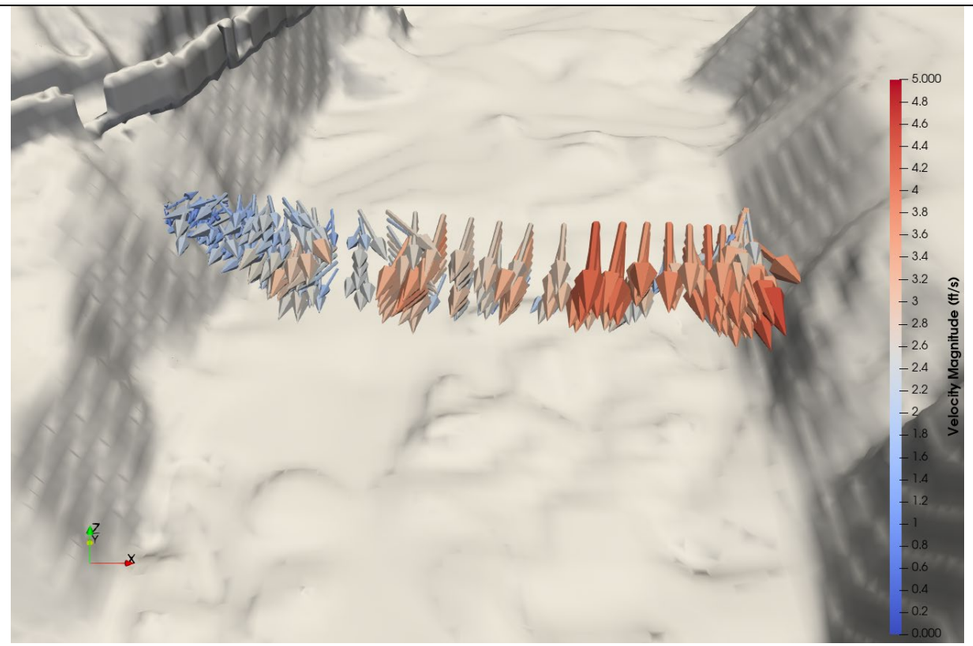


Field Measured Velocities

Figure 6.1.2-7: Simulated and Field Measured Velocities at TR5



Simulated Velocities

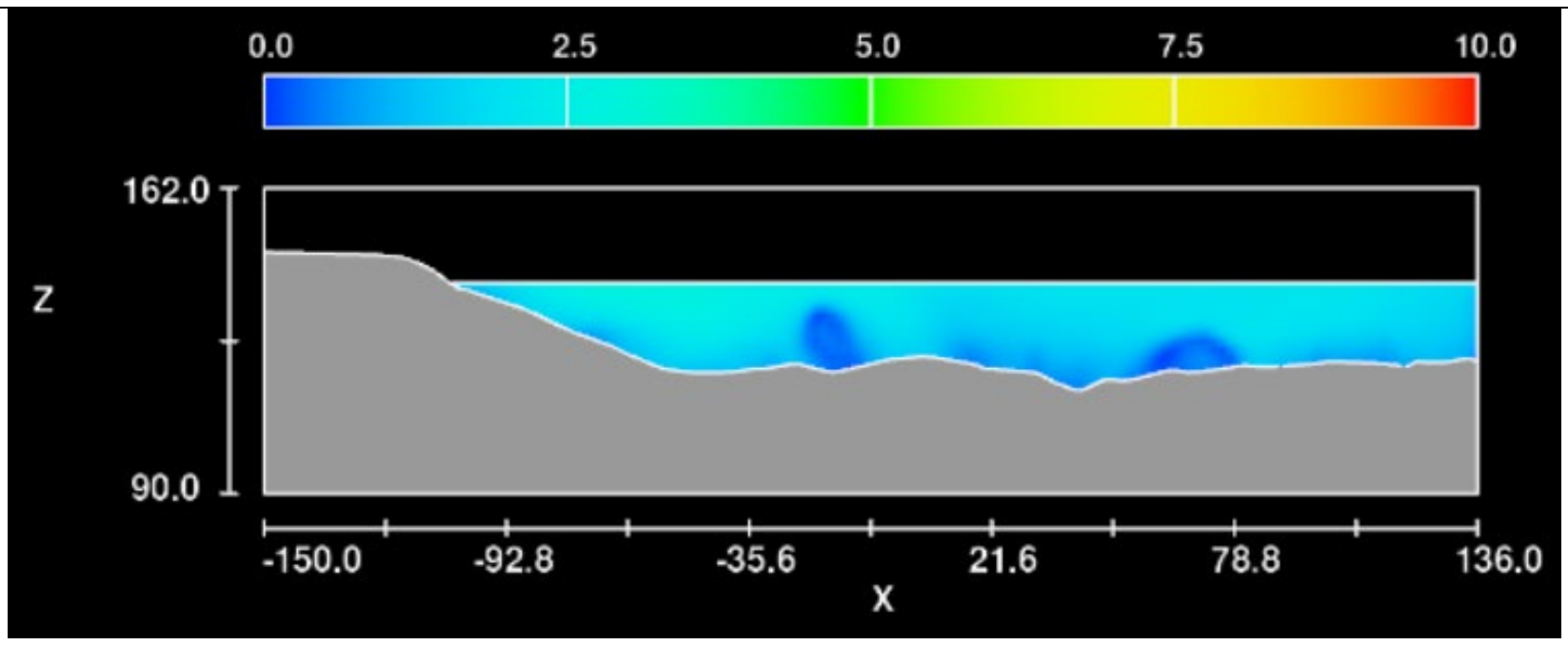


Field Measured Velocities

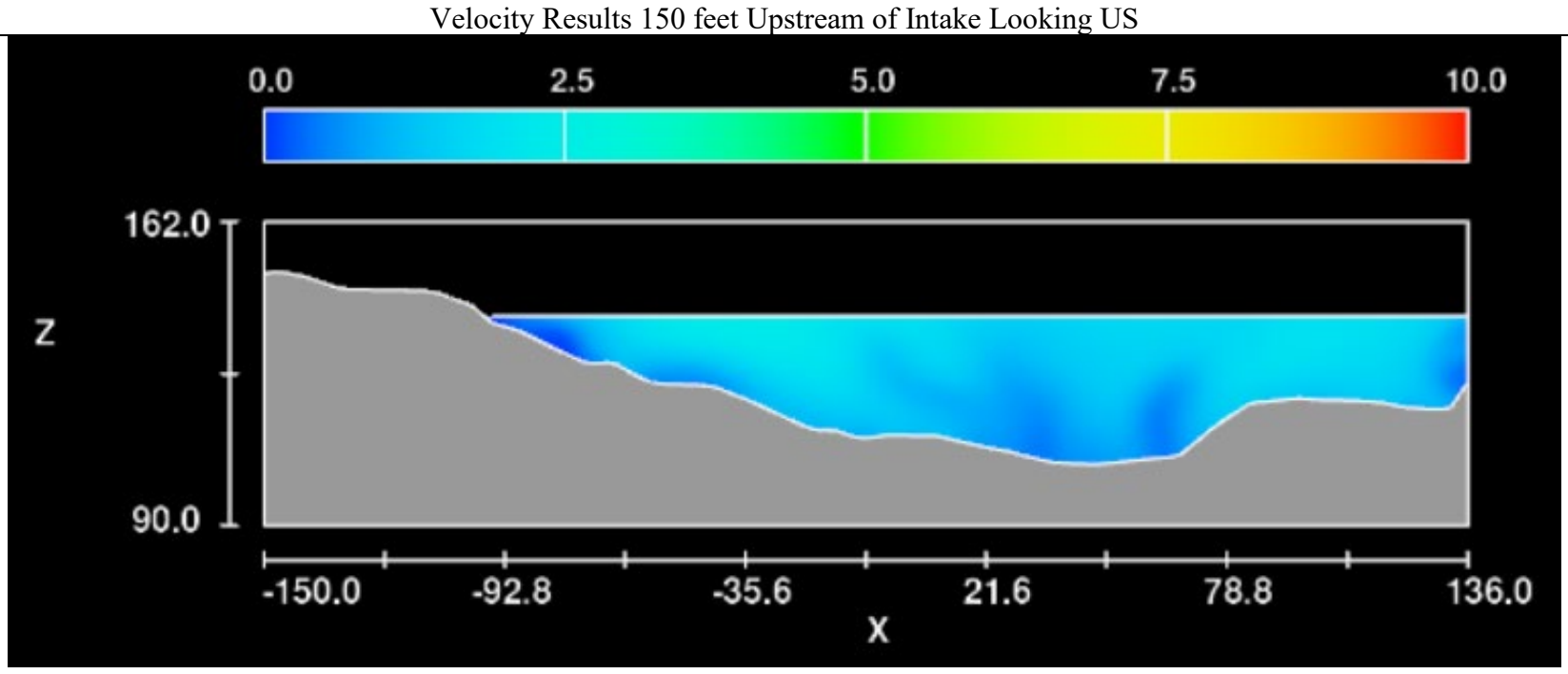
Figure 6.2.1-1: Location of Forebay Model Velocity Planes



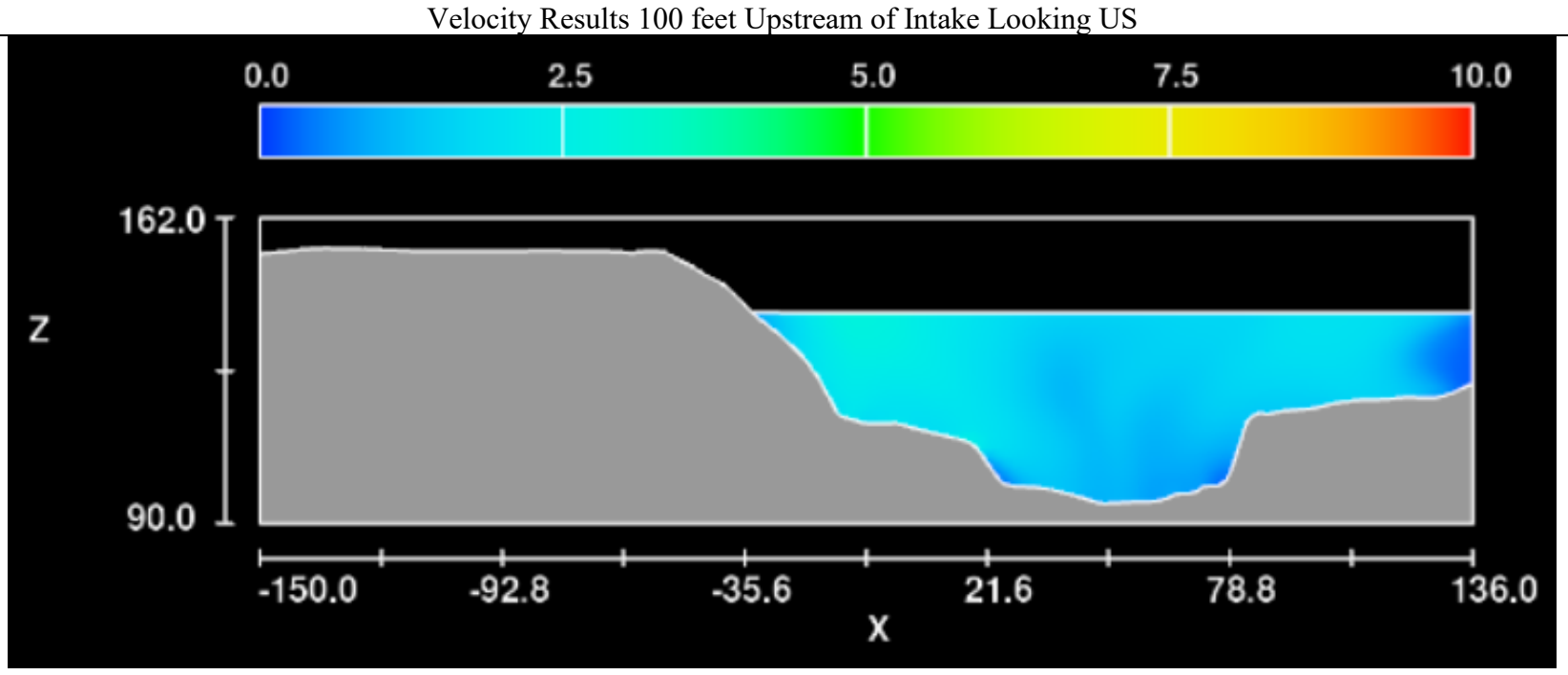
Figure 6.2.1-2: Simulated Velocities at Three Locations in Front of the Intake for Highest Production Flow (7,595 cfs)



Velocity Results 150 feet Upstream of Intake Looking US



Velocity Results 100 feet Upstream of Intake Looking US



Velocity Results 50 feet Upstream of Intake Looking US

Figure 6.2.1-3: Velocity Magnitude and Orientation for Highest Production Flow (7,595 cfs) 50 feet Upstream of Intake

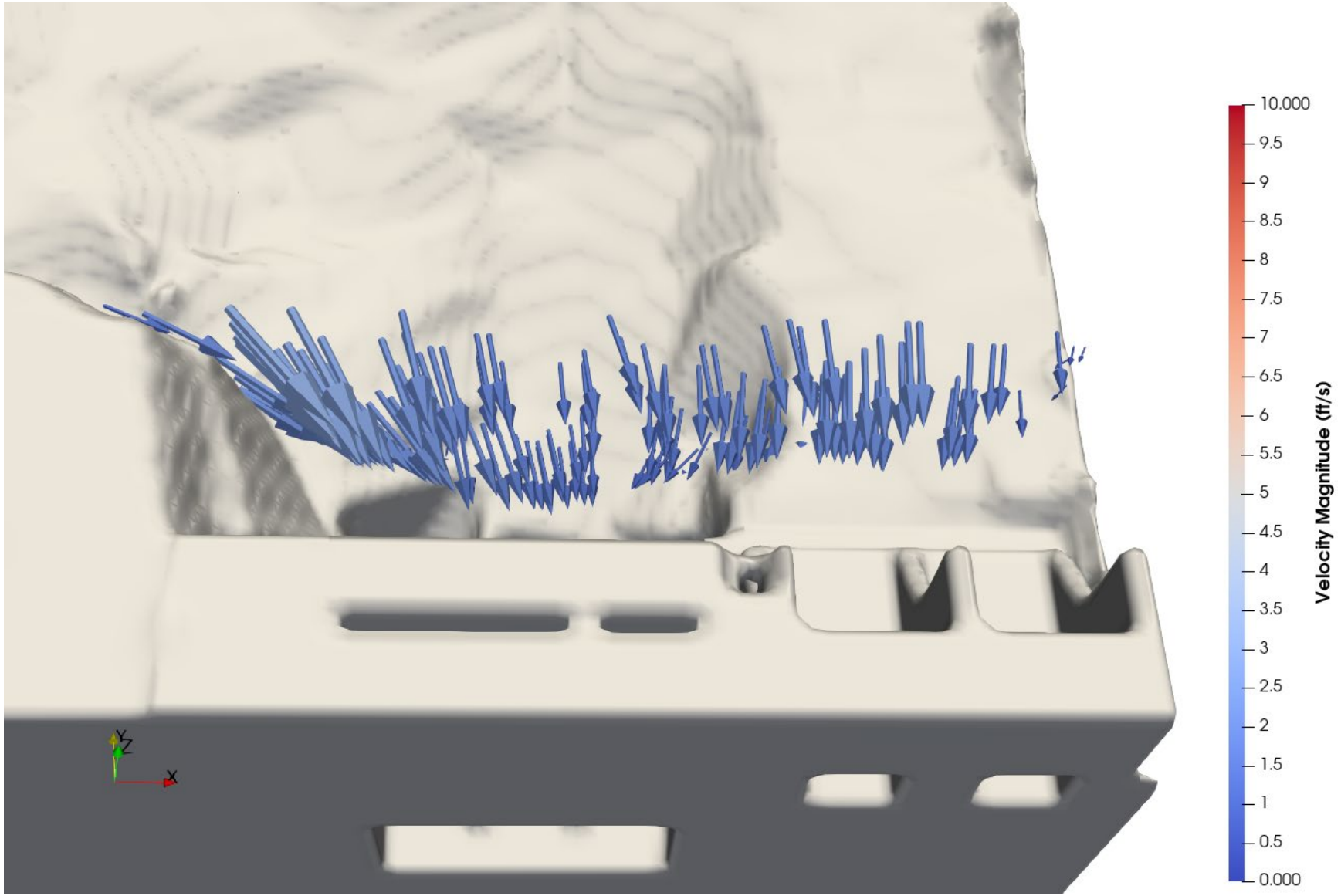


Figure 6.2.1-4: Velocity Magnitude and Orientation for Highest Production Flow (7,595 cfs) 100 feet Upstream of Intake

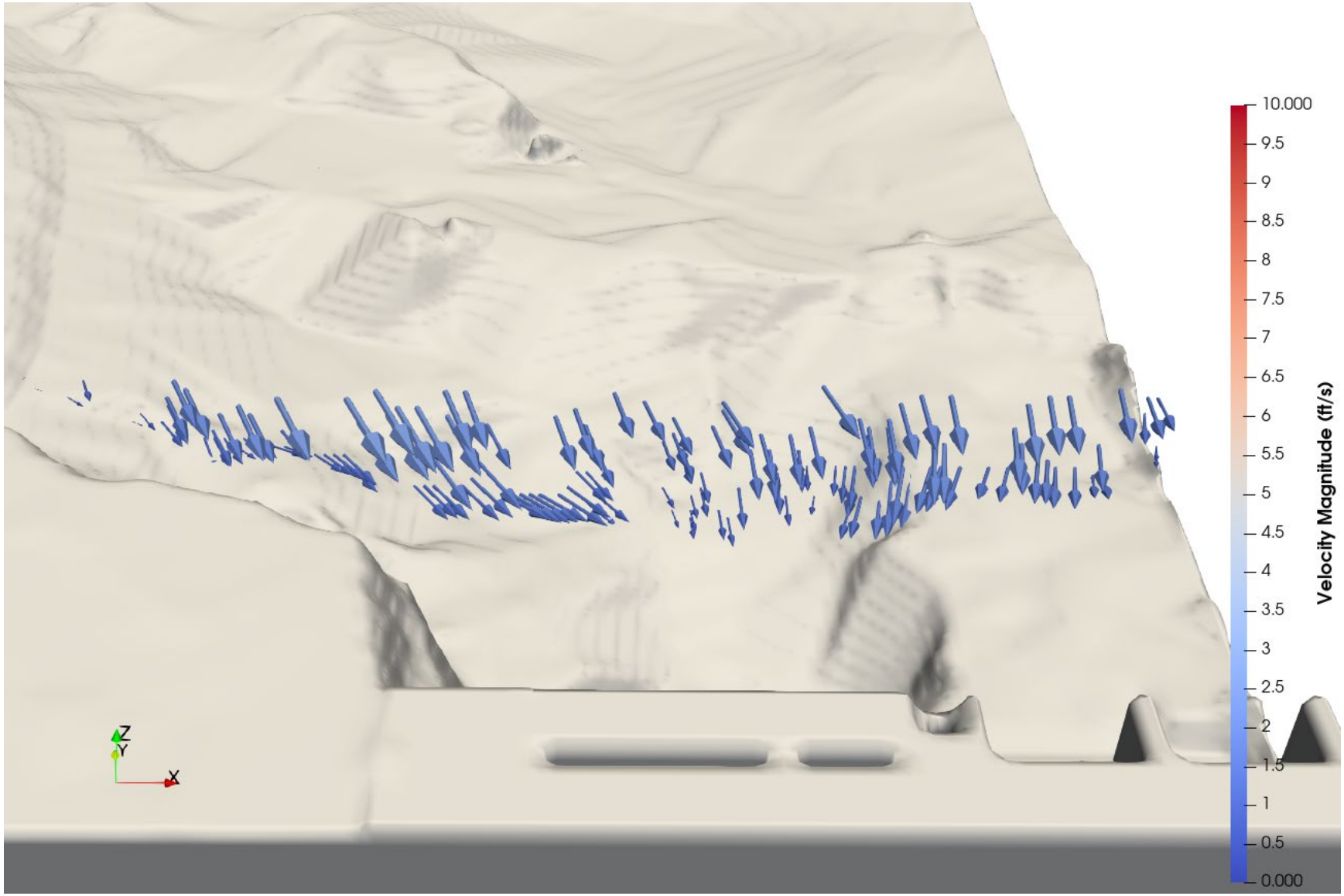


Figure 6.2.1-5: Velocity Magnitude and Orientation for Highest Production Flow (7,595 cfs) 150 feet Upstream of Intake

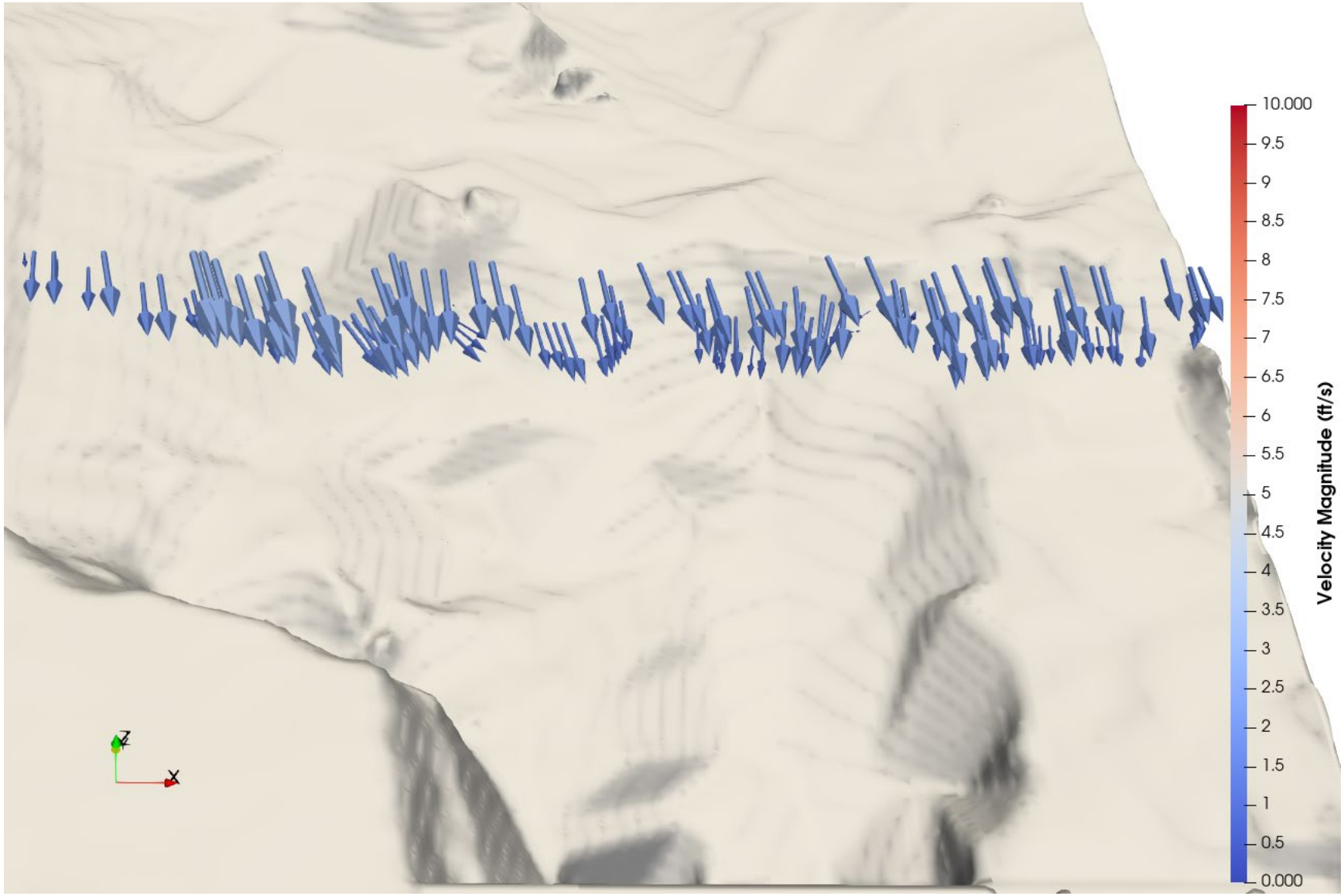
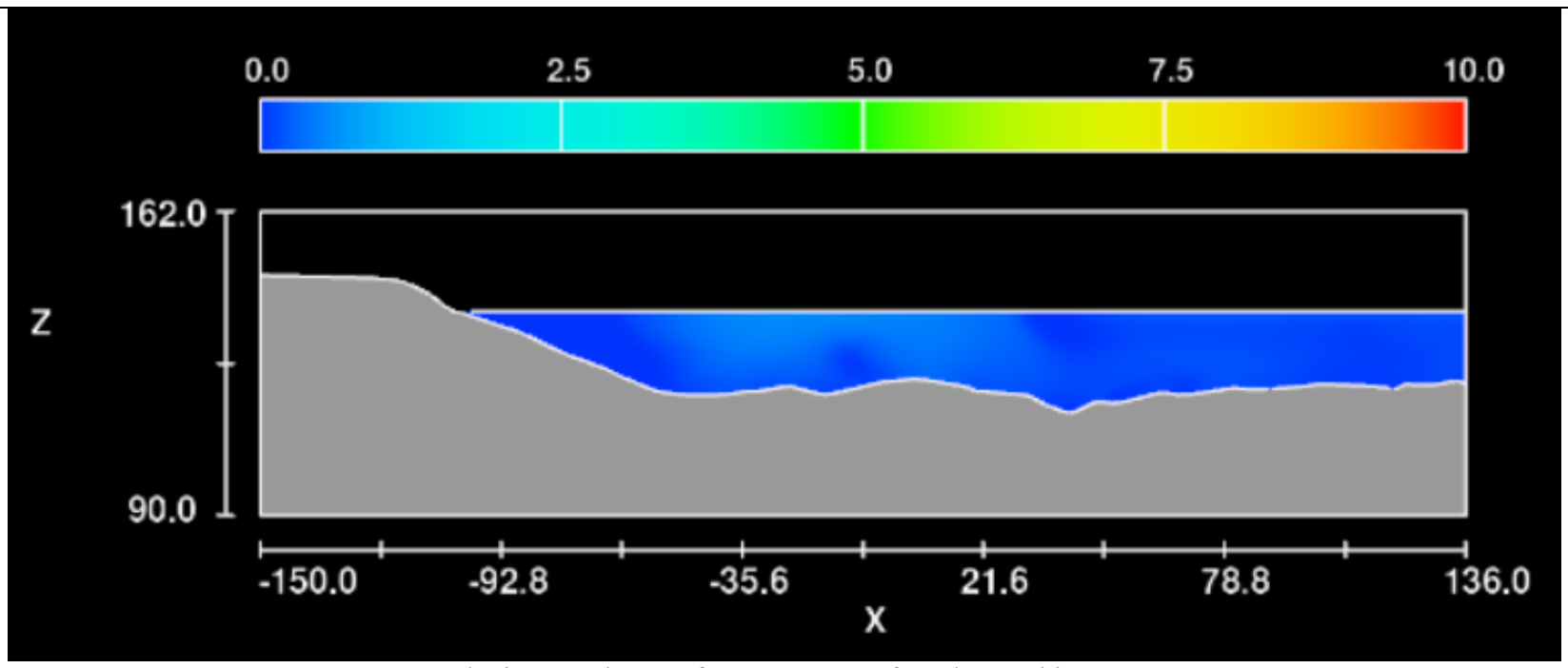
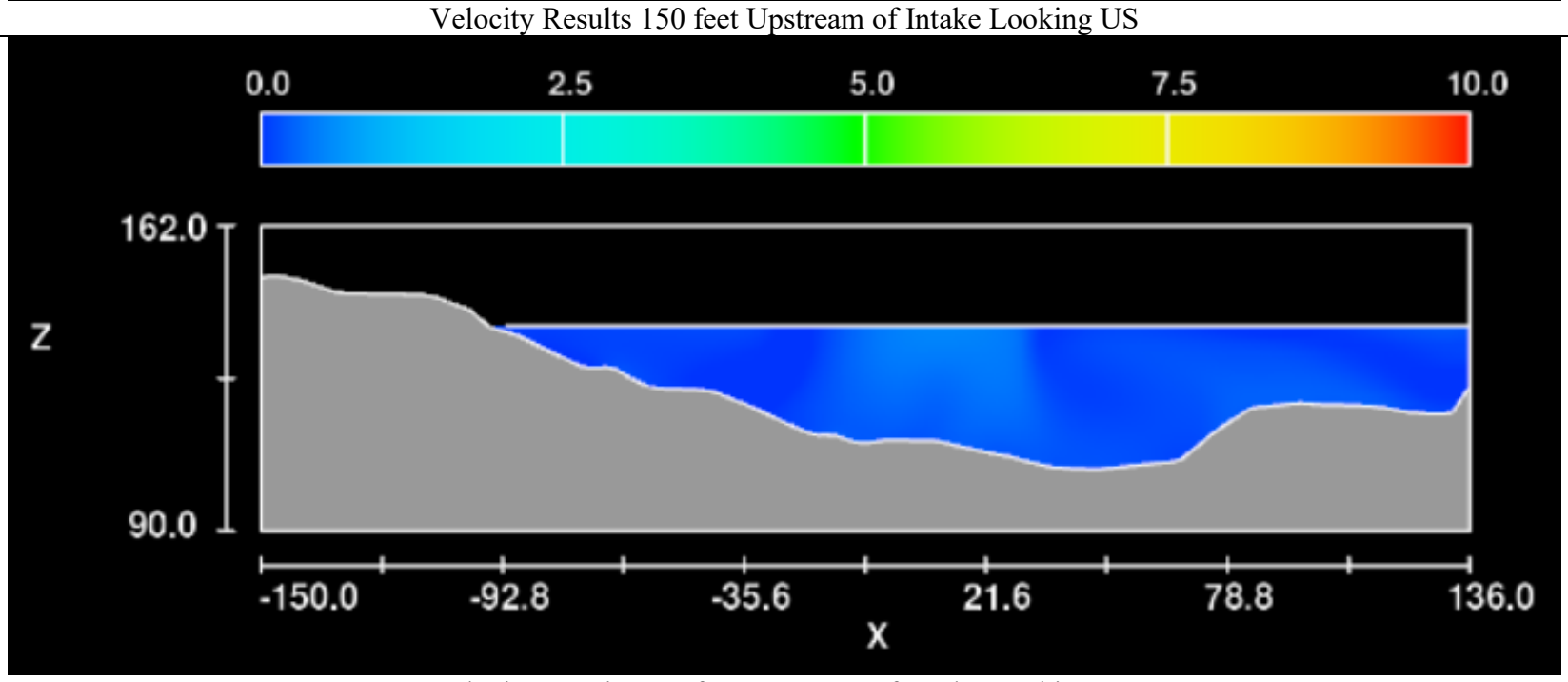


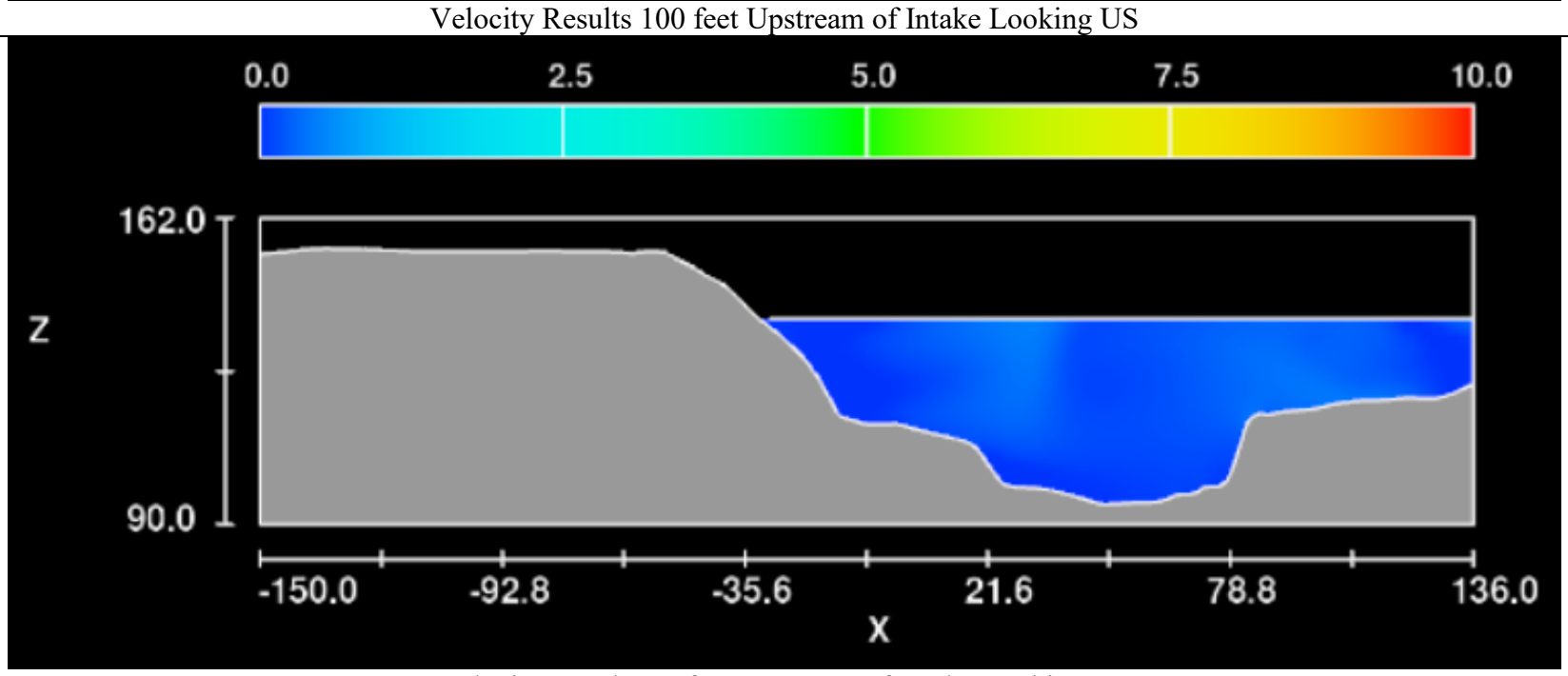
Figure 6.2.1-6: Simulated Velocities at Three Locations in Front of the Intake for Lowest Production Flow (1,320 cfs)



Velocity Results 150 feet Upstream of Intake Looking US



Velocity Results 100 feet Upstream of Intake Looking US



Velocity Results 50 feet Upstream of Intake Looking US

Figure 6.2.1-7: Velocity Magnitude and Orientation for Lowest Production Flow 50 feet Upstream of Intake

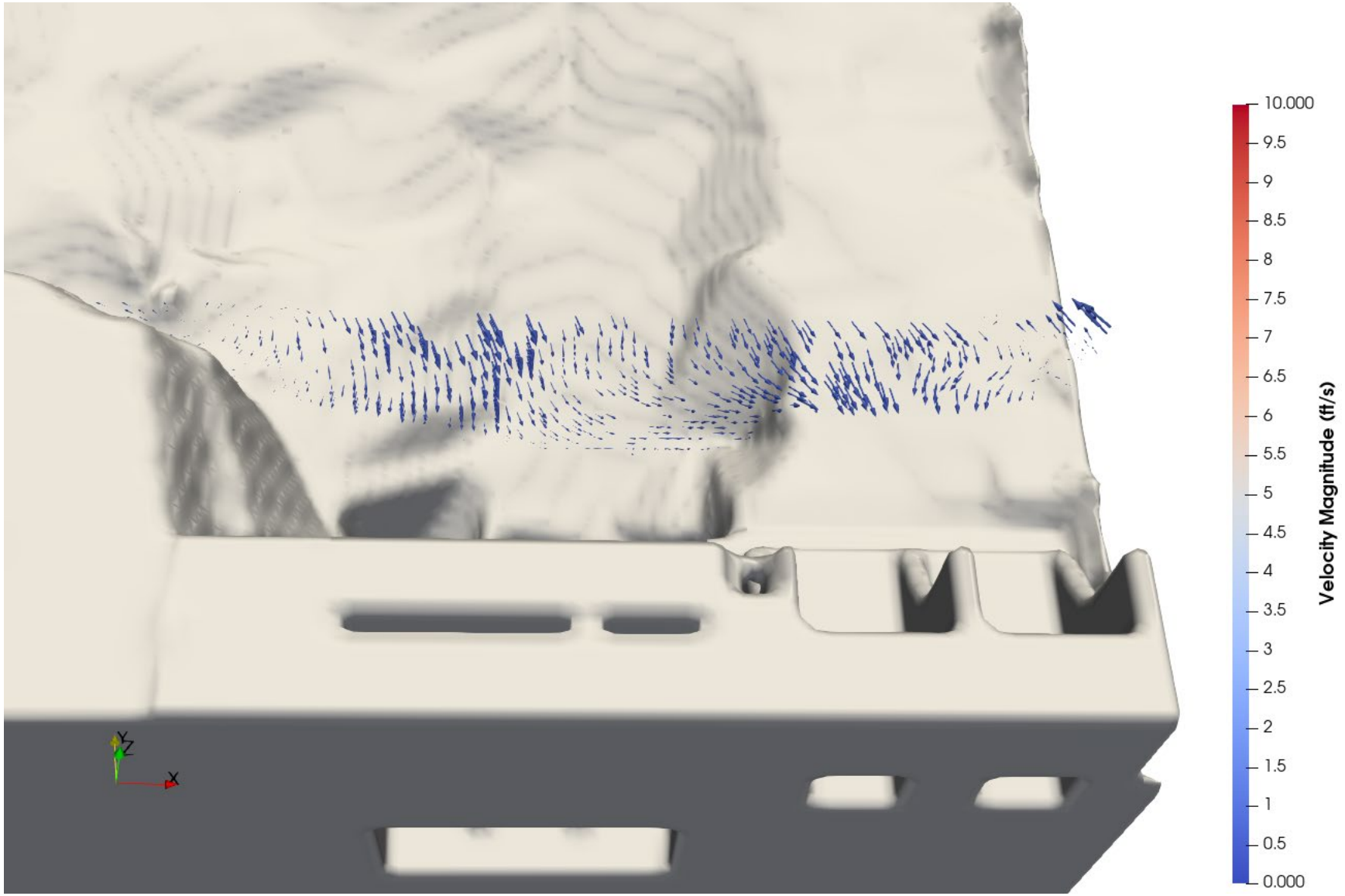


Figure 6.2.1-8: Velocity Magnitude and Orientation for Lowest Production Flow 100 feet Upstream of Intake

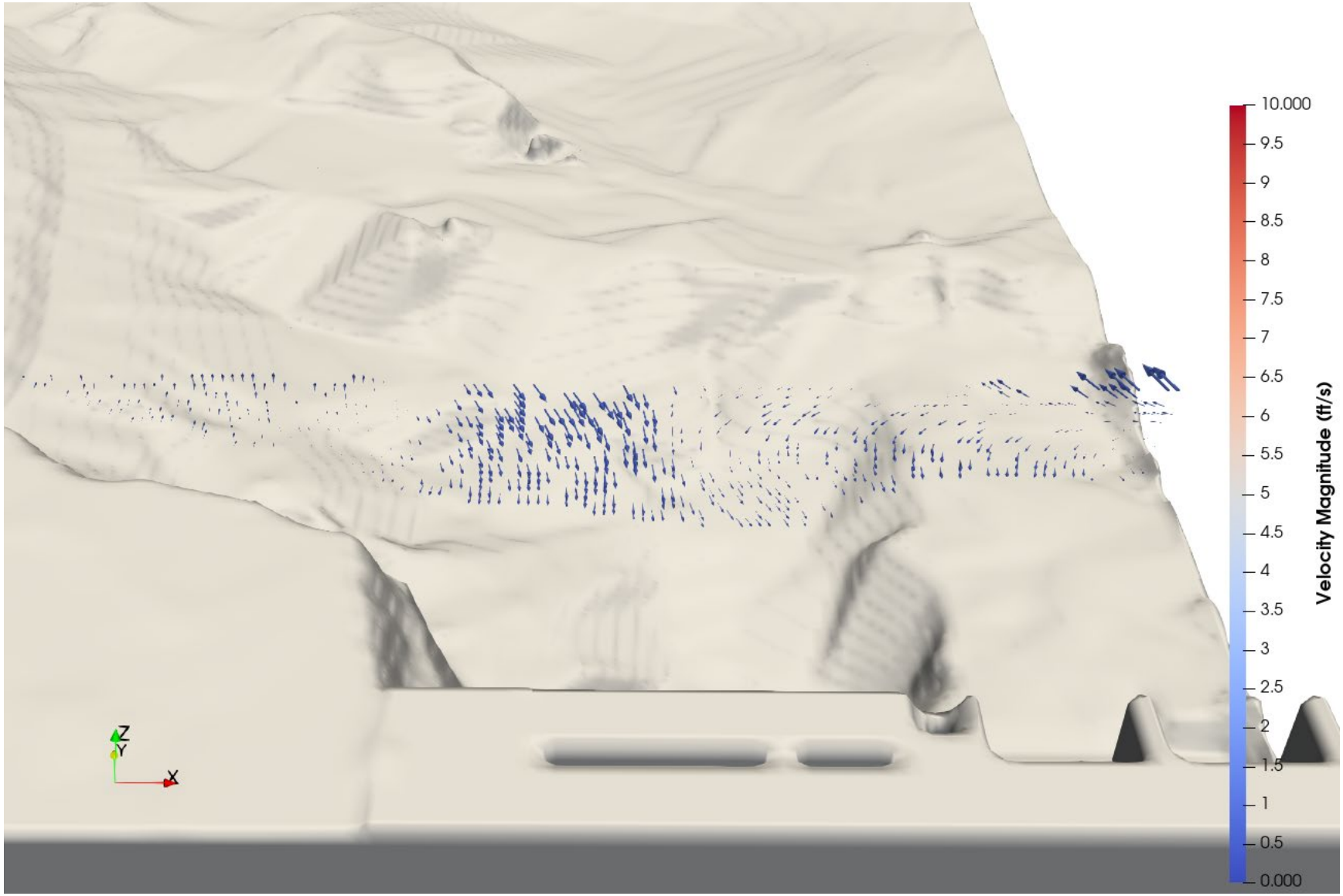


Figure 6.2.1-9: Velocity Magnitude and Orientation for Lowest Production Flow 150 feet Upstream of Intake

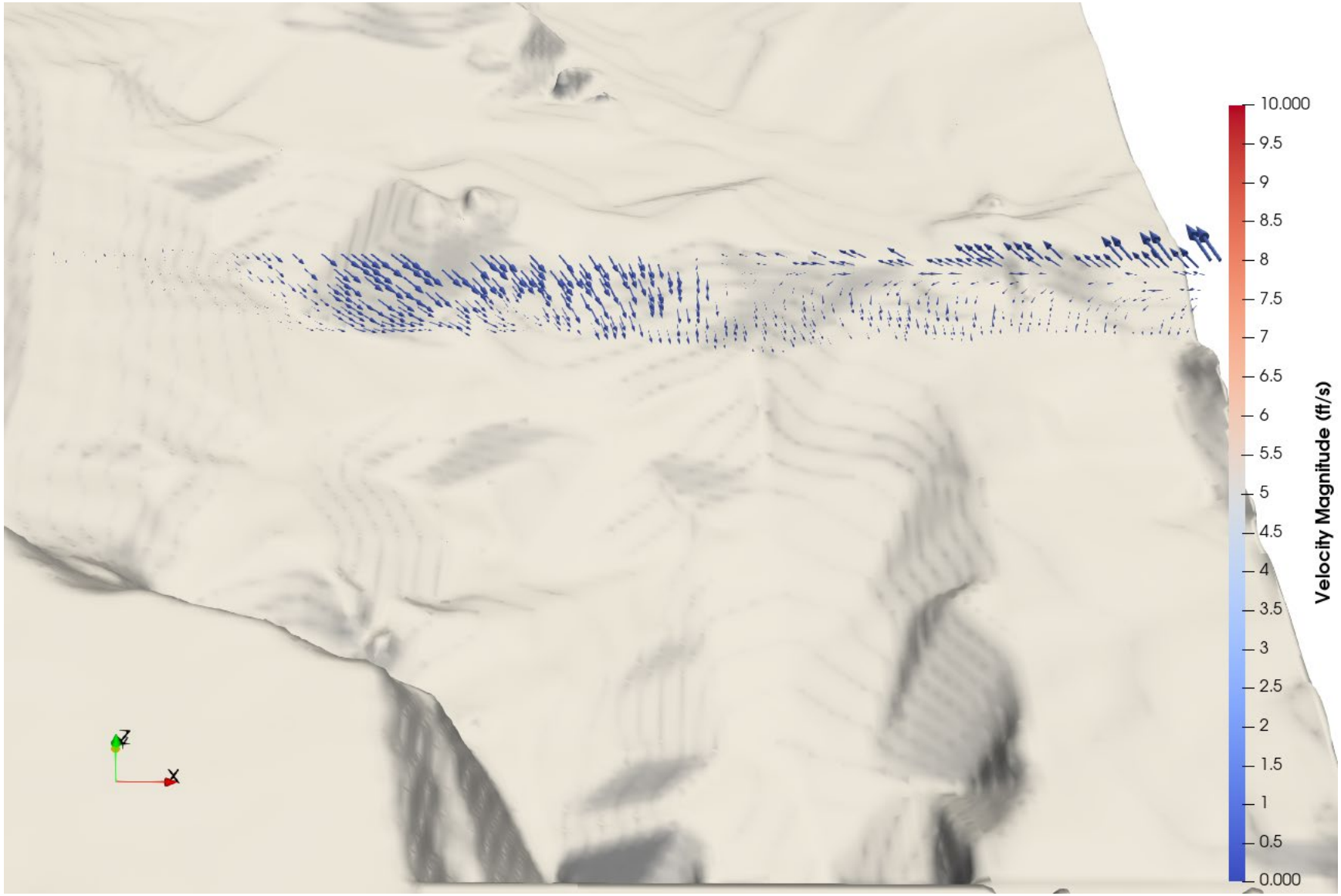
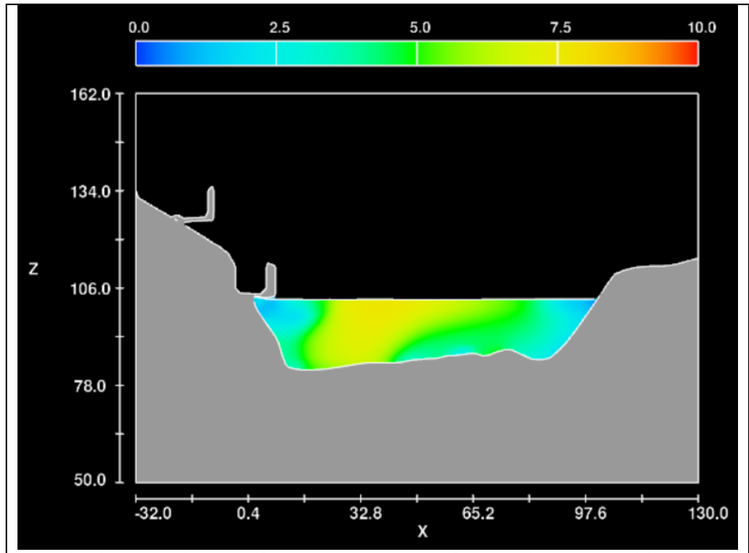


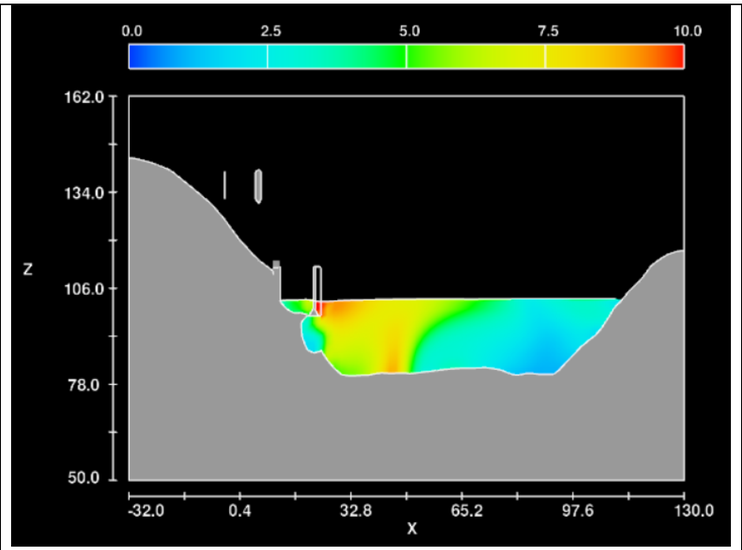
Figure 6.2.2-1: Location of Tailrace Model Velocity Planes



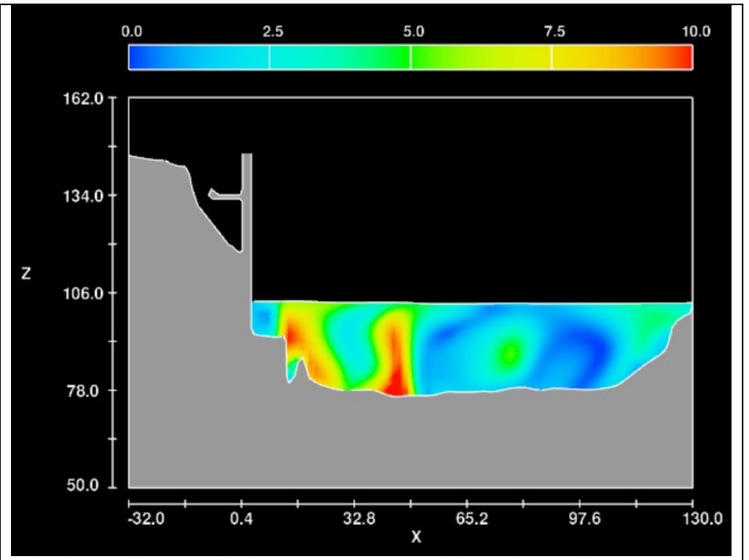
Figure 6.2.2-2: Simulated Velocities at Three Locations Downstream of the Powerhouse for Highest Production Flow (7,595 cfs)



Velocity Results 150 feet Downstream of Powerhouse Looking US

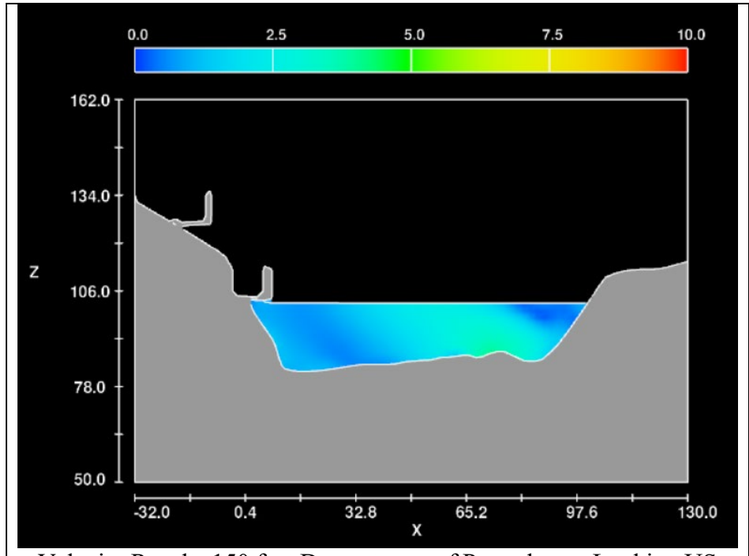


Velocity Results 100 feet Downstream of Powerhouse Looking US

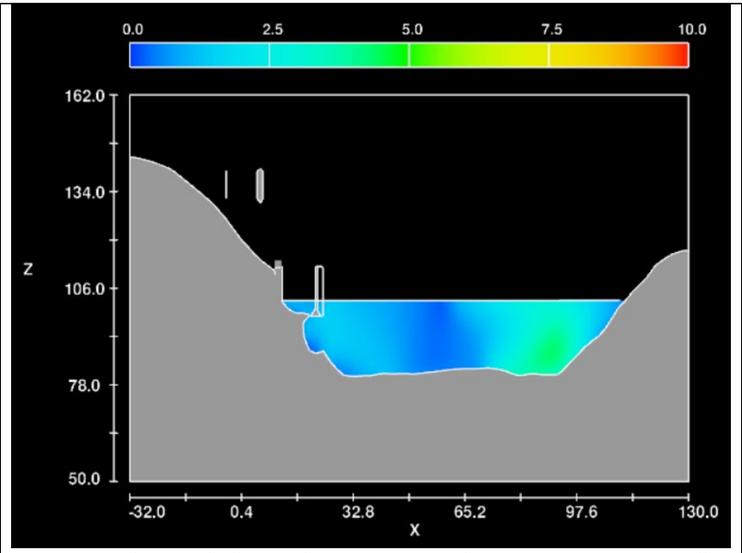


Velocity Results 50 feet Downstream of Powerhouse Looking US

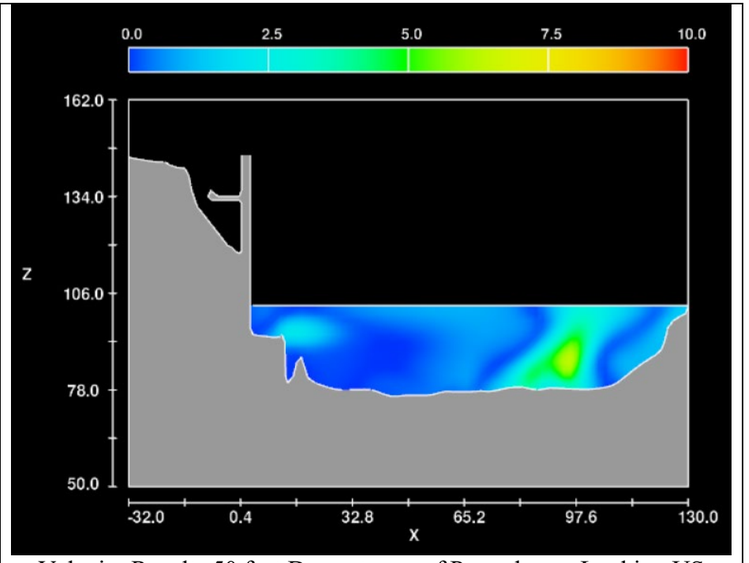
Figure 6.2.2-3: Simulated Velocities at Three Locations Downstream of the Powerhouse for Lowest Production Flow (1,320 cfs)



Velocity Results 150 feet Downstream of Powerhouse Looking US



Velocity Results 100 feet Downstream of Powerhouse Looking US



Velocity Results 50 feet Downstream of Powerhouse Looking US

Figure 6.2.2-4: Velocity Magnitude and Orientation for Highest Production Flow (7,595 cfs) 50 feet Downstream of Powerhouse

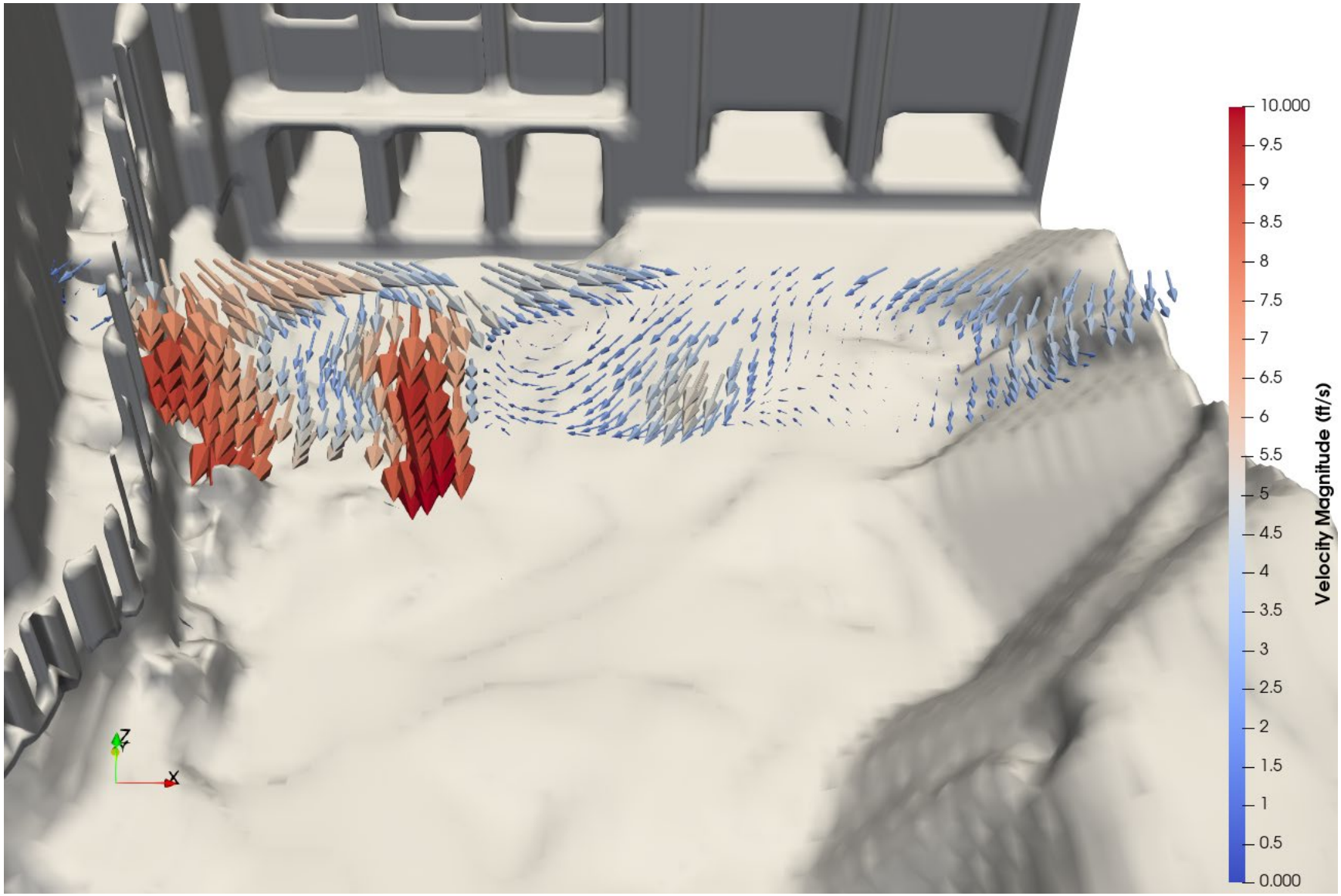


Figure 6.2.2-5: Velocity Magnitude and Orientation Highest Production Flow (7,595 cfs) 100 feet Downstream of Powerhouse

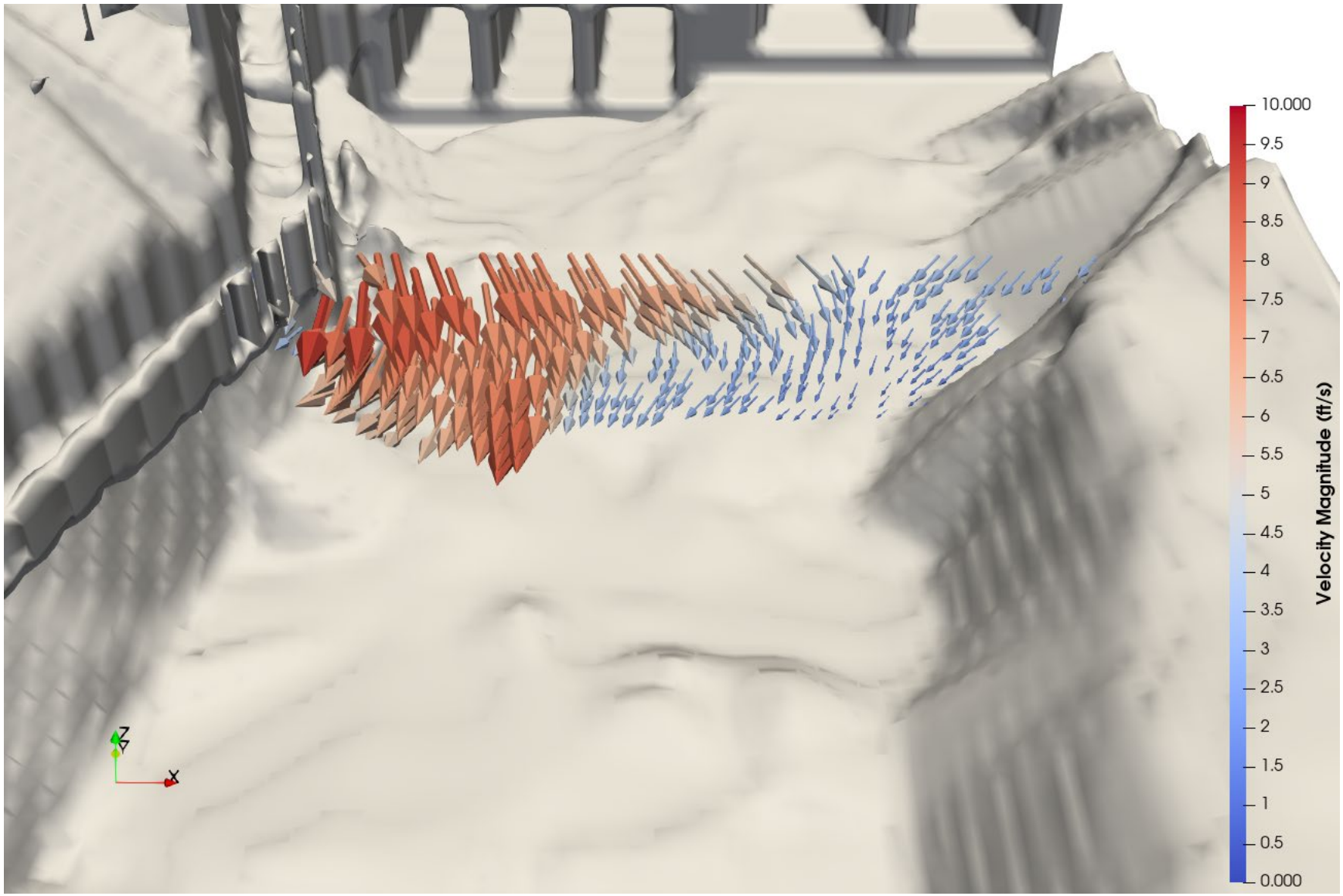


Figure 6.2.2-6: Velocity Magnitude and Orientation for Highest Production Flow (7,595 cfs) 150 feet Downstream of Powerhouse

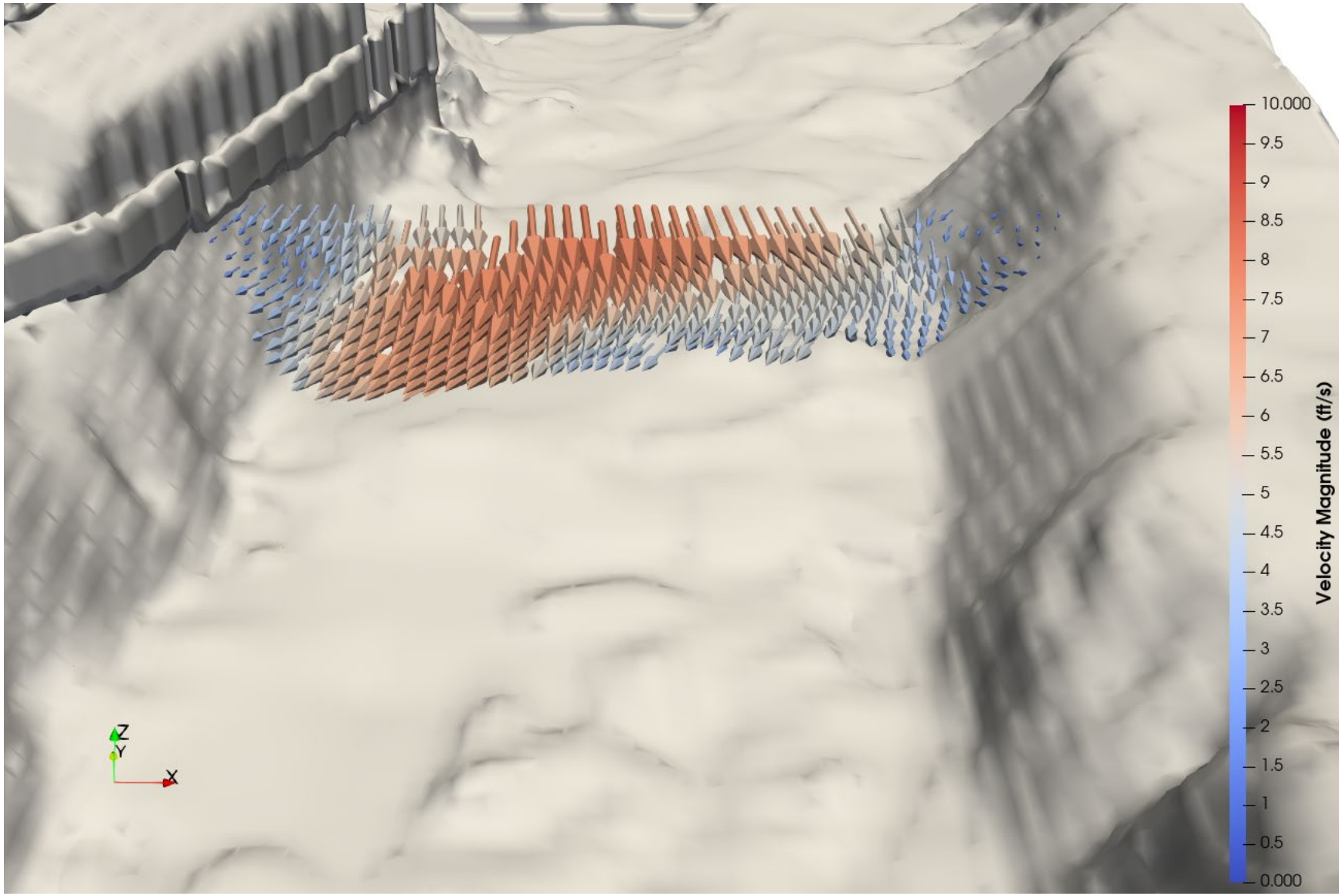


Figure 6.2.2-7: Velocity Magnitude and Orientation for Lowest Production Flow (1,320 cfs) 50 feet Downstream of Powerhouse

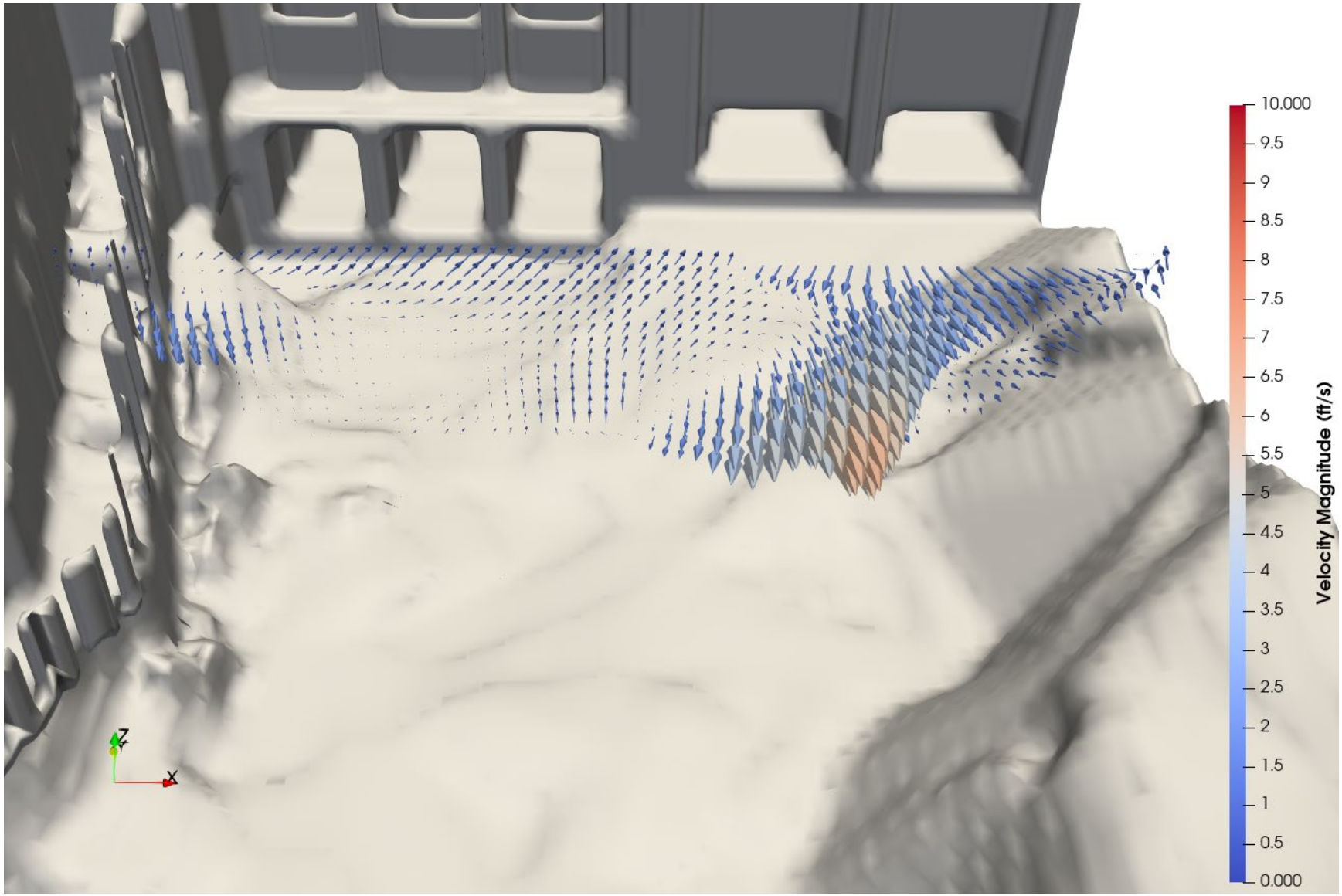


Figure 6.2.2-8: Velocity Magnitude and Orientation for Lowest Production Flow (1,320 cfs) 100 ft Downstream of Powerhouse

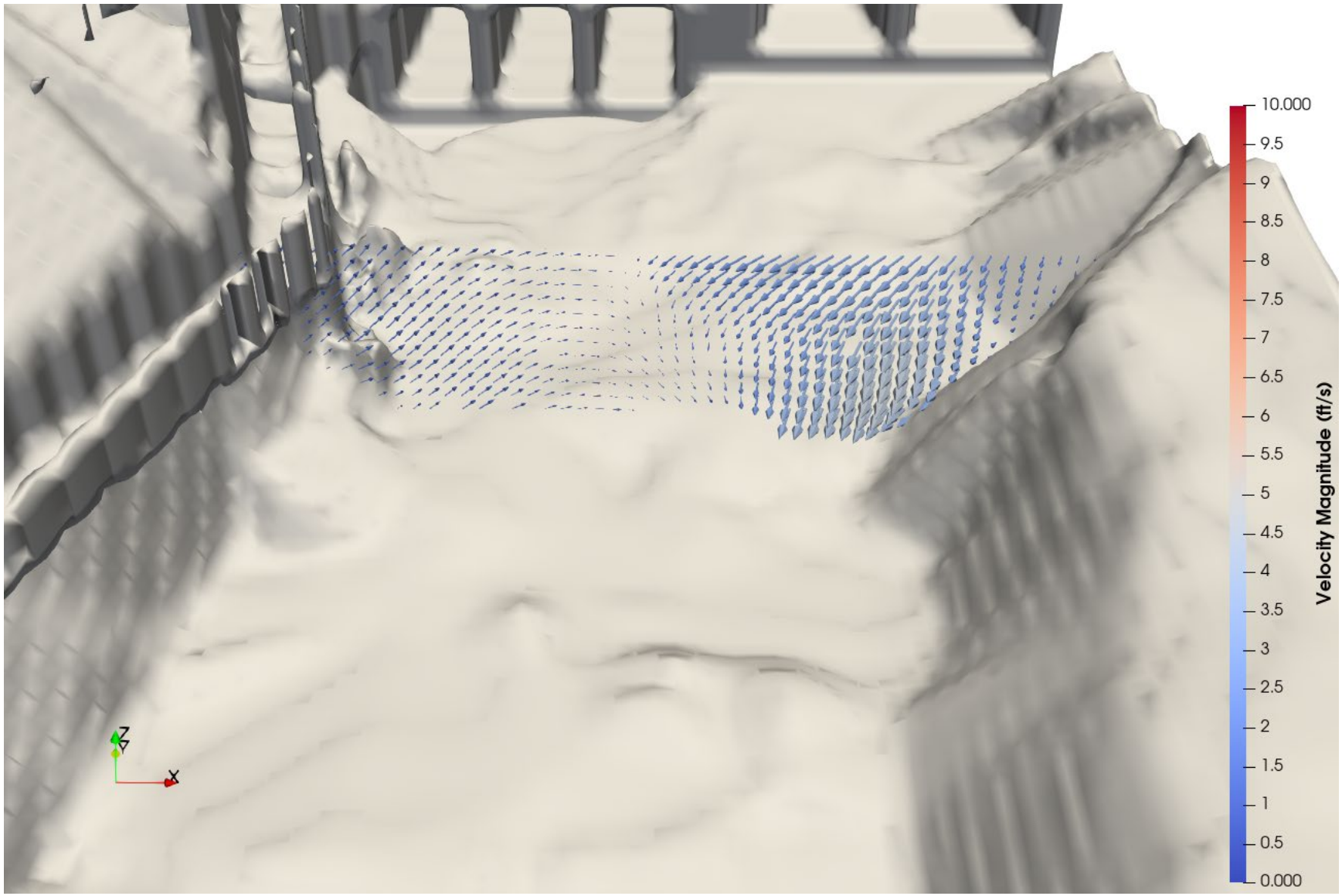


Figure 6.2.2-9: Velocity Magnitude and Orientation for Lowest Production Flow (1,320 cfs) 150 ft Downstream of Powerhouse

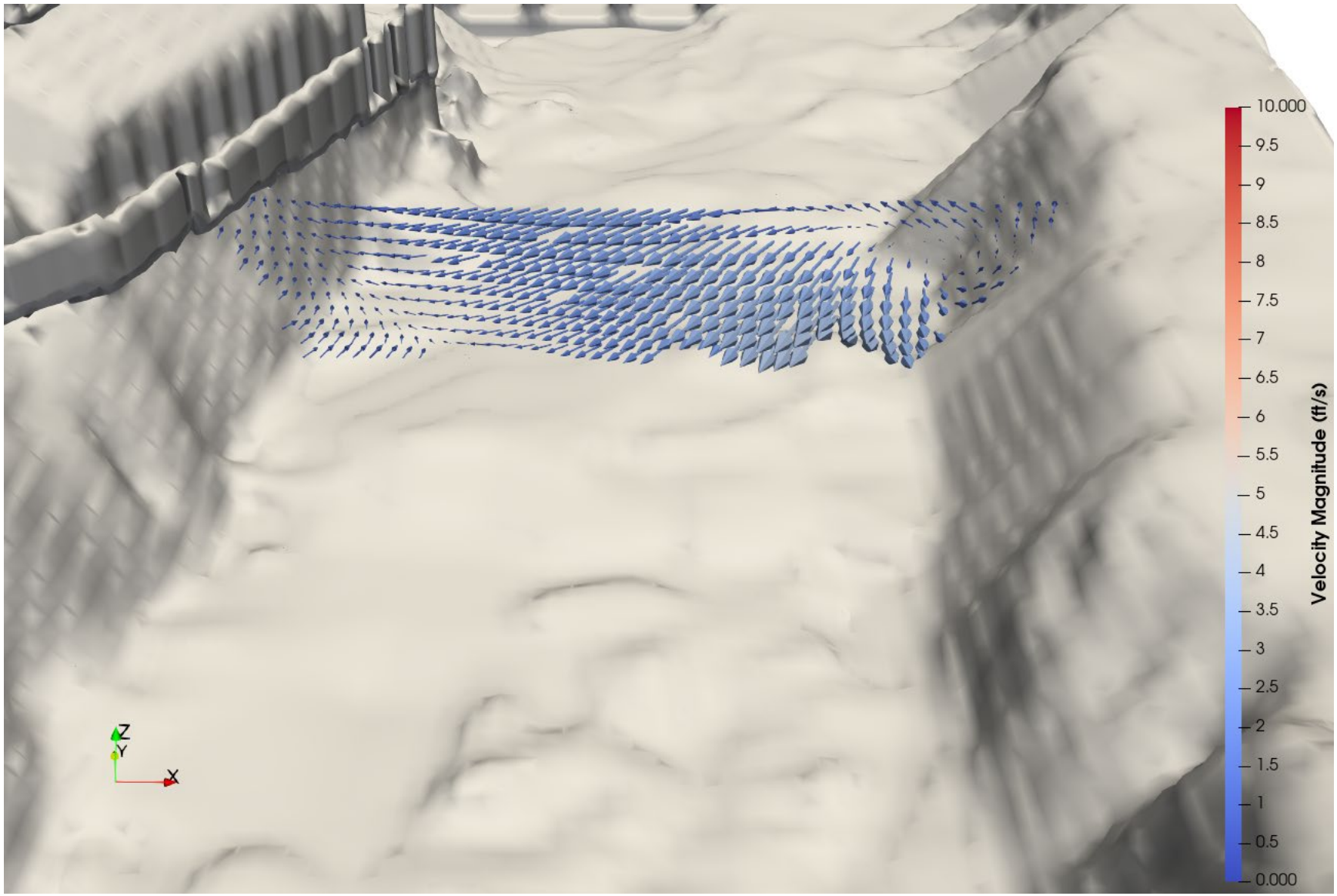


Figure 6.2.3-1: Simulated Depths in the Bypass Channel (100 cfs)

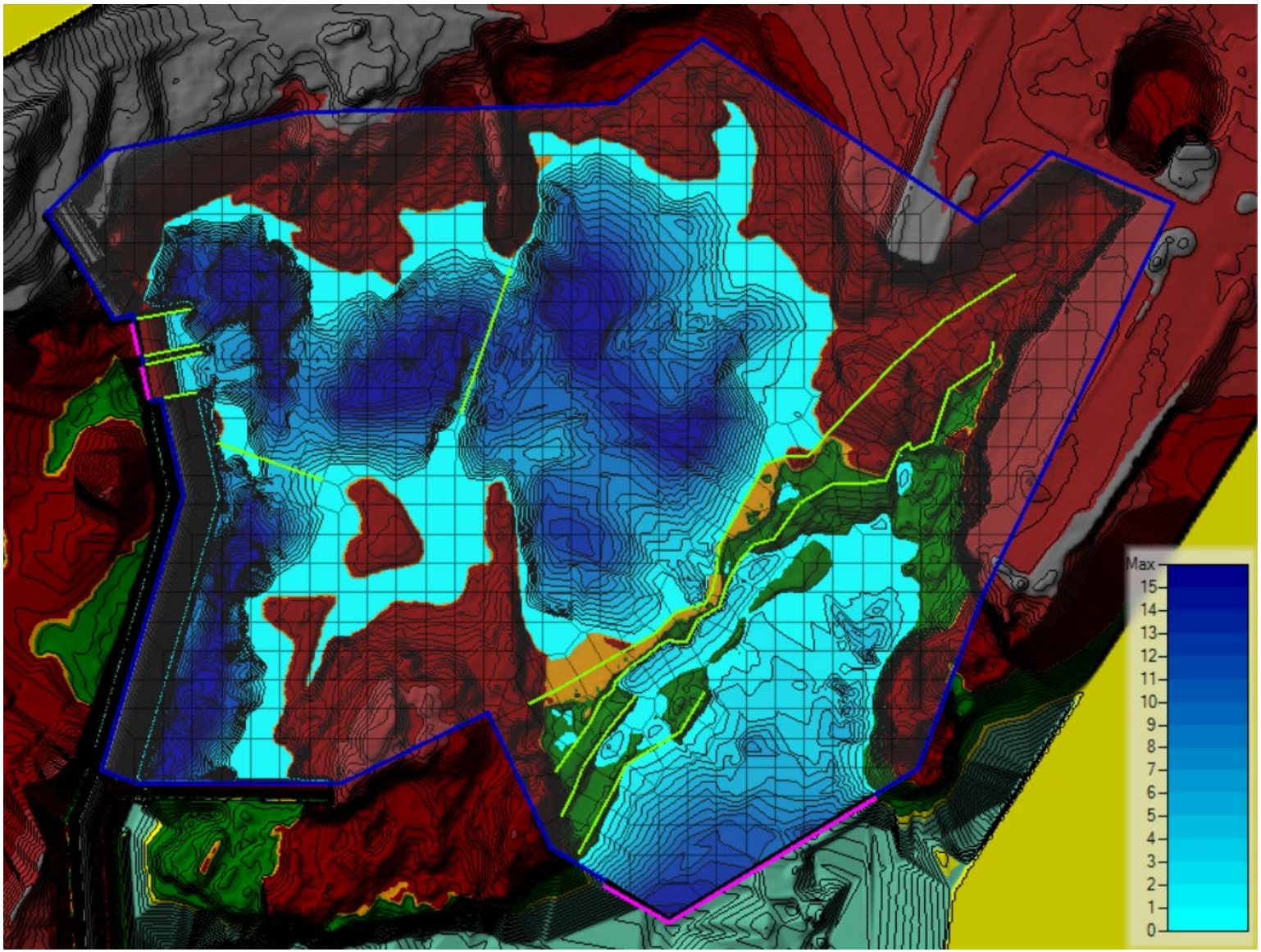


Figure 6.2.3-2: Simulated Velocities in the Bypass Channel (100 cfs)

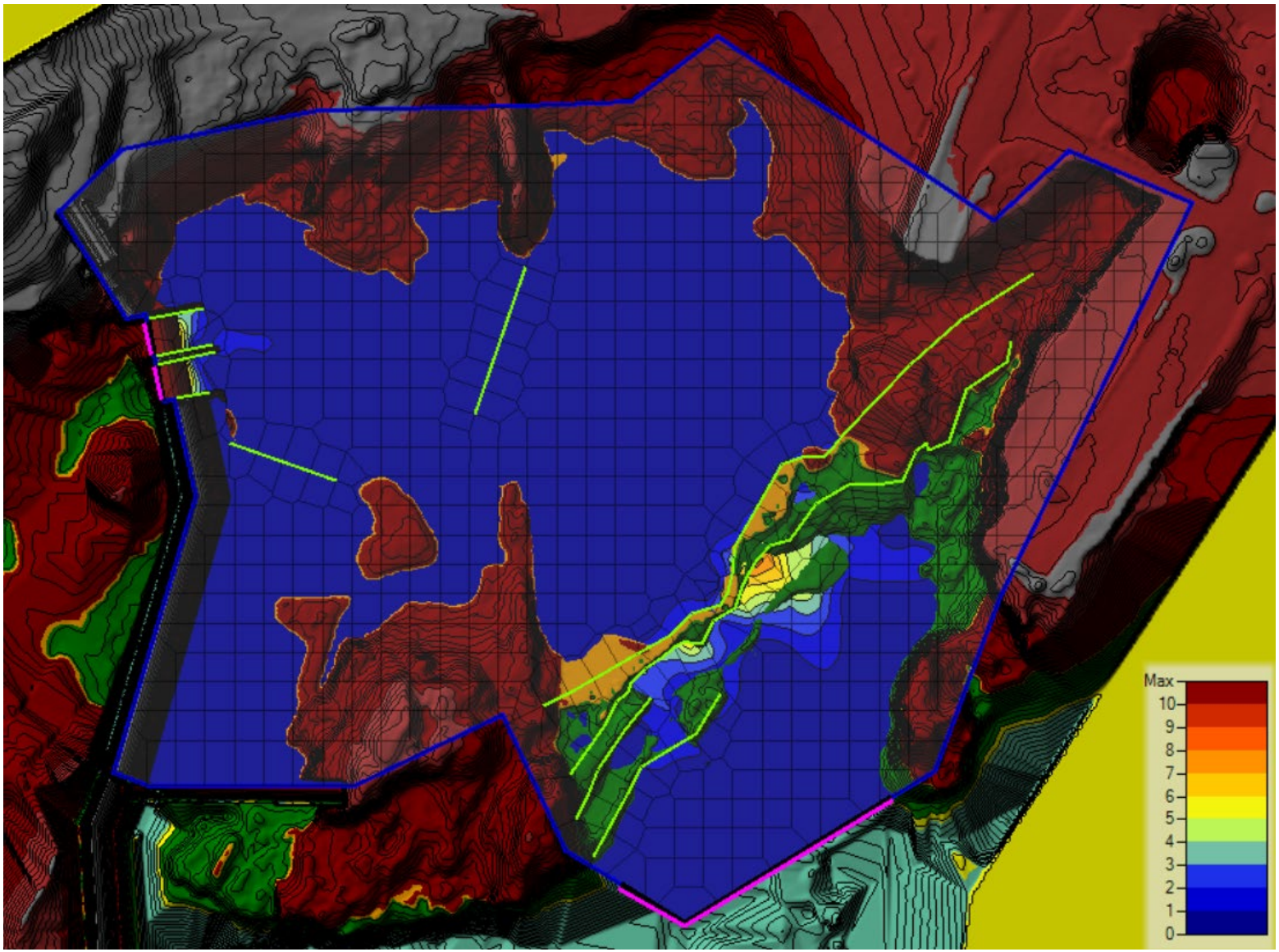


Figure 6.2.3-3: Simulated Depths in the Bypass Channel (930 cfs)

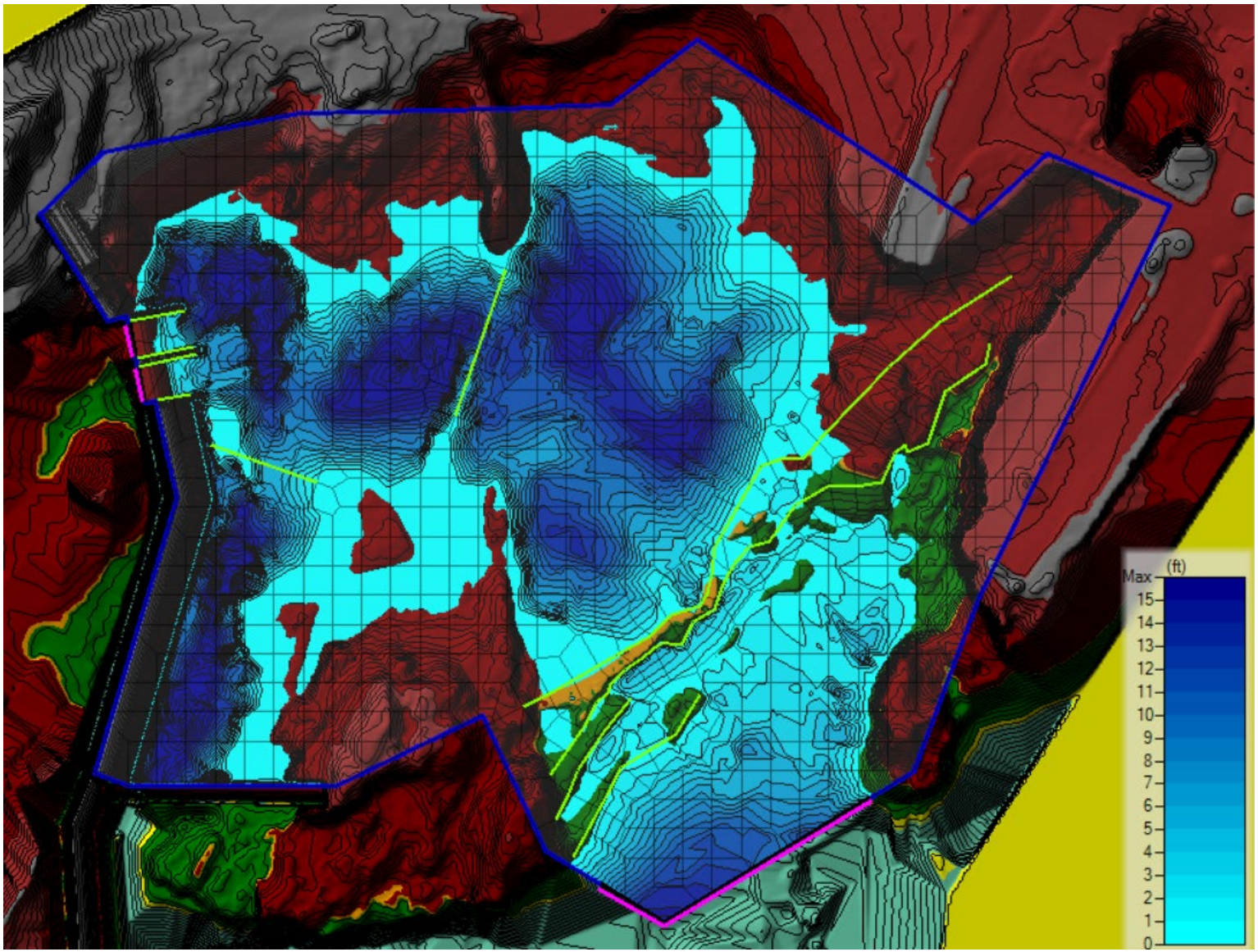


Figure 6.2.3-4: Simulated Velocities in the Bypass Channel (930 cfs)

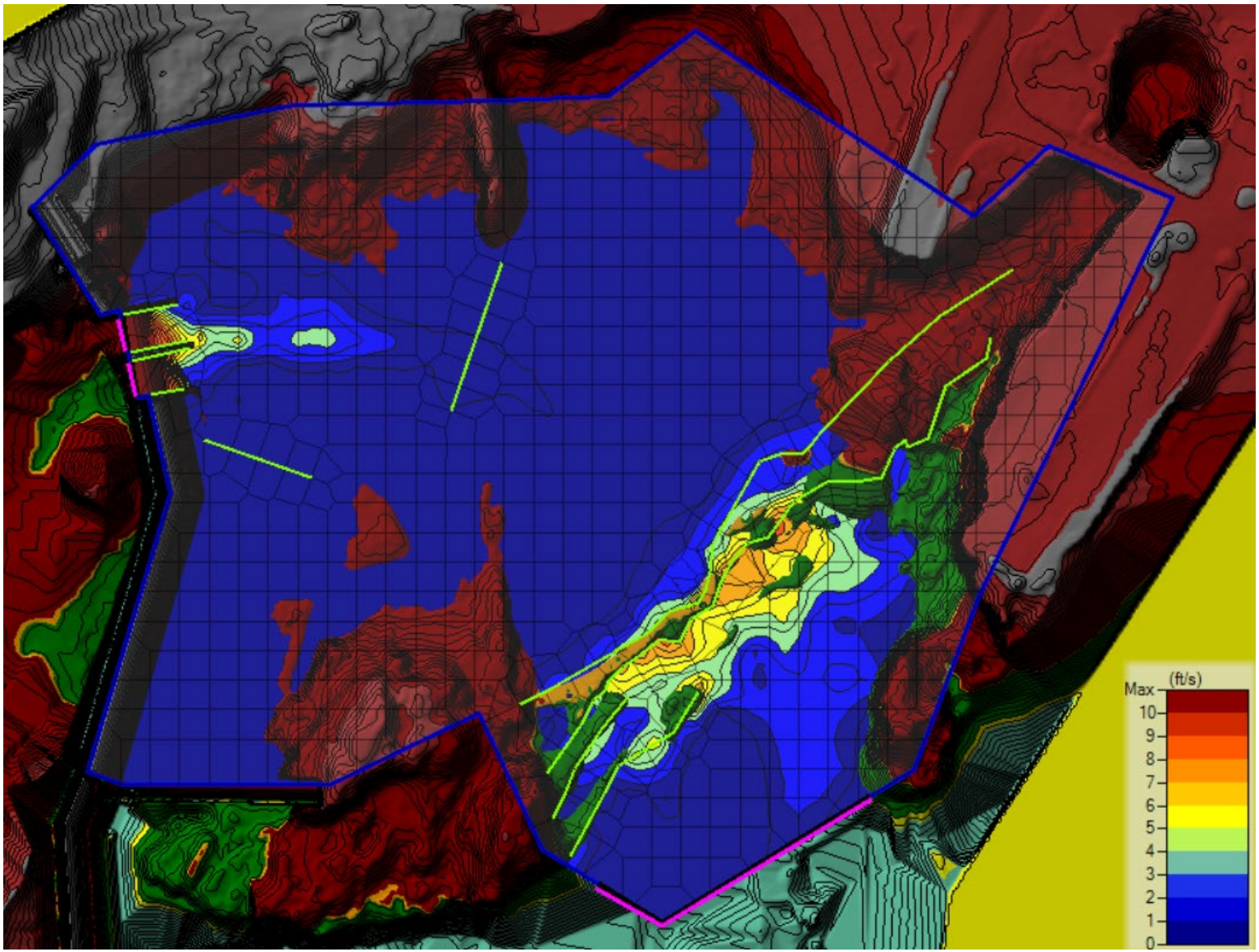


Figure 6.2.3-5: Simulated Depths in the Bypass Channel (1,760 cfs)

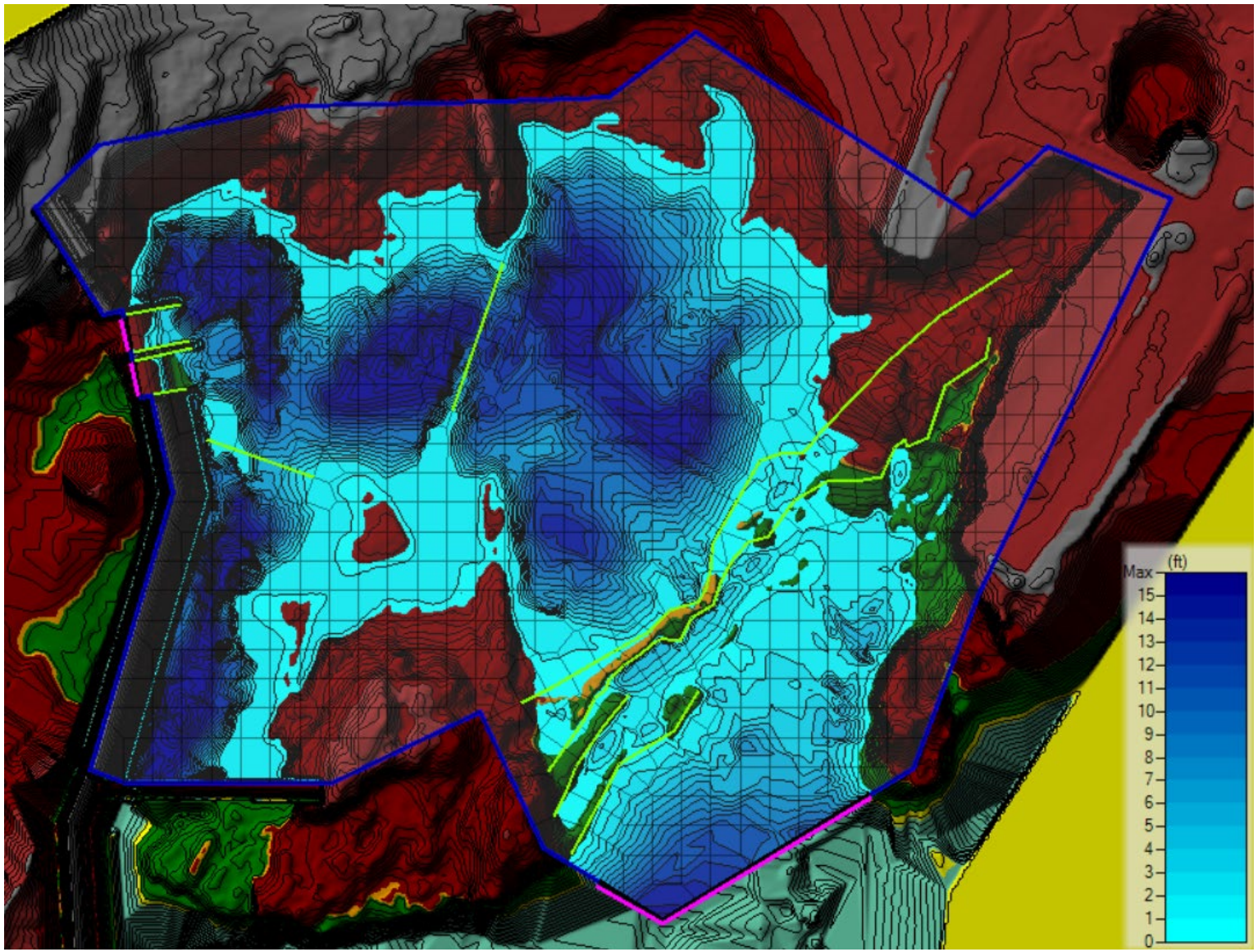


Figure 6.2.3-6: Simulated Velocities in the Bypass Channel (1,760 cfs)

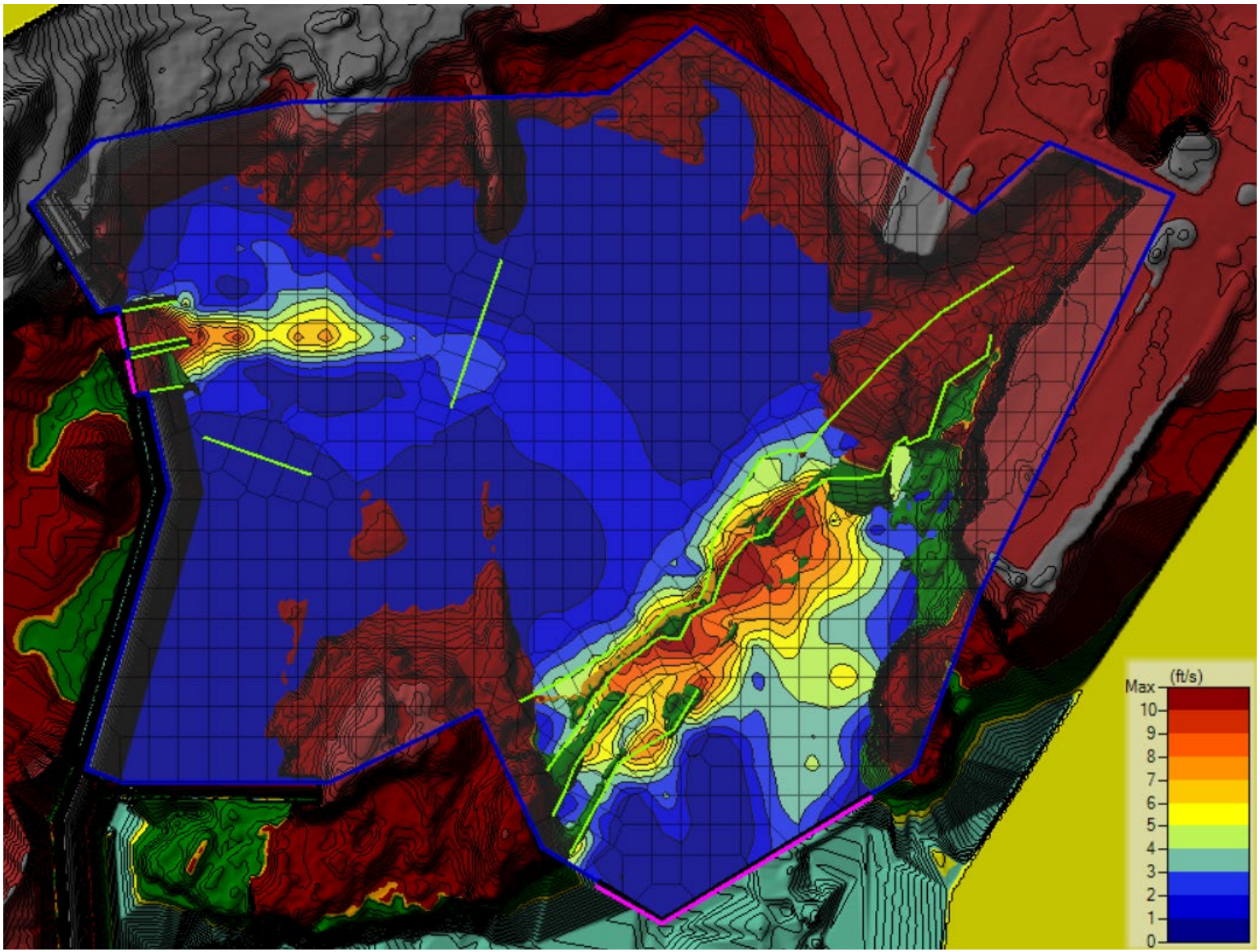


Figure 6.2.3-7: Simulated Depths in the Bypass Channel (2,690 cfs)

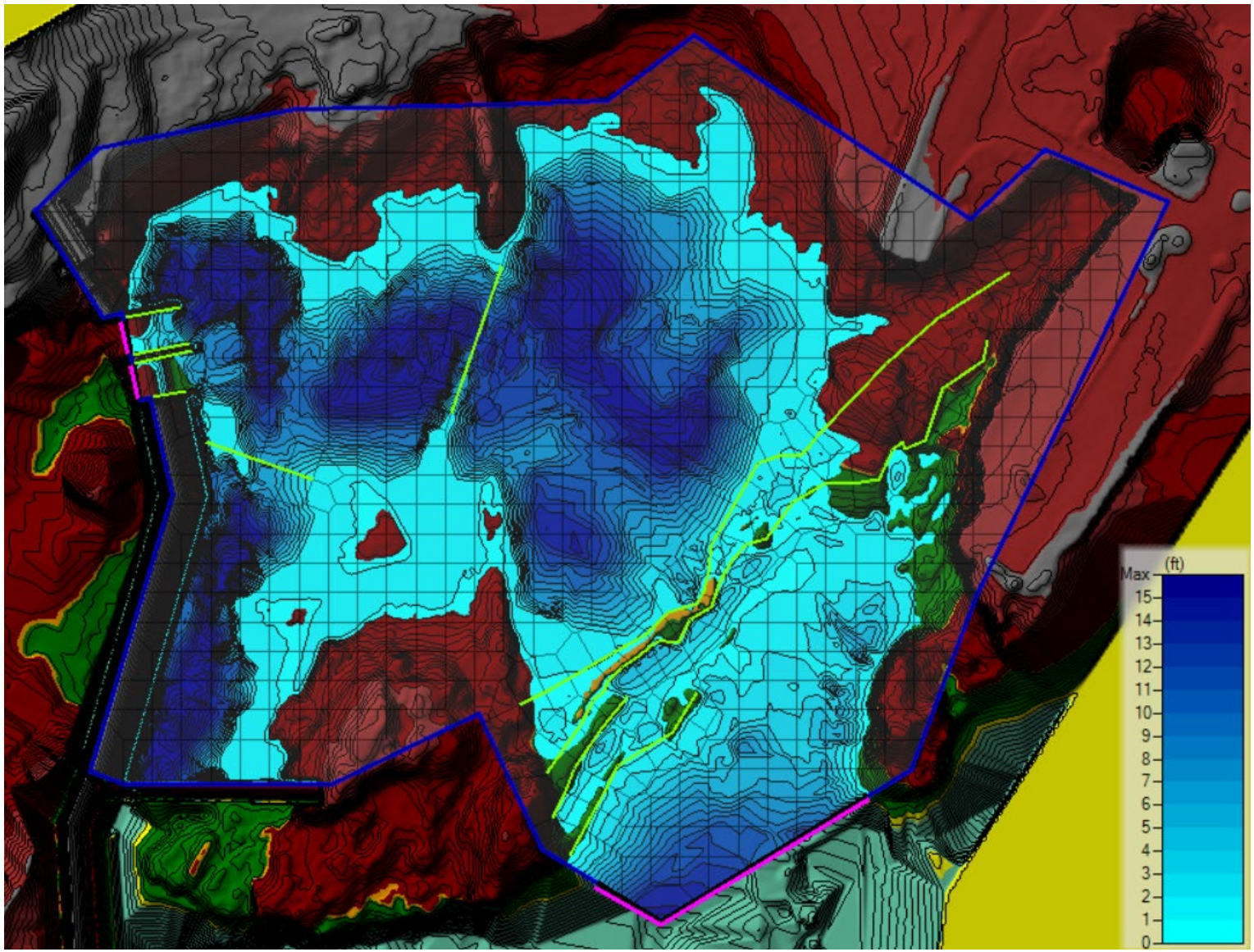


Figure 6.2.3-8: Simulated Velocities in the Bypass Channel (2,690 cfs)

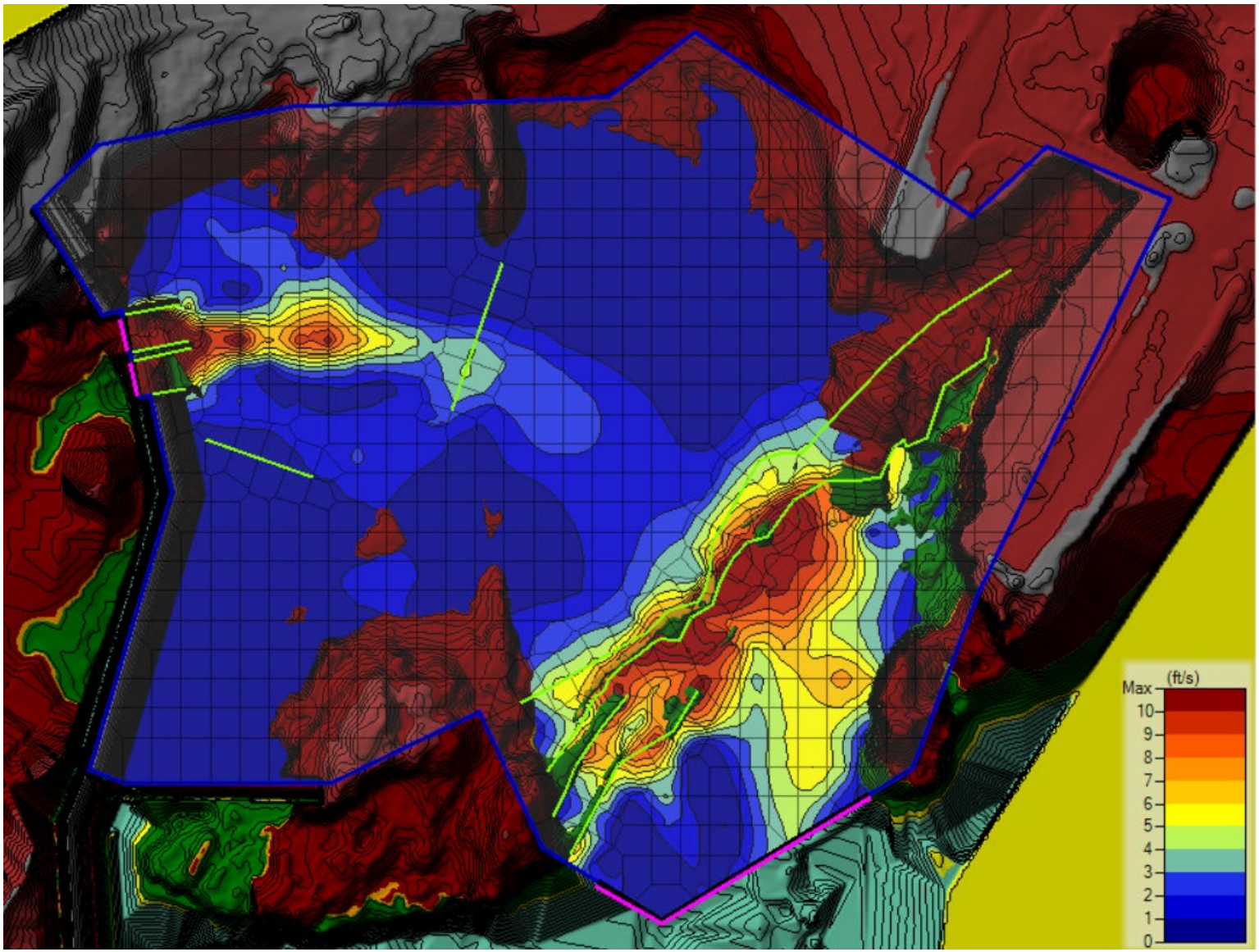


Figure 6.2.3-9: Simulated Depths in the Bypass Channel (3,625 cfs)

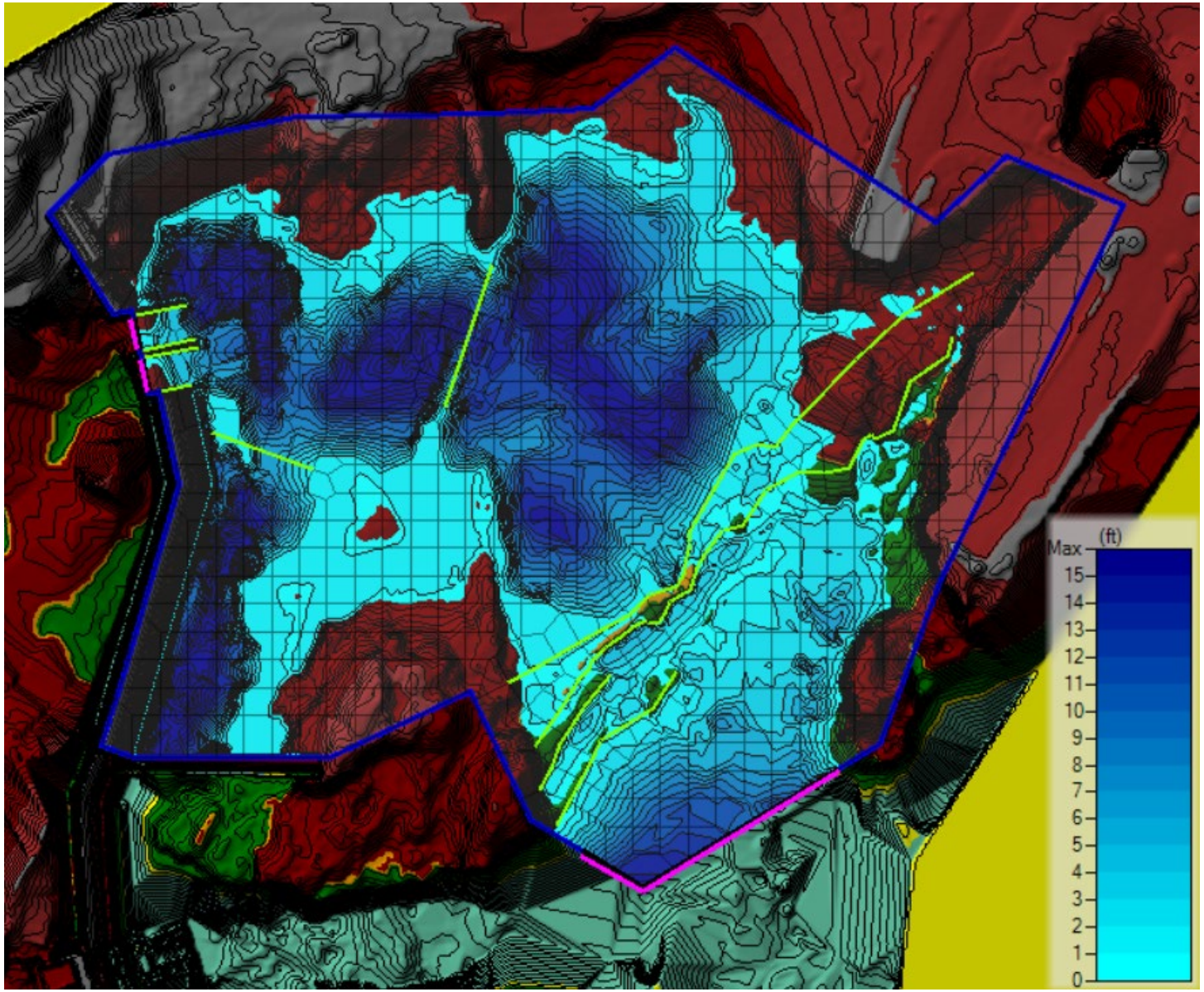


Figure 6.2.3-10: Simulated Velocities in the Bypass Channel (3,625 cfs)

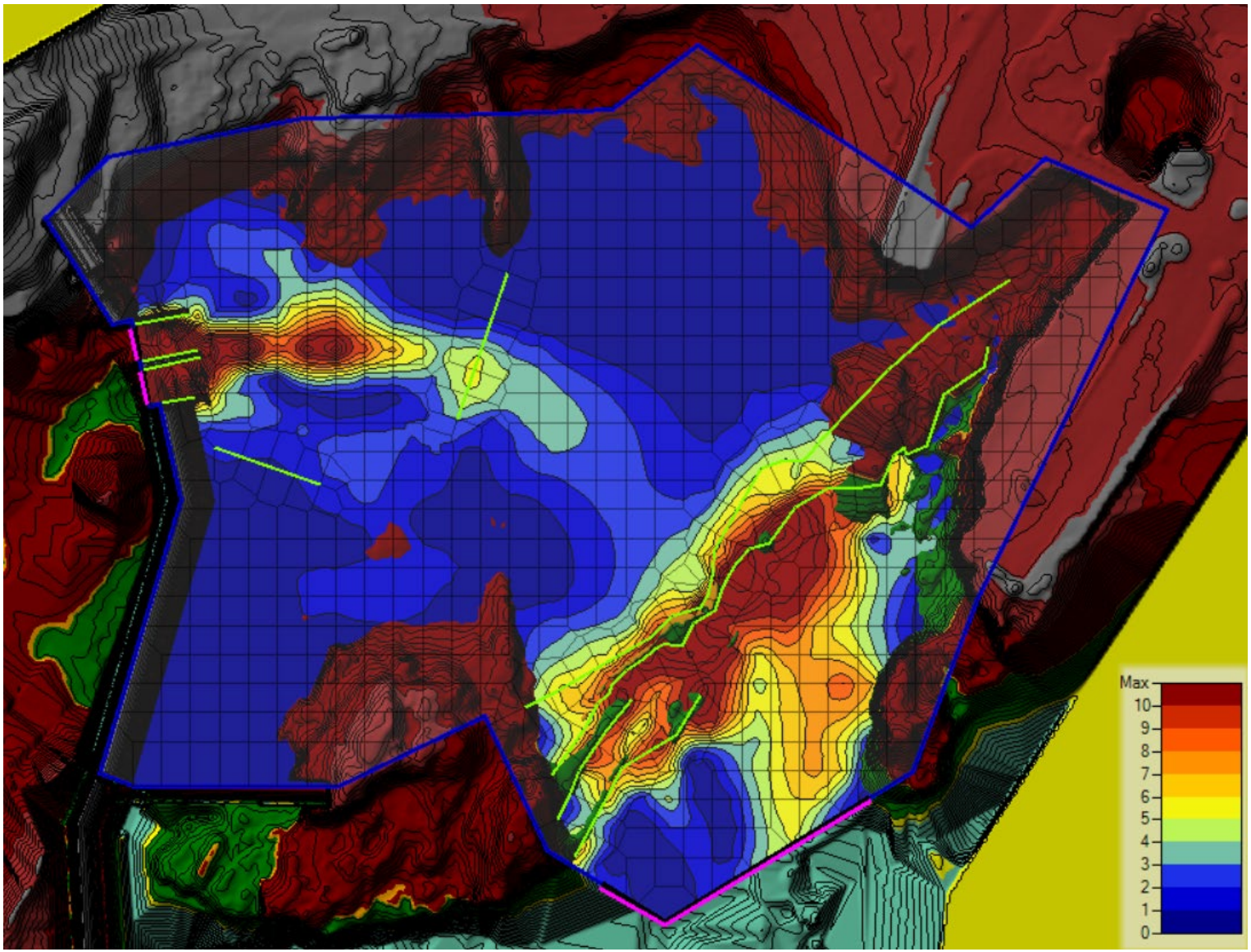


Figure 6.2.3-11: Simulated Depths in the Bypass Channel (7,250 cfs)

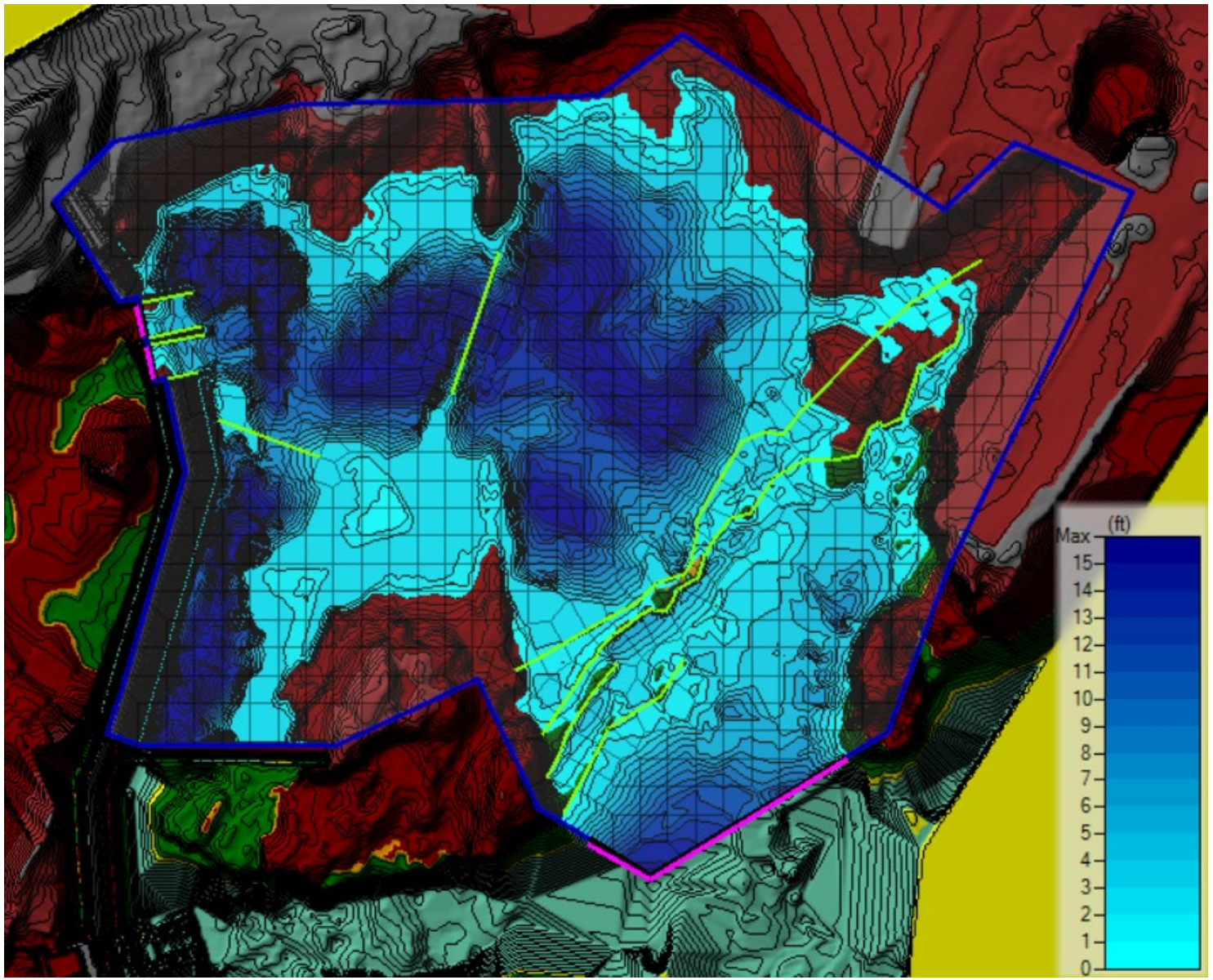


Figure 6.2.3-12: Simulated Velocities in the Bypass Channel (7,250 cfs)

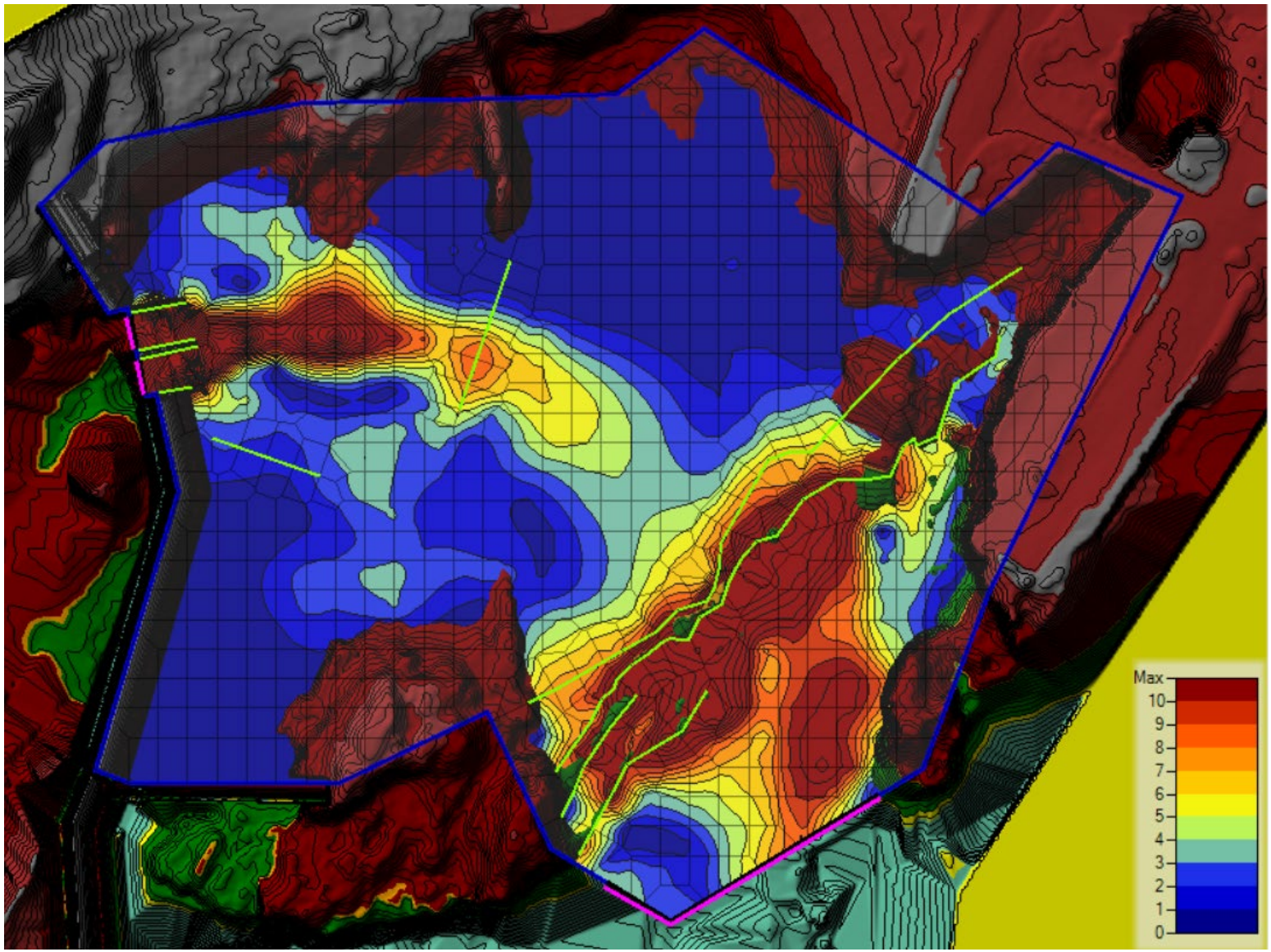


Figure 6.2.3-13: Simulated Depths in the Bypass Channel (10,875 cfs)

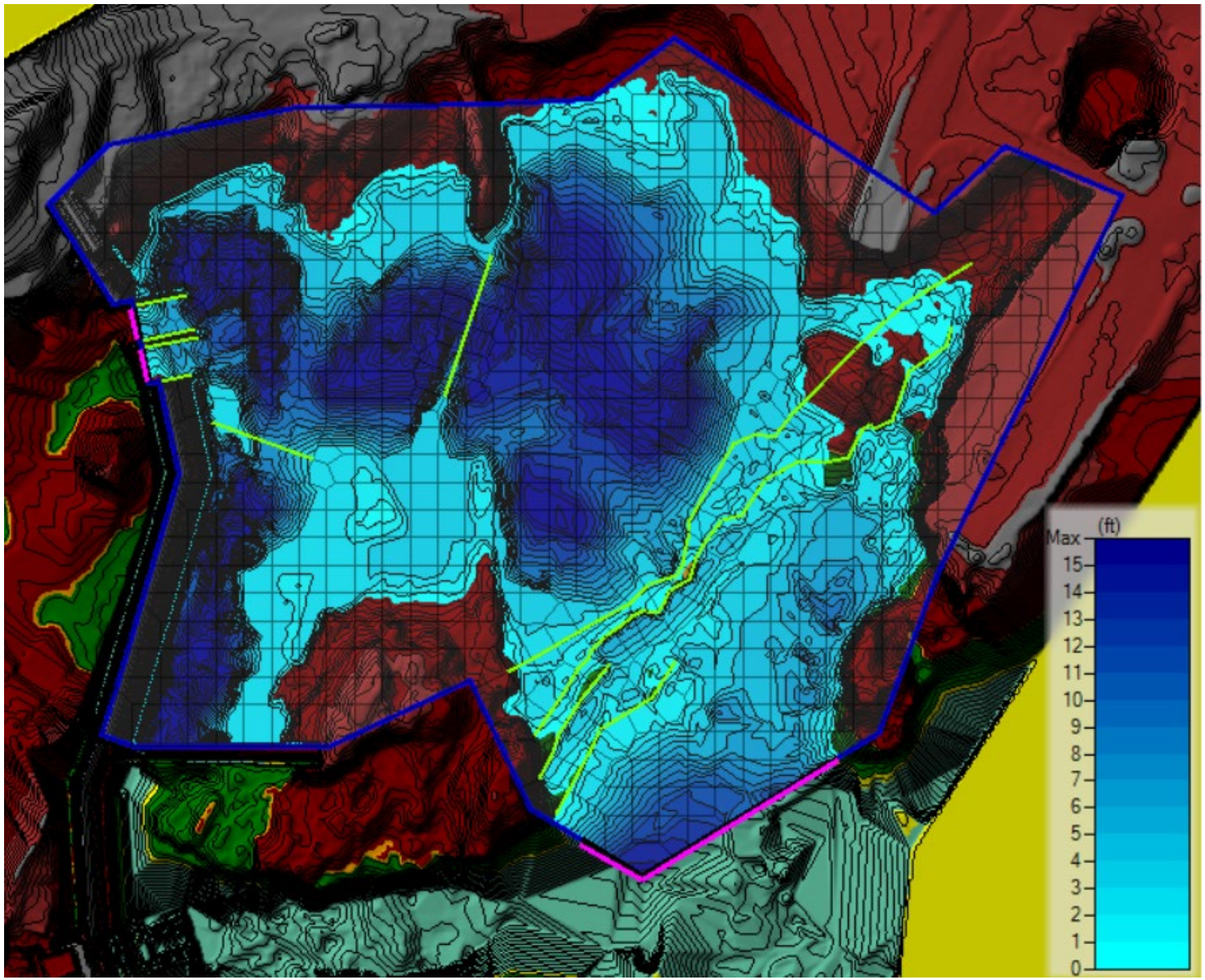


Figure 6.2.3-14: Simulated Velocities in the Bypass Channel (10,875 cfs)

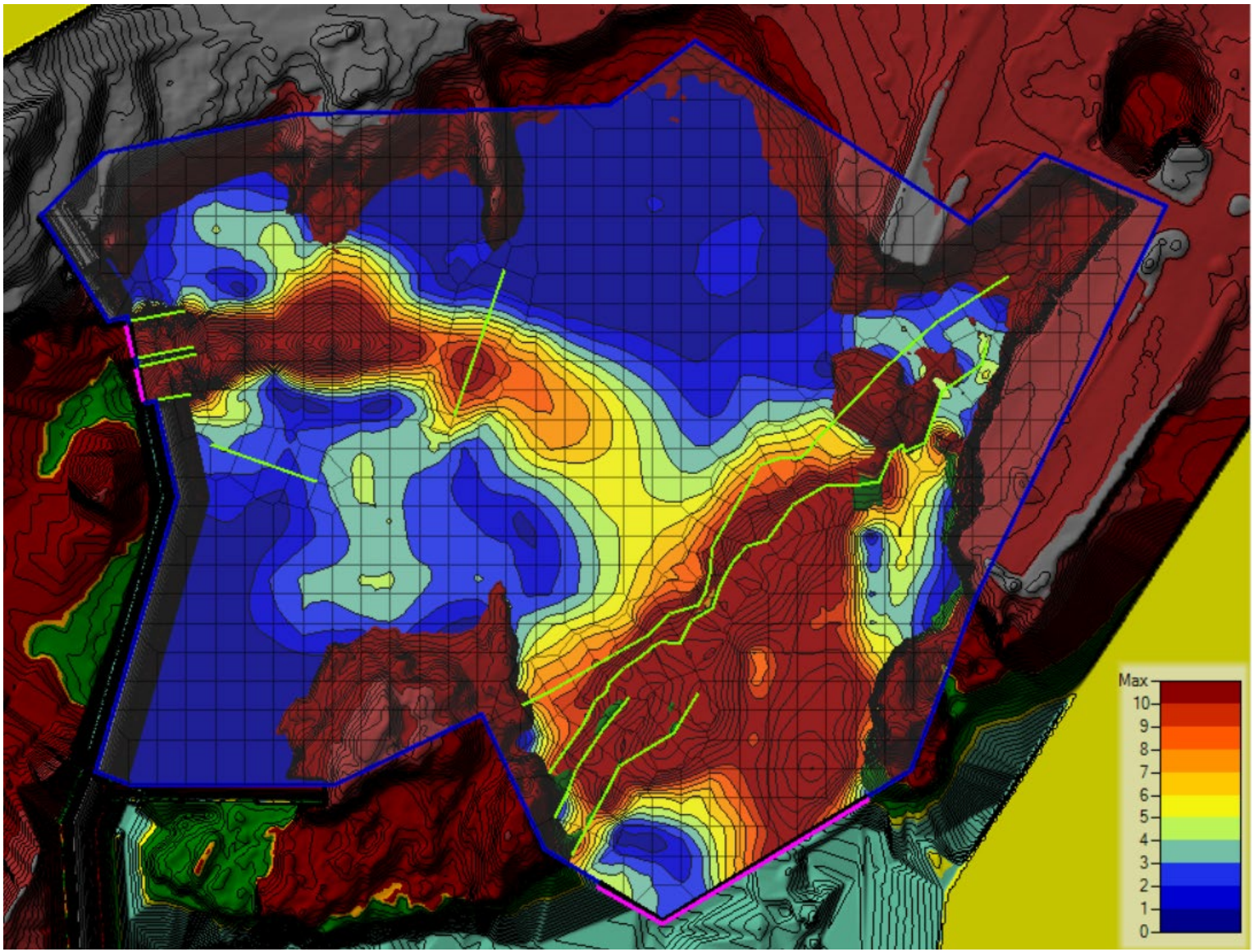


Figure 6.2.3-15: Simulated Depths in the Bypass Channel (14,500 cfs)

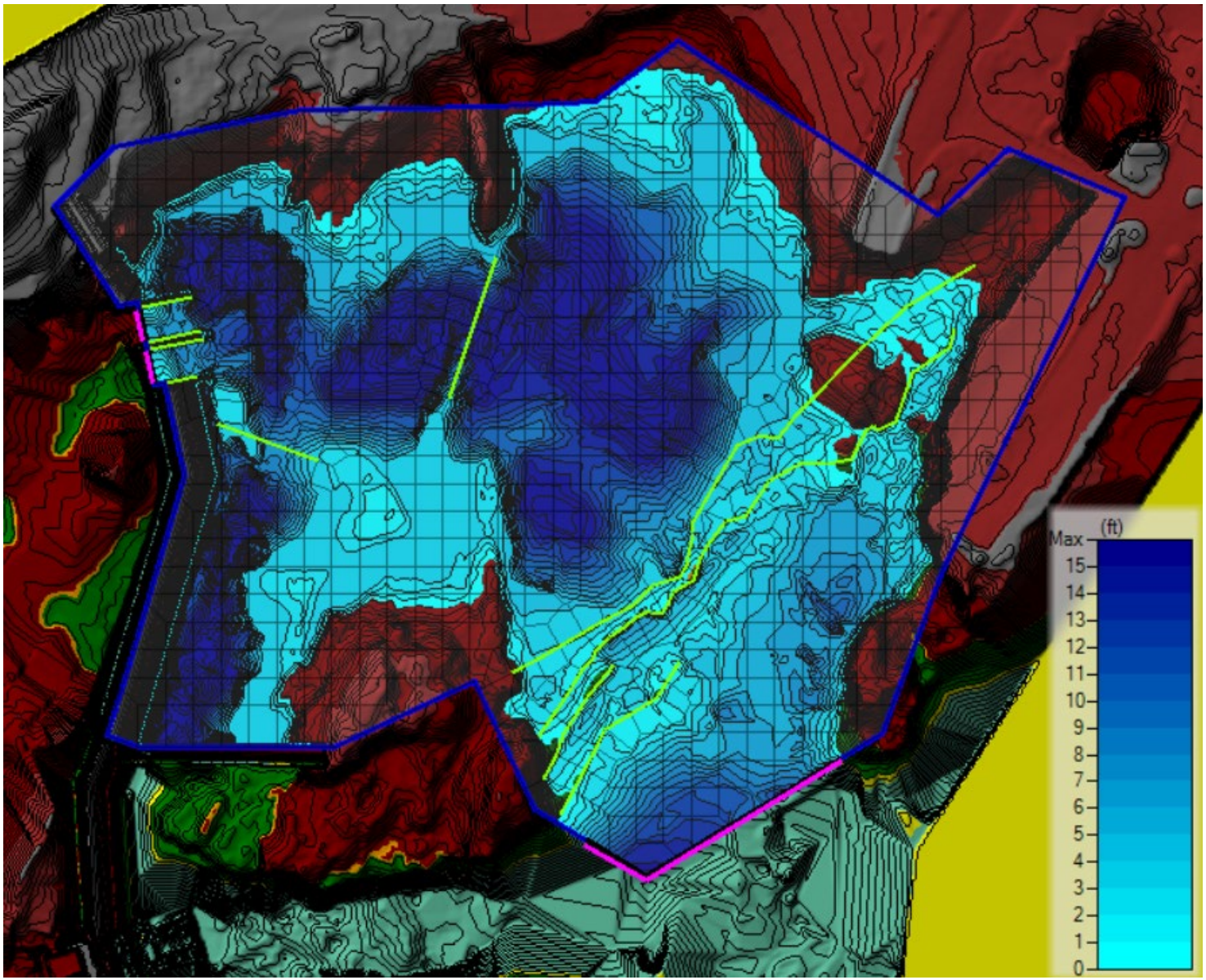
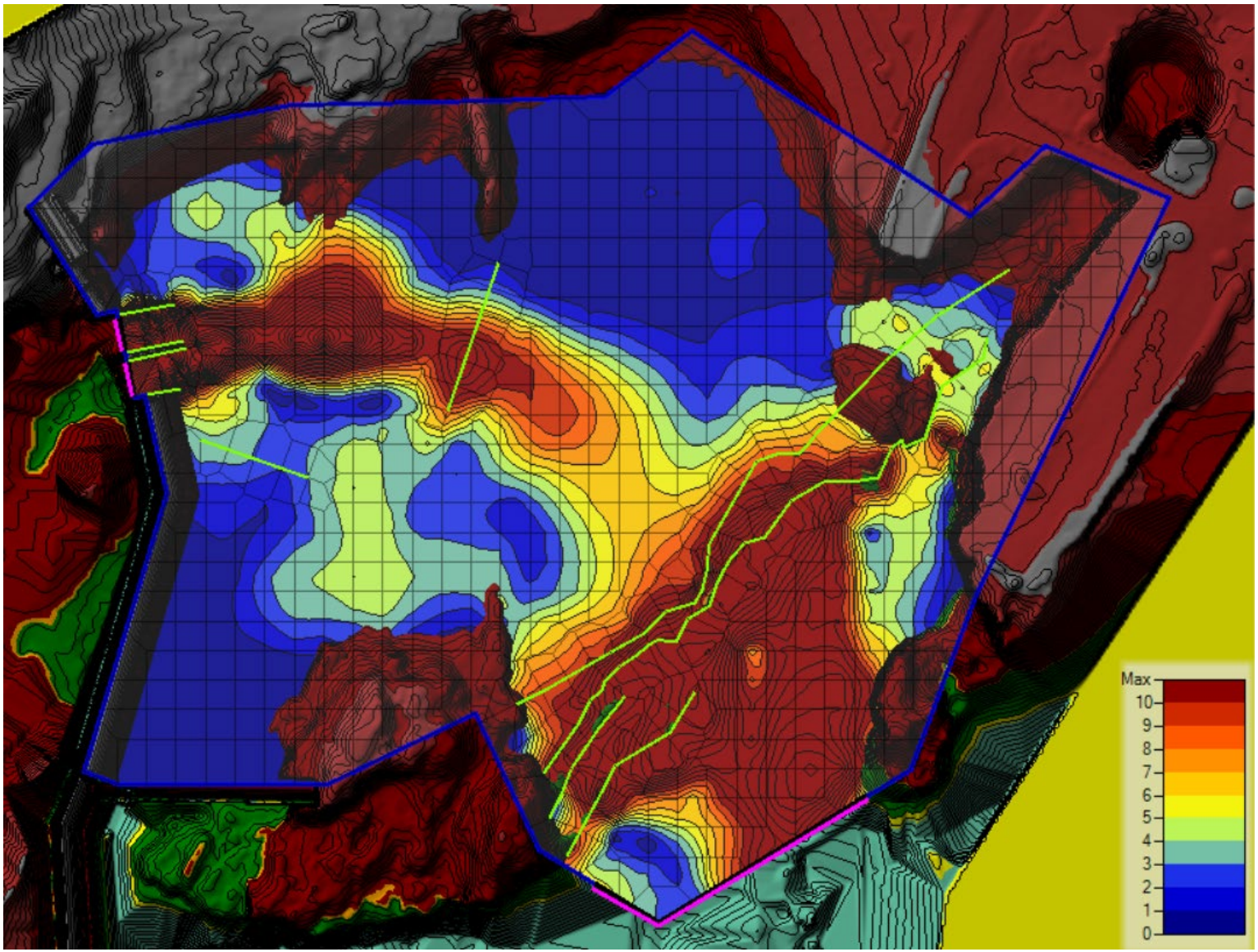


Figure 6.2.3-16: Simulated Velocities in the Bypass Channel (14,500 cfs)



7.0 REFERENCES

Brookfield Renewable. 2024. Revised Study Plan for the Brunswick Hydroelectric Project. Prepared by Gomez and Sullivan Engineers. Filed with FERC December 2024.

Flow Science, Inc. 2025. FLOW-3D Users Manual.

OCM Partners, 2026: 2020 USGS Lidar DEM: South Coastal Maine (QL2), https://www.fisheries.noaa.gov/inport/item/75243.

APPENDIX A: TAILRACE MODEL RESULTS

Figure A-1: TR_P-01 (Total Flow = 7,595 cfs) – Velocity at Elevation 1.00 (Approximately 1.5-feet below the water surface)

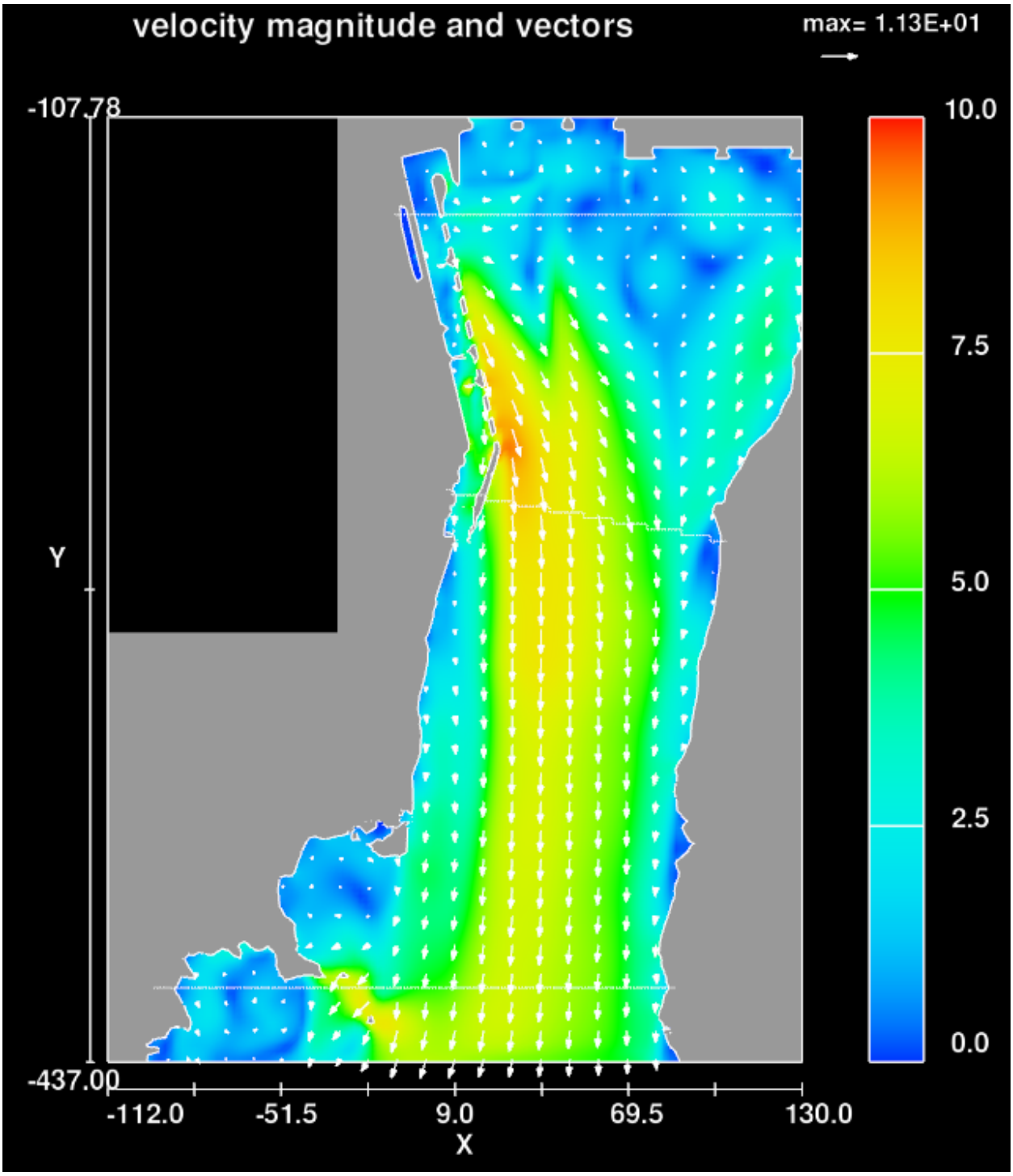


Figure A-2: TR_P-01 (Total Flow = 7,595 cfs) Velocity at Elevation -5.00 (Approximately 7.5-feet below the water surface)

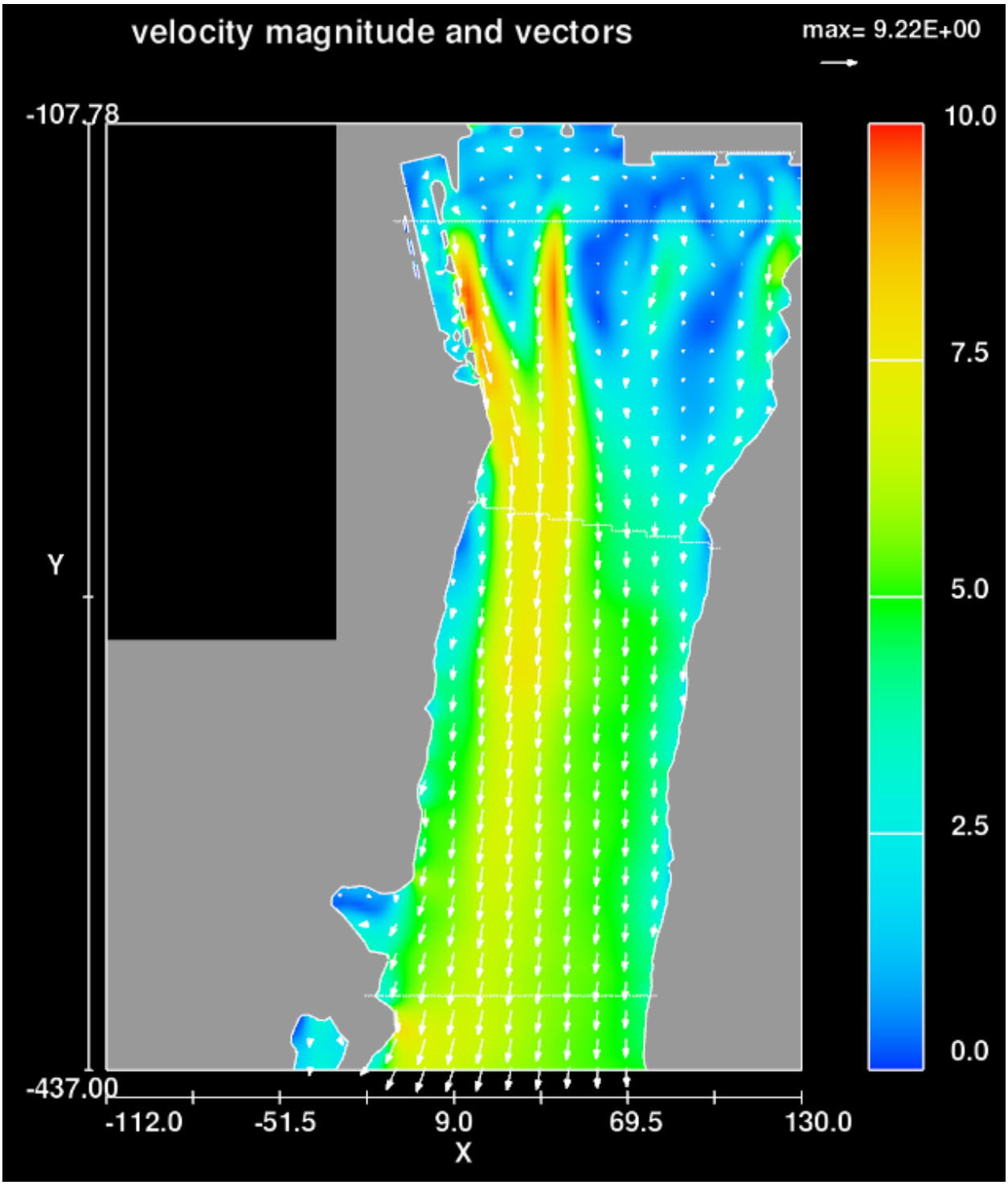


Figure A-3: TR_P-01 (Total Flow = 7,595 cfs) Velocity at Elevation -9.00 (Approximately 11.5-feet below the water surface)

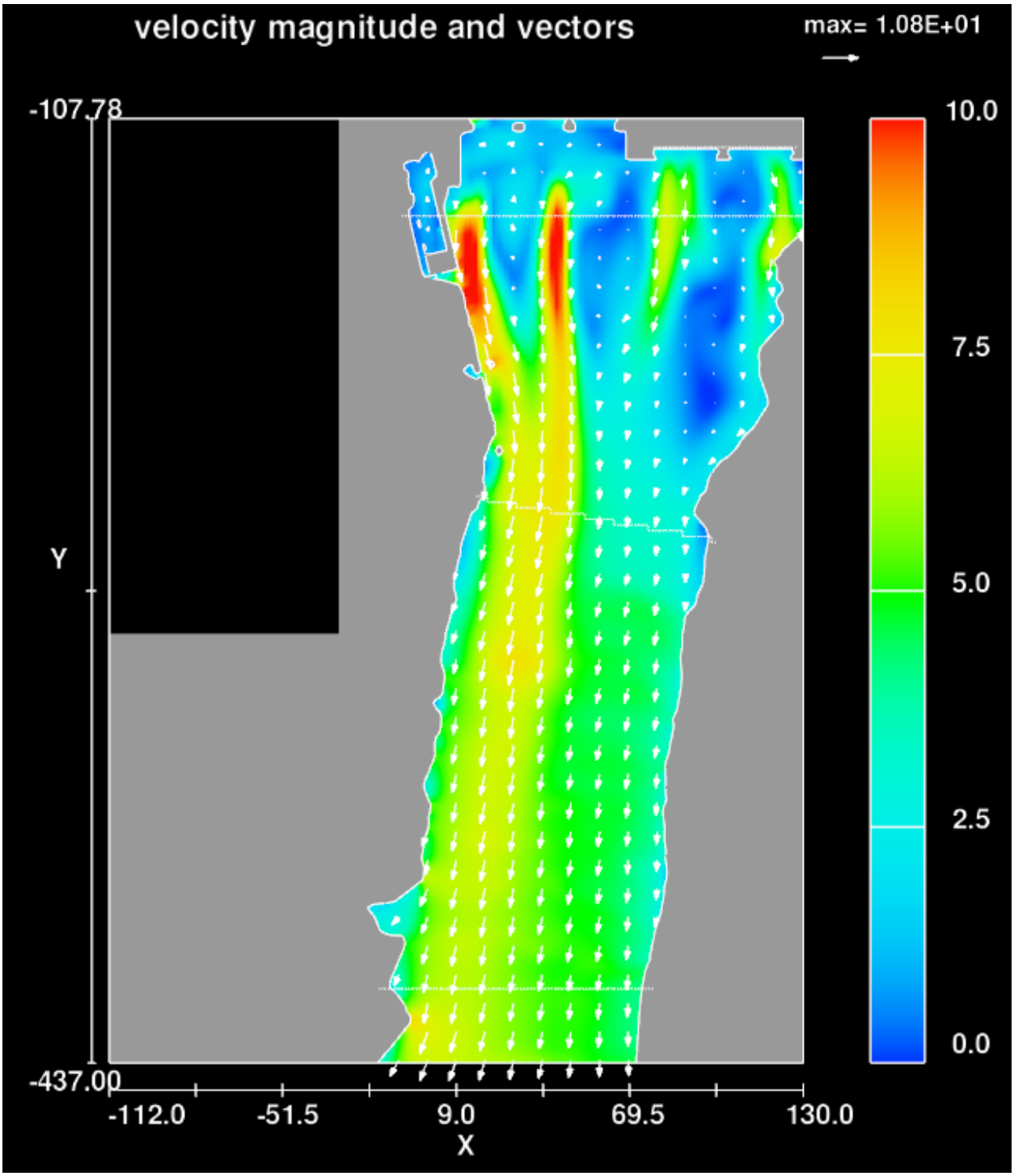


Figure A-4: TR_P-02 (Total Flow = 1,320 cfs) – Velocity at Elevation 1.00 (Approximately 1.5-feet below the water surface)

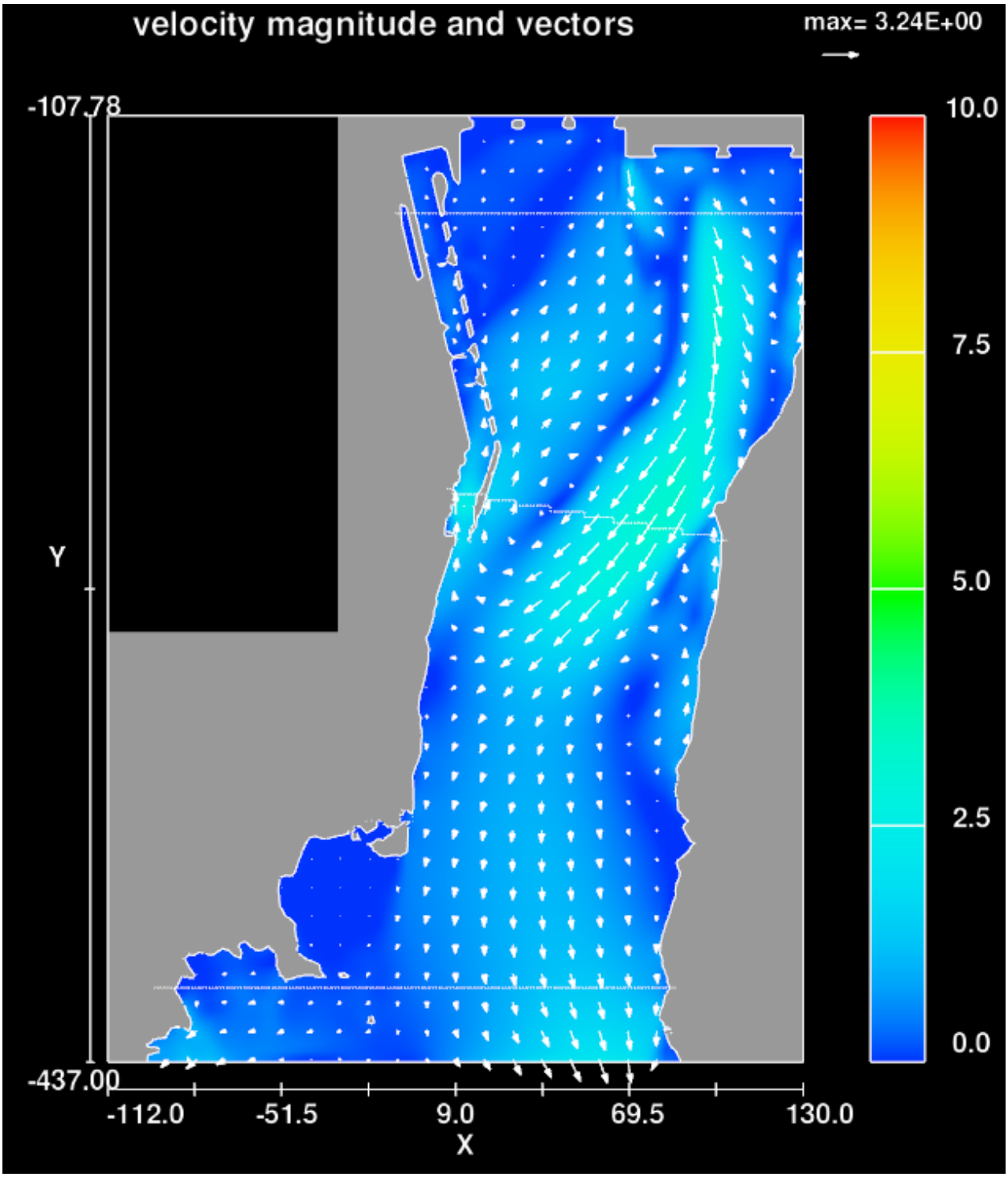


Figure A-5: TR_P-02 (Total Flow = 1,320 cfs) Velocity at Elevation -5.00 (Approximately 7.5-feet below the water surface)

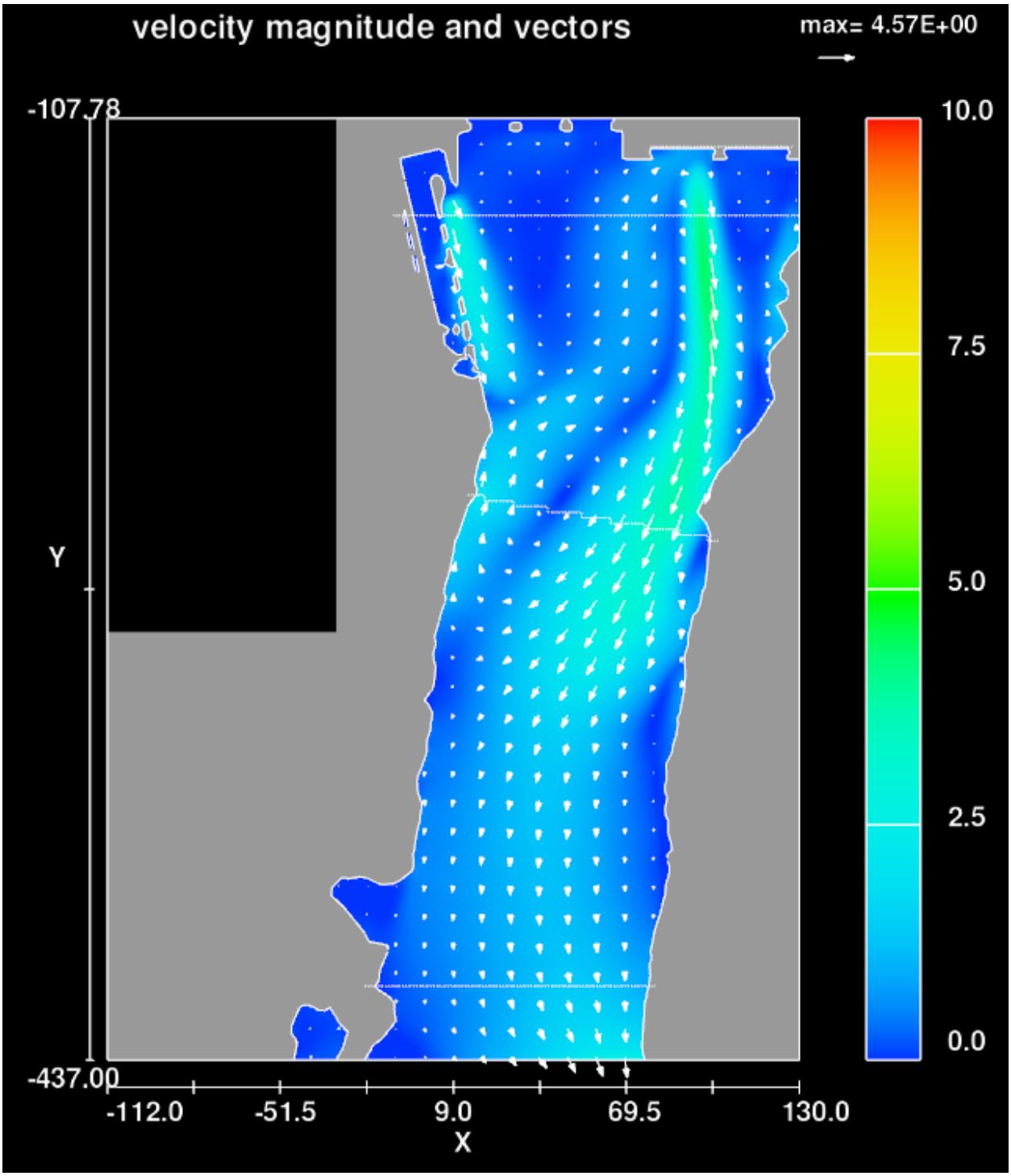


Figure A-6: TR_P-02 (Total Flow = 1,320 cfs) Velocity at Elevation -9.00 (Approximately 11.5-feet below the water surface)

